Safety in Mines Research Advisory Committee

Draft Final Project Report

The effect of structural discontinuities on coal pillar strength as a basis for improving safety in the design of coal pillar systems

GS Esterhuizen

Executive summary

The stability of underground coal mine workings depends on the integrity of the pillars which are required to support the overlying strata. Should the pillars collapse, the safety of the persons in the workings will be threatened.

The strength of a coal pillar is affected by the strength of the coal material which forms the pillar. Coal contains many natural discontinuities which adversely affect its strength. Discontinuities are not explicitly taken into account in the empirical methods of pillar design currently used in South Africa. As a result, pillars which are formed in coal with a high intensity of discontinuities may be under designed, while pillars in undisturbed coal may be over designed. This study sets out to investigate the effect of discontinuities on the strength of coal pillars.

Data on the characteristics of discontinuities were collected from a variety of operating coal mines in South Africa. Laboratory tests and field data collection techniques were used to determine the shear strength of discontinuities in coal. The condition of coal pillars in underground workings was evaluated, which showed that discontinuities have an adverse effect on pillar stability. Strength tests on laboratory samples were carried out to assess the effect of discontinuities on their strength. Rock mass classification techniques were used to estimate the large scale strength of coal. Numerical models were used to assess the effects of discontinuities on pillar strength, taking into consideration the width to height ratio of the pillars and the orientation of discontinuities in the pillars.

The field data showed that three distinct types of discontinuities were present coal, being small scale cleats, joints and slips. It was found that the intensity of discontinuities is highly variable in the different coal seams being mined, and within individual mine sites. This variability is likely to result in variable pilar strength.

The results of laboratory strength tests showed that the reduction in strength of coal samples as their volume increases could be explained by the increased intensity of discontinuities in the larger samples. The application of rock mass classification methods showed that realistic strength values could be obtained for the large scale coal mass. The technique results in a large scatter of the strength, which would result in excessively high factors of safety being required when designing pillars.

Numerical model studies showed that as the width to height ratio of a pillar increased, the effect of discontinuities became less pronounced. The strength of pillars with width to height ratios in excess of 6,0 was essentially unaffected by the presence of discontinuities. However, the strength of pillars was extremely sensitive to the strength of the contact surfaces between the coal and the surrounding strata, even at large width to height ratios.

It is concluded that discontinuities have a weakening effect on pillars in South African coal mines. The high variability of discontinuities in coal seams results in variable pillar strength, which may result in local instability of pillars. A design method is required which will allow rock engineers to carry out a site specific design in which the effect of discontinuities is taken into account. The results of this research may be used to develop such a design method.

Contents

List of figures

List of tables

Glossary of symbols and abbreviations

Symbols

k	:	large scale strength of coal material
σ_n	:	normal stress
τ	:	shear stress
L	:	block edge length
σ_c	:	uniaxial compressive strength
d	:	sample diameter
l	:	fracture trace length
l_e	:	equivalent dimension of a sample
F_s	:	frequency of slips
F_j	:	frequency of joints
σ_1	:	maximum principal stress
σ_3	:	minimum principal stress
m, s, a	:	parameters in Hoek-Brown strength criterion
σ_m	:	strength of rock/coal mass
ϕ	:	friction angle
ϕ_r	:	residual friction angle
β	:	angle between normal to a plane and the maximum principal stress
σ_p	:	pillar strength
w, h	:	width and height of a pillar
α, β	:	empirical constants in pillar strength equation
J_n	:	joint set number
J_a	:	joint alteration
J_r	:	joint roughness
J_w	:	joint water reduction factor
J_f	:	joint frequency
c	:	cohesion

Abbreviations

FOS	:	Factor of safety
GSI	:	Geological strength index
JRC	:	Joint roughness coefficient
JCS	:	Joint wall compressive strength
RMR	:	Rock mass rating
UDEC	:	Universal distinct element code (a computer program)
UCS	:	Unixial compressive strength
W:H	:	Width to height ratio
3DEC	:	Three dimensional version of UDEC

1 Introduction

1.1 Background

Underground coal mines rely extensively on pillars of coal to provide support to the overlying strata. When designing pillars it is necessary to determine the strength of the pillars so that appropriate safety factors can be applied to the design. Should pillars be under designed, the collapse of large areas is possible, which represents a major safety hazard to operating coal mines. Natural discontinuities in coal, such as cleats, joints and slips, may weaken the pillars and result in the collapse of the coal mine workings. It is therefore necessary that discontinuities be accounted for when designing pillars. Currently the equation of Salamon & Munro (1967) is widely used to design coal pillars in South Africa. The equation does not explicitly account for the presence of discontinuities in coal. It provides the same result, whether the pillars being designed contain discontinuities or not.

Inspection of coal mine workings has indicated that the intensity of jointing and other discontinuities in coal seams is highly variable. The discontinuities are expected to result in a considerable variation in the strength of coal pillars, but methods of estimating the effects of the discontinuities on the coal pillar strength do not exist. The Coal Rock Engineering Advisory Committee of the Safety in Mines Research Advisory Committee (SIMRAC) decided that this problem should be researched and the project COL005A was awarded to the Department of Mining Engineering, University of Pretoria. The project formed part of a larger project, COL021, aimed at developing improved methods of coal pillar design.

1.2 Objectives

The objective of the research presented in this report is to improve the understanding of the effect of discontinuities on the strength of coal pillars allowing design of coal mine pillars to be carried out with greater confidence. The following sub-objectives were set as a strategy to meet the main objective of the research:

- Determine the properties of discontinuities in coal seams in South Africa. The strength, persistence, frequency and variation of each property within a single mine and over several mine properties had to be determined. Understanding the characteristics of discontinuities was required to allow further investigation of their effect on coal pillar strength.

- Determine the effect of discontinuities on the condition of pillars in existing mine workings. The correlation between the intensity of discontinuities and condition of the pillars could be used as an indicator of the effect of discontinuities.

- Investigate the effect of discontinuities on the strength of small scale coal samples. These results were expected to provide insight into the effect of discontinuities on large scale coal pillars.

- Establish the effect of discontinuities on large scale coal pillars through numerical models. The emphasis was again to determine how discontinuities would affect the strength of pillars at different width to height ratios.

1.3 Research methodology

1.3.1 Field data collection

The research commenced with collecting data on discontinuities in coal seams. Detailed mapping of discontinuities was carried out in the main coal seams being mined in South Africa. It was soon found that standard rock mass discontinuity mapping procedures were not suited to coal, owing to the large variation in scale of discontinuities, ranging from millimetres to several tens of meters. In addition large variations in the frequency of discontinuities made standard methods of mapping impractical. The mapping method was modified so that it was based on discontinuity frequency, in which a coal seam is mapped on a one metre scale, a 10m scale and on a 100m scale. Data were collected at 86 different underground locations. The mapping results and results of a survey of the condition of the pillars was used to establish whether the discontinuities had an effect on the condition of the pillars.

1.3.2 Laboratory tests

Laboratory tests on coal samples were used as a source of data on the effect of discontinuities on the strength of coal at a small scale. The results of the strength tests together with detailed mapping of all visible discontinuities in the samples were used as a method of establishing the effect of the minor discontinuities on the strength of the coal.

1.3.3 Model analysis

Owing to the excessive cost and technical difficulty of determining the strength of full scale pillars, numerical models were used to investigate the effects of single and multiple discontinuities on pillars. Two and three dimensional numerical models were created using finite difference computer programs. Many combinations of discontinuity types and pillar geometries were analysed. The effect of discontinuity orientation, strength, frequency and location was evaluated.

1.3.4 Evaluation

The results of the analyses were evaluated and a number of conclusions are presented relating discontinuities to the strength of coal pillars. The objective of improving the understanding of the effect of discontinuities on coal pillar strength has been met.

1.3.5 Limitations

The research was limited to obtaining information on discontinuities in South African coal seams and assessing their effect on pillar strength. The research did not attempt to develop a methodology for designing pillars which takes into account the effect of discontinuities. The development of a methodology formed part of the objectives of Project COL021A and Project COL223.

2   Discontinuities in South African coal seams

2.1 South African coal deposits and their structure

2.1.1 Formation of South African coals
Coal consists of an assembly of organic materials, called macerals, just as minerals are the constituents of rocks and orebodies. The macerals are the fragmented and partially decomposed remains of the original vegetable matter. Mineral matter in coal originates from the inorganic matter in coal forming plants and inorganic matter added to the coal forming deposit after the death of the plants (Gaigher, 1980). Coal is stratified and may contain individual layers which are no more than a few centimetres thick. Coal has a typically macroscopic structure perpendicular to the bedding planes, known as the main cleating and another structure perpendicular to the other, known as cross-cleating, (Green, 1982). Coal may be categorised by its rank, which is the maturity of the coal induced by time, temperature and overburden pressure. Coal forming matter initially forms peat beds in shallow depositional basins and matures to lignite (brown coal), bituminous coal (black coal) and finally to anthracite, the highest rank.

South African coals are rich in minerals and are highly variable in rank, (Falcon & Ham, 1988). The coal was formed in Permian swamps under cold temperate conditions associated with the waning of a massive ice age. The coal bearing sediments accumulated in relatively stable continental depressions forming mineral rich, peat forming swamps which developed into wide spread, relatively thick coal seams. The seams remained at relatively shallow depths, but they were subject to frequent intrusions of hot igneous lavas in vertical and horizontal directions which resulted in uneven increases in maturation and rank within localized areas. A present the seams are at a relatively shallow depth and are almost horizontal in dip. The coal seams in South Africa are generally described as bituminous coals with the exception of locally heat-affected regions where the coal becomes meta-anthracite in rank.

2.1.2 Coal fields
South African coal deposits are located in a number of coal fields (de Jager, 1976), shown in figure 2.1. The numbers indicated in figure 2.1 are mine sites where data were collected as part of the research presented in this report. The deposits in the Main Karoo Basin have been divided into a number of coal fields, based on differences in lithology, properties of coal seams and coal qualities. The coal in the Main Karoo Basin is found in the Vryheid Formation of the Karoo Supergroup. It is a sedimentary unit consisting of alternating shale and sandstone layers, with sandstone dominating. The coal seams are well defined with sharp contacts between the overlying and underlying clastic rocks.

In the other smaller coal bearing basins the coal is developed in the equivalent of the Vryheid formation but also in the overlying formation, which is equivalent to the Volksrust formation in the Main Karoo Basin. The coal zone may reach thicknesses of up to 80m, but it is always contaminated by shale bands which are intimately associated with the coal.

2.1.3 Major structural features of coal fields
The South African coal fields are characterised by the presence of dolerite intrusions in the form of dykes and sills, (Faucconier & Kersten, 1982). These structures have result in difficulties in applying total extraction mining methods such as longwall mining. Dykes tend to compartmentalise the coal seams into blocks which are not suitable for high extraction mining and sills result in caving problems of the overlying strata. The compartments formed by the dykes tend to be shallow dipping and are relatively undisturbed.

Faults and dolerite dykes often form the boundaries of mining blocks. It is in these undisturbed blocks of coal that coal pillars are formed. Access to the blocks of coal is often obtained by developing through disturbed ground. During development through ground disturbed by faulting or a dolerite dyke, the method of mining is altered so that only a few headings are mined through. The stability of the workings changes from a pillar stability problem to a heading stability problem. The stability of the pillars between the headings becomes of minor importance, since control of the immediate roof and sidewalls of the headings is the major concern.

The research presented in this report has therefore been aimed at identifying the structures in the "undisturbed" blocks of coal where the vast majority of coal pillars are formed. These structures exist on a local scale and affect the strength of individual coal pillars.

2.2 Initial mapping of discontinuities

To obtain data on the discontinuities within mineable blocks of coal, field mapping was carried out at sites 1 to 6 shown in figure 2.1. The objective was to determine the spacing, orientation, length and strength properties of the discontinuities in the different coal seams. Standard scan line mapping methods were used. Although not comprehensive, the initial sampling set the basis for developing a discontinuity recording system which was suited to coal.

It was soon found that censoring of the joints at some minimum length had to be done so that the numerous minor discontinuities (cleats) did not have to be recorded. In some cases there were more than 20 cleats per linear metre. It was decided that only joints with a length of greater than 1m would be recorded.

2.2.1 Discontinuity orientations

The discontinuity orientations are summarised in figures 2.2 to 2.7, which presents lower hemisphere, equal area contour plots of the poles of the discontinuities mapped at the different sites. The number of poles measured at some of the sites was not sufficient to produce accurate stereoplots. This is an indication of the paucity of major structures at these sites. The total length of scan line exceeded 350m at each site.

Inspection of the stereoplots indicates that at sites 2, 3 and 4 the most prominent joints were steeply dipping. At sites 1, 5 and 6 shallow dipping joints were observed, with the prominent joint set dipping at between 50^0 and 70^0. At site 2, shallow dipping joint sets were indicated, striking approximately parallel to the major steep set.

2.2.2 Geotechnical properties of discontinuities

The geotechnical properties of the discontinuities observed at all six sites are summarised in table 2.1. The observed discontinuity length reported in table 2.1, was limited by the span of the excavation. Inspection of major discontinuities underground indicated that they could be several tens of metres long in the strike direction.

N

Limpopo

Pafuri

Soutpansberg

Waterberg

Springbok flats

Komatipoort

Springs-Witbank

10 12 4 17 3
9 15 14
8
Highveld
11

Eastern
Trans-
vaal 5 6
16
19 20

Swaziland

South
Rand

Vereeniging
- Sasolburg

2 Vryheid
18

Zululand

13

21

Utrecht

Freestate

Klipriver

Lesotho

INDIAN OCEAN

Molteno - Indwe

0   100 km

Scale
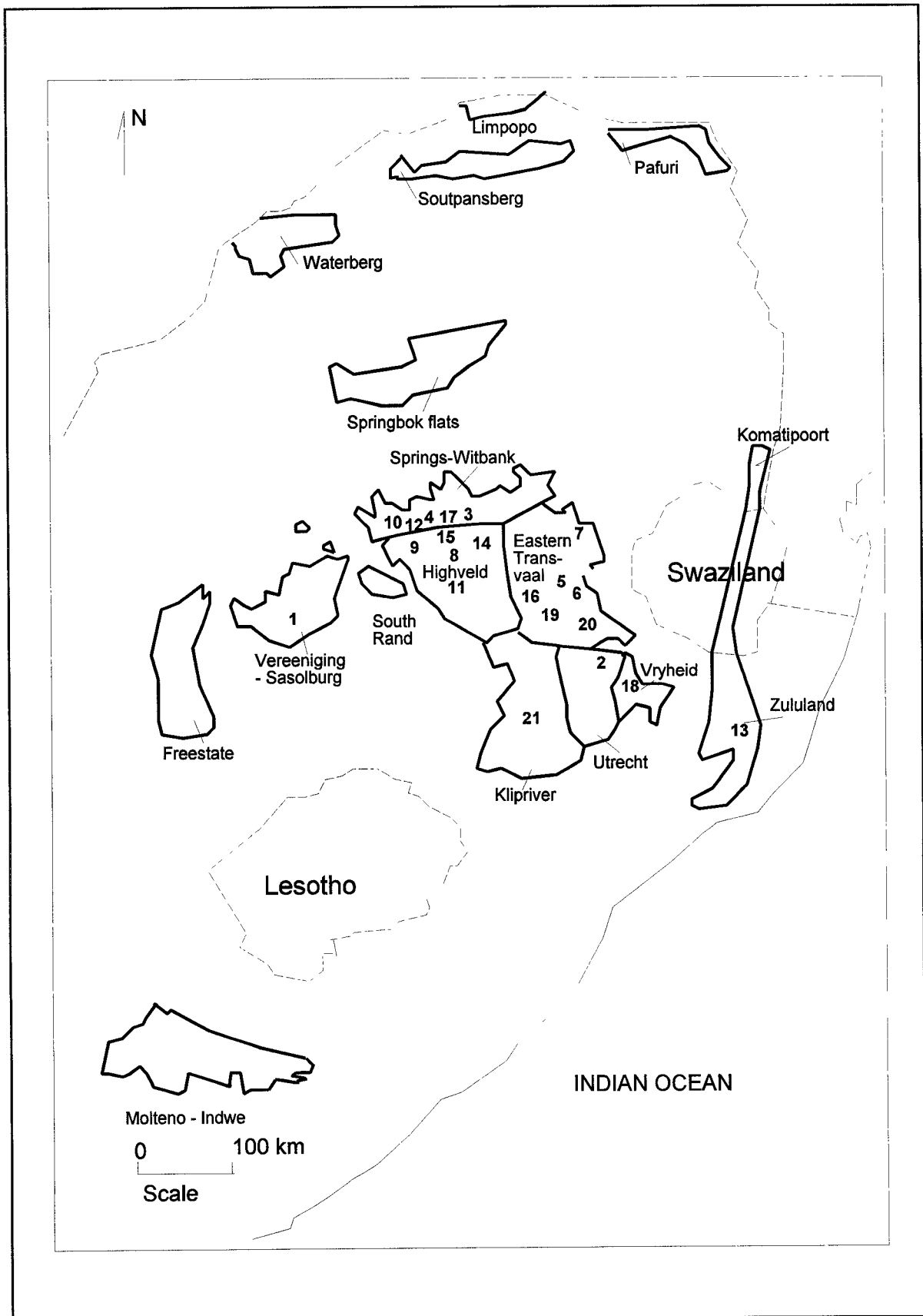
Figure 2.1   Locality plan of South African Coal Fields. Numbers indicate mine sites where data were collected
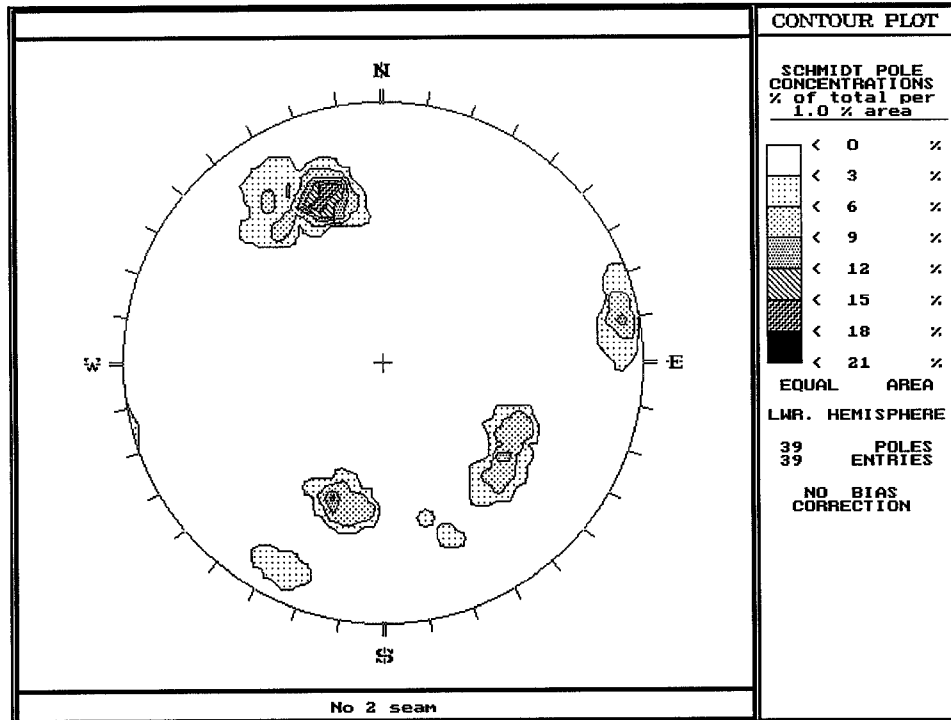
Figure 2.2 Discontinuity orientations at site 1
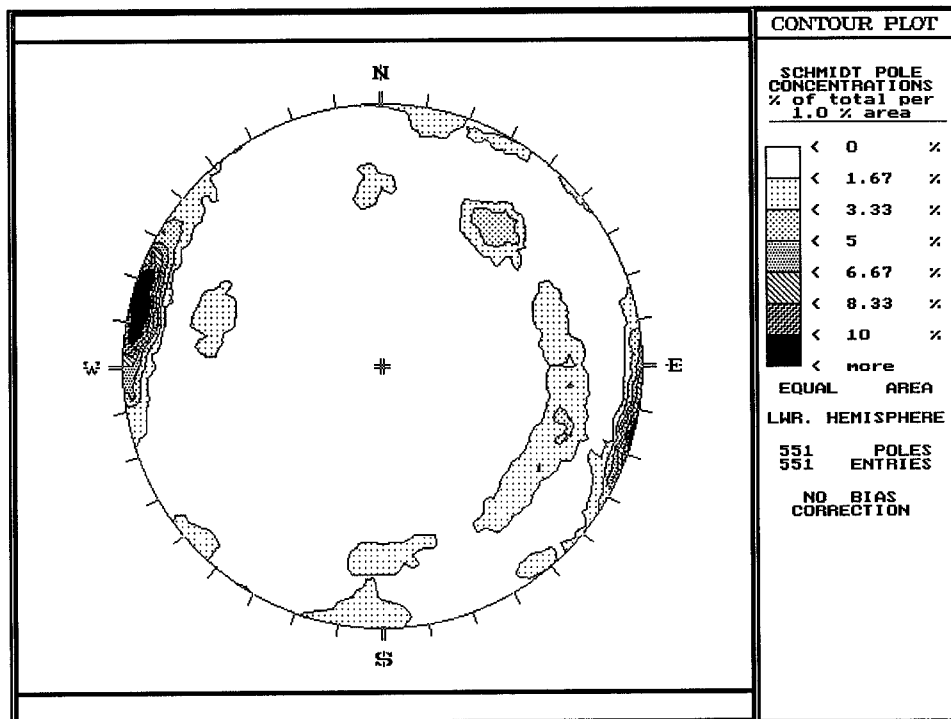
Figure 2.3 Discontinuity orientations at site 2.
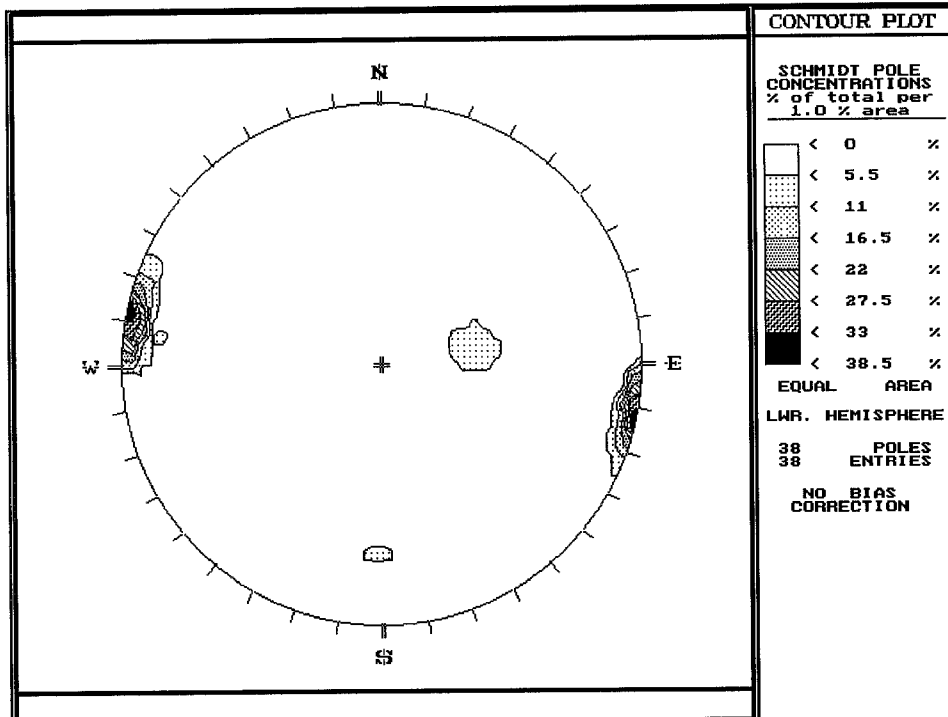
Figure 2.4 Discontinuity orientations at site 3
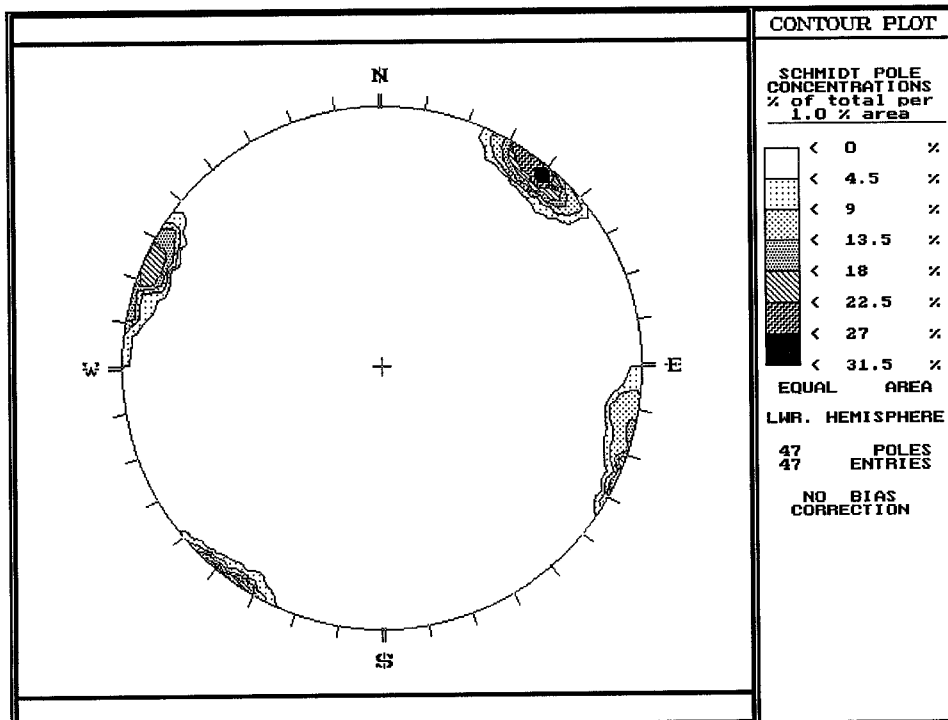
Figure 2.5 Discontinuity orientations at site 4
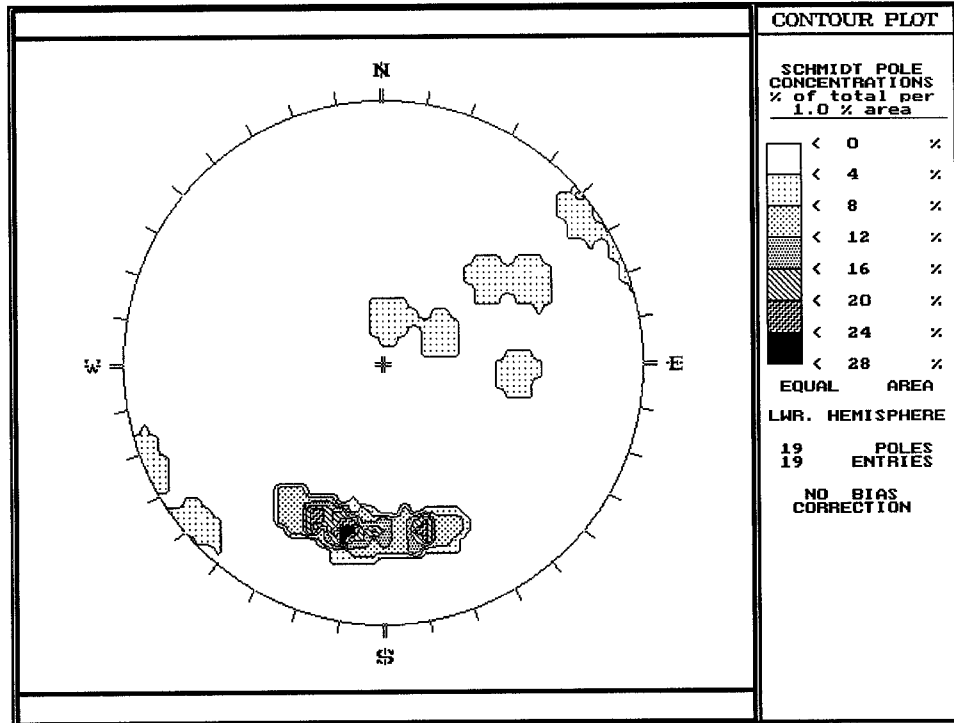
Figure 2.6 Discontinuity orientations at site 5
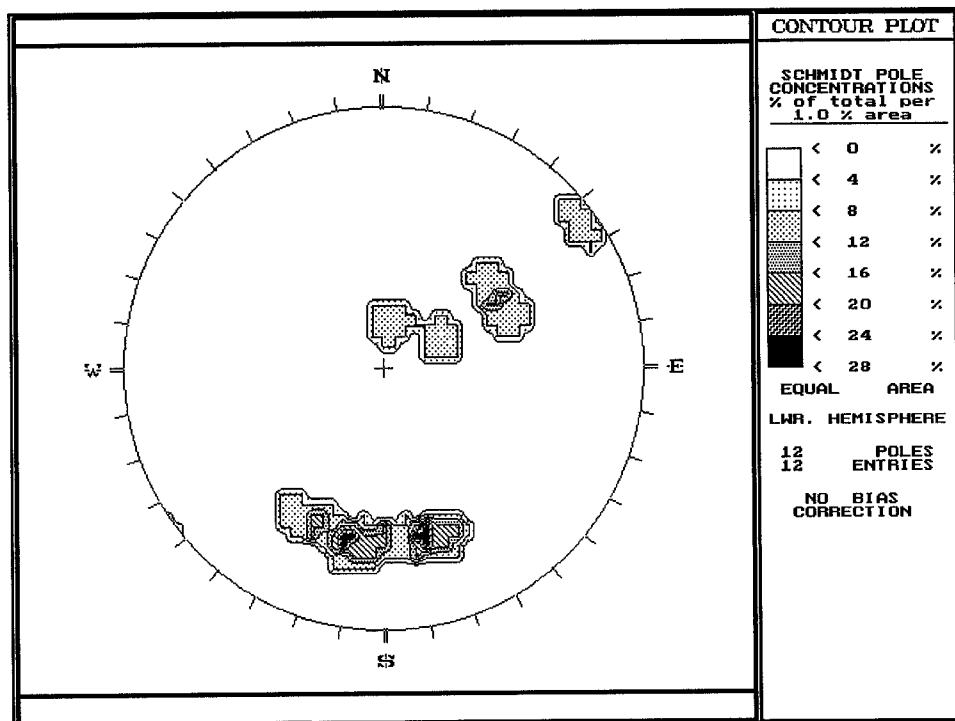
Figure 2.7 Discontinuity orientations at site 6

At site 1 the discontinuities were continuous into the roof strata. It was not possible to observe whether they were continuous into the floor. It was observed in all the locations that the discontinuity surfaces were infilled with soft calcite. Although the surfaces were relatively rough, they were often striated and slickensided in the dip direction.

At site 2, the discontinuities were found to be rougher than at other sites although they may be polished in the dip direction. The discontinuity frequency was higher than at the other sites, with frequent discontinuities extending from the roof to the floor of the seam. No discontinuities were found to extend into the roof strata. The infilling material was again calcite, sometimes with montmorillonite clay and the wall strength was considerably lower than at the other sites, often being weak and crumbly when impacted with a geological pick.

The joints at site 3 were found to be infrequent, with only 38 major discontinuities being observed at six different mapping sites. Each site consisted of conducting scan line mapping around a pillar, a total length of some 60 m. At one of the locations no major discontinuities were found.

At site 4, the discontinuity lengths were found to be near the limit of 1m, which was selected as the cut-off for major discontinuities. The discontinuities were typically between 1,0 m and 0,6 m long. It was decided to measure these discontinuities. The frequency was high and spacings of between 5 cm and 10cm were observed.

At sites 5 and 6, the discontinuities were very infrequent, with only 19 being observed at site 5 and 12 at site 6. Several of the locations mapped did not have any major discontinuities. At site 6 it was observed that the upper layer of the coal seam contained minor discontinuities spaced about 10cm apart, which were approximately 40 cm long. They were not mapped individually but indicated that a different method of collecting discontinuity data was required.

2.2.3 Discussion of initial mapping results

Mapping of discontinuities in coal seams using standard scan line mapping techniques poses problems in that large numbers of minor discontinuities (cleats) exist in coal. At the other end of the scale, major discontinuities (slips) can be tens of metres long and tens of metres apart. The minor discontinuities are often spaced 2 to 5 cm apart and totally overwhelm the less frequent major discontinuities. During the initial mapping it was necessary to truncate data collection of discontinuities which are shorter than 10cm.

The mapping results indicated that there was a large variation in the frequency of discontinuities in the different coal seams. Spacings in excess of 10m were observed as well as spacings down to as little as 5 cm. Most of the discontinuities were steeply dipping, which would be favourable from a pillar stability point of view. Infrequent shallow dipping joints were observed in most of the seams. In the Gus seam, large numbers of discontinuities dipping at 50^0 to 60^0 were observed, and these may be expected to have a detrimental effect on pillar strength.

The roughness, infilling and waviness, indicated by the amplitude of the joints was similar in the different seams. It was found that the infilling material was mostly a soft calcitic material which was weaker than coal. The infilling was typically 1mm to 2mm wide. The joint surfaces were relatively rough. In some cases the surfaces were slickensided, but a roughness of approximately 3,0 on Barton's scale appears to be typical of the roughness.

Table 2.1 Mean values of observed major discontinuity parameters at initial mapping sites

	Seam							
	Site 1			Site 2	Site 3	Site 4	Site 5	Site 6
Parameter	No. 2A	No. 2B	No. 3	Gus	No. 2	No. 5	No. 3	No. 3
Spacing (m)	6,5	7	> 10	0,1 to 1,0	1,4	0,08	> 10	> 10
Joint alteration J_a	2,2	4,0	1,6	3,0	1,8	3,0	2,5	2,8
Estimated joint wall strength (MPa)	7,9	7,0	7,3	3,8	13,8	4,1	13,5	20
Roughness (1 - 10)	1,7	2,75	2,0	7,2	3,4	3,5	2,3	4,8
Trace length (m)	7,1	7,5	3,5	4,2	2,16	0,75	2,7	5,0
Amplitude (cm)	10,9	6,1	5,7	8,0	6,3	2	5	7,9
Separation (mm)	2,6	6,5	1,5	1,5	1,1	1	1,5	1,8
Infill type	Calcite	Calcite	Calcite	Calcite/mont-morillonite	Calcite	Surface staining only	Calcite	Calcite

11

Coal pillars in the Vereniging-Sasolburg coal field have been shown to be weaker than elsewhere in South Africa, (van der Merwe, 1993). Discontinuities were mapped in three different seams in this coal field at site 1, shown in figure 2.1. The discontinuities were widely spaced, typically more than 5m apart which is a very low frequency compared to most other sites visited. It is, therefore, unlikely that discontinuities are responsible for the lower coal strength in this coal field.

2.3   Shear strength of discontinuities

In the development of a mapping system for coal seams it was necessary to investigate the shear strength of discontinuities, so that a practical method of assessing shear strength could be developed. The shear strength of discontinuities may be estimated using field methods (Barton & Choubey, 1977) or measured directly using a shear testing apparatus. During the course of mapping discontinuities, data was collected to allow the Barton & Choubey method of shear strength estimation to be used. A limited number of shear tests were conducted in the laboratory to measure the shear strength.

2.3.1   Shear strength based on field estimation techniques
The equation of Barton & Choubey (1977) for the estimation of shear strength is as follows:

$$\tau = \sigma_n \tan\left(\phi + JRC \ \log_{10}\frac{JCS}{\sigma_n}\right) \tag{2.1}$$

where σ_n is the normal stress across the discontinuity surface in MPa, ϕ is the base friction angle measured along a smooth cut surface, JRC is the joint roughness coefficient and JCS is the joint wall compressive strength in MPa. The base friction angle was determined by conducting sliding tests on coal samples using a tilt table. The friction angle was determined to be between 21^0 and 24^0 for coal from the Vereeniging and Highveld coal fields. The JRC value was determined by comparing traces of joint surface profiles with the published traces of joint roughness of Barton & Choubey. The value of JCS was determined by field estimation using Schmidt hammer tests and strength estimation techniques of Robertson (1971). In most cases the joint walls were coated with calcite or were weak and crumbly, having a low strength (about 3 MPa). Unaltered joint walls were rarely seen. The results of the field work on joint strength are summarised in table 2.1. Plots of the field estimates of shear strength at site 4 are shown in figure 2.8. The observed values of JRC and JCS for each discontinuity were used with a base friction angle of 21^0 in the Barton & Choubey equation. It can be seen that most of the predicted shear strengths are clustered at the lower bound of the group, with only one or two of the joints having a higher strength owing to greater roughness and wall strength.

The results at site 4 are typical of the shear strengths determined at the other sites. If all the results for the JRC and JCS values are combined, the results shown in table 2.2 are obtained.
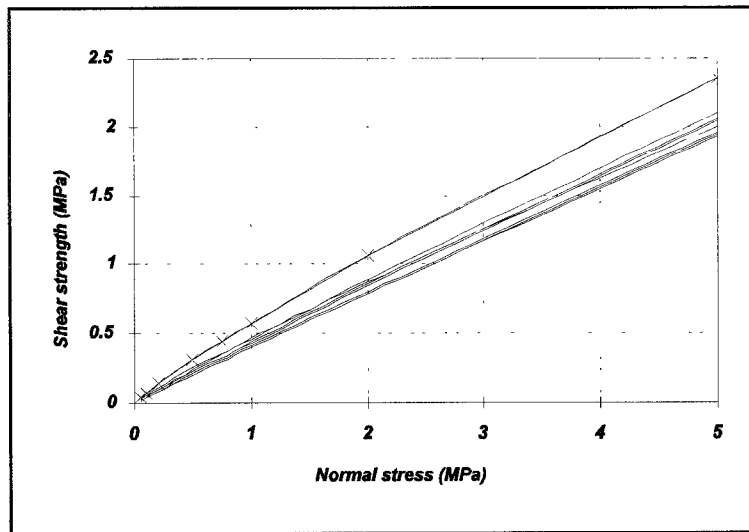
Figure 2.8   Field estimates of shear strength of seventeen joints at site 4.

Table 2.2   Statistics of joint properties of six sites

Property	Mean value	Standard deviation
Joint roughness	3,45	1,45
Joint wall strength (MPa)	9,67	2,51

The point estimate method (Harr, 1986) was used to determine the mean joint strength and the 95% confidence limits of the strength. In the calculations, the effect of variations in the base friction angle was eliminated by assuming it was constant at $21°$. The results are shown in figure 2.9 where it can be seen that the shear strength, based on field estimates, falls in a narrow range. Fitting a straight line Coulomb equation through the mean strength curve for the joints, the following strength equation is obtained if the curve fit is done from zero to five MPa :

$$\tau = \sigma_n \tan(21,8°) + 0,0318 \quad (MPa) \qquad (2.2)$$

If a curve is fitted to the normal stress range of zero to one MPa the resulting equation is:

$$\tau = \sigma_n \tan(24,8°) + 0,0132 \quad (MPa) \qquad (2.3)$$

The second equation shows that at lower stresses the effect of joint roughness is more pronounced, resulting in a higher value of the friction angle but a lower value in the apparent cohesion.
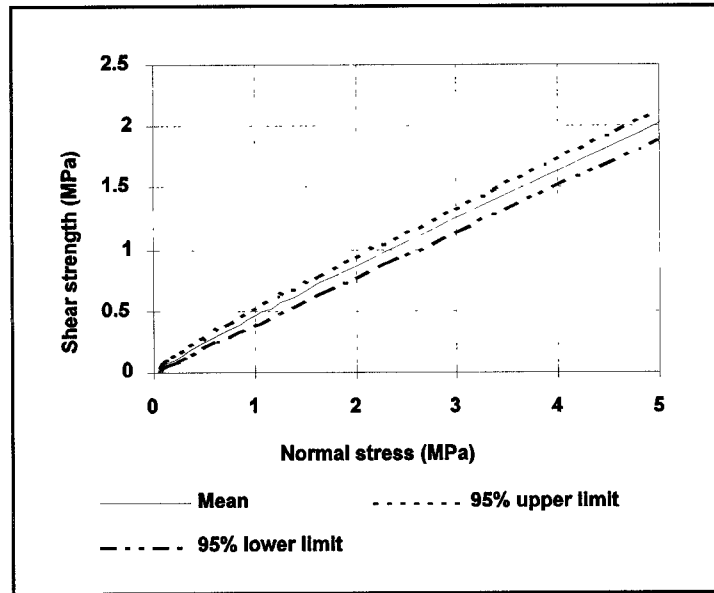
Figure 2.9 Graph showing 95% confidence limits of field estimates of discontinuity shear strength.

2.3.2 Shear strength tests on discontinuities

Direct shear tests were carried out on samples of coal containing unfilled discontinuities and saw cut surfaces. The tests were carried out in a rig in which the normal loading to the samples was provided by gravity. Shear loading was provided by a horizontal hydraulic jack. The applied shear force and shear displacement were monitored during the tests. The tests were carried out a normal stresses of 0,1 to 0,3 MPa. At the low normal stress values, the effect of roughness plays an important role on the apparent friction angle. The normal
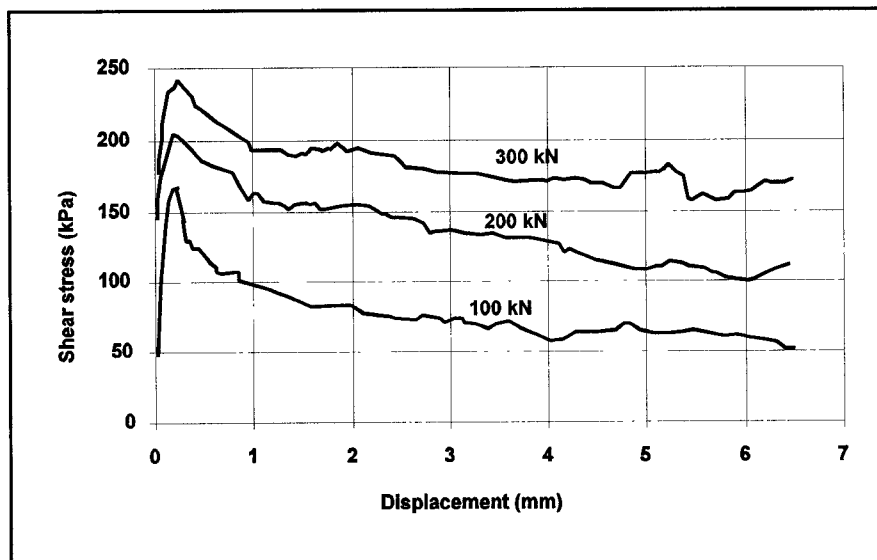
Figure 2.10 Shear test results of natural discontinuity in coal.
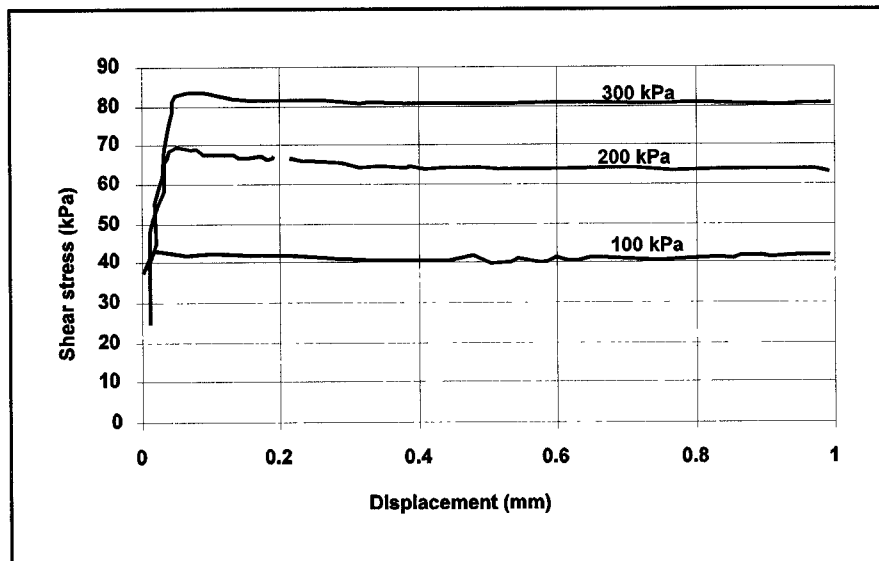
Figure 2.11 Shear test results of saw cut surface in coal.

stresses were insufficient to cause comminution of the asperities along the surface, and the residual strengths represent the frictional resistance of two diamond saw cut surfaces sliding over each other.

Figure 2.10 and 2.11 illustrate the results of a test on a natural discontinuity and a saw cut surface respectively. The test results are summarised in table 2.3. It can be seen that the

Table 2.3 Summary of shear test results on discontinuities in coal

	Peak strength		Residual strength	
	Cohesion (kPa)	Friction angle	Cohesion (kPa)	Friction angle
Saw cut surface	9,3	22,3°	7,2	18,9°
Natural discontinuity	132	21,6°	1,7	28,9°

friction angle at the peak shear strength was 21,6 degrees which is similar to the friction angle obtained by sliding tests. The residual friction angle obtained in the shear tests of the natural discontinuity was 28,9 degrees, which is higher than expected. The high value may be explained by the fact that the normal stresses were insufficient to cause comminution of the asperities on the joint surfaces. The residual friction angle therefore represents the effect of two rough surfaces sliding over one another. The shear test results for the peak strength were plotted in figure 2.12 together with the field estimates of shear strength. It can be seen that the laboratory test results provided a higher strength than predicted for field conditions.

One of the reasons for this difference is the scale effect of joint strength. The samples tested measured about 50 mm across, whilst the field estimates are based on 100 mm to 1000 mm

Table 2.4 Scaling of laboratory shear strength tests to field values

Parameter	Laboratory value	Scaled field value
Length	50 mm	1000 mm
JRC	12	5.8
JCS	30	10.2
φr	21°	21°

samples. The effect of scale on the shear strength of joints has been widely discussed and researched (Barton and Choubey, 1977, Bandis, 1980 and Cunha, 1990). Barton and Bandis (1982) have suggested that the values of JRC and JCS should be modified from laboratory scale to in situ scale. They propose the following two equations:

$$JRC_n = JRC_0 \left(\frac{L_n}{L_0} \right)^{-0.02 \; JRC_0}$$

(2.4)

and

$$JCS_n = JCS_0 \left(\frac{L_n}{L_0} \right)^{-0.03 \; JRC_0}$$

(2.5)

where the subscript 0 refers to the laboratory scale value and subscript n refers to the field sample size. L is the block edge length. Using the above two equations, the laboratory test results were scaled to field strength values. Table 2.4 shows the laboratory values and the scaled field values obtained. Using the derived field values, the shear strength was calculated using the Barton and Choubey equation and plotted in figure 2.12, where it can be seen that the scaled laboratory test results fall within the 95% confidence limits of the estimated field strength of joints in coal.
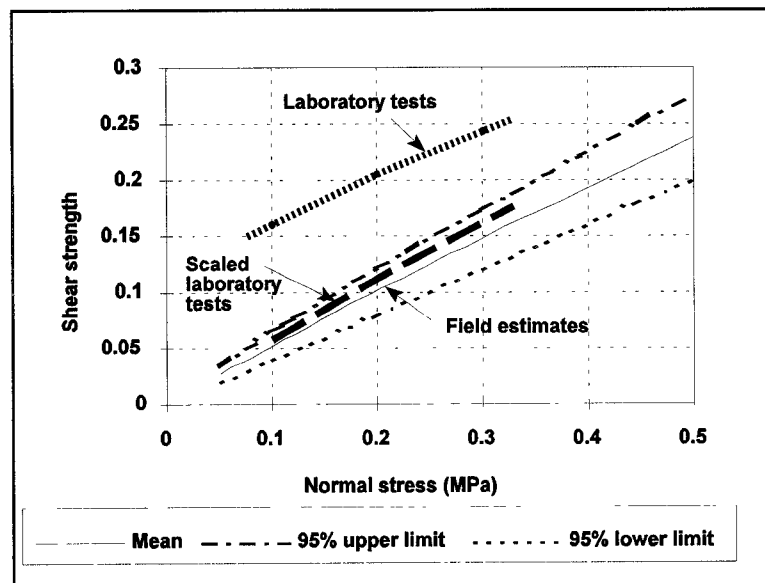
Figure 2.12 Comparison between shear test results indicated as dots and field estimates of shear strength at low normal stresses.

2.3.3 Discussion of shear strength

The field estimation method of determining discontinuity shear strength provided large numbers of data points. The results showed that there was a fairly large scatter in the joint roughness, having a coefficient of variation of 42%. The variation in the estimated joint wall strength was less, having a coefficient of variation of 26%. Using the point estimate method, the 95% confidence limits of joint shear strength were relatively narrow, the coefficient of variation was about 15% for joint shear strength. The results imply that joint shear strength is not very sensitive to the variations in joint roughness and joint wall compressive strength. In design applications or modelling of discontinuities in coal, the error will be small if average values of friction angle and cohesion are used. It also implies that the details of the joint surface conditions are not critical when gathering data on jointing in coal for the purpose of strength analysis. The accuracy of the field method of strength estimation was confirmed by limited laboratory testing.

2.4 Development of a discontinuity recording system for coal

The initial mapping of major discontinuities showed that a system had to be developed in which numerous discontinuities with lengths of less than 10 cm had to be accounted for on the one end of the scale and discontinuities with lengths of more than 100m at the other end. The spacing of the discontinuities could vary between 1 cm and 100 m. Ordinary scan line mapping techniques are not suited to this large variation in scale and large numbers of discontinuities. A different mapping system had to be developed.

2.4.1 Classification of coal according to discontinuities

As a first step in developing a mapping system, it was decided to classify the coal seams into categories according to the type and frequency of discontinuities. The discontinuities were classified into three types shown in table 2.5.

This definition of the types of discontinuities was used to draw up a simplified visual classification of coal seams which is illustrated in figure 2.13. The first four classes are related to the cleats in the coal and are used to describe the coal structure. Class 5 describes coal containing joints whilst class 6 describes coal with major slips. Most coal seams are combinations of the classes. For example a seam may be described as class 3-5-0 which indicates that it contains cleats with jointing but no slips. The visual classification was
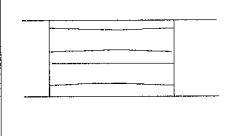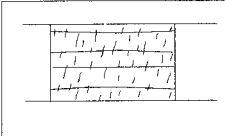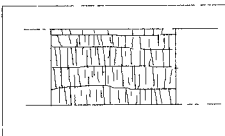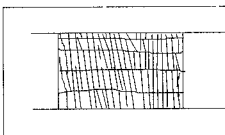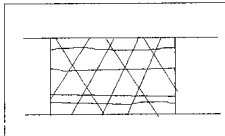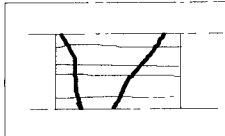
CLASSES OF DISCONTINUITIES IN COAL SEAMS

Class

	Class	Description
	1	Massive coal , no visible cleats/joints longer than 5cm. Coal may be horizontally layered.
	2	Massive coal, irregular cleats/joints, less than 30cm long, less than 10 per meter.
	3	Blocky coal, regular cleats/joints in bands, typically less than 1m long with frequency of more than 10 per meter.
	4	Highly disturbed coal, continuous cleats/joints more than 1m long with frequency of more than 10 per meter.
	5	Jointed coal, smooth planar joints, usually inclined with infilling. Joints are not limited to individual coal layers, typically longer than 1m. One or more sets may be present.
	6	Coal contains major slips with undulating surfaces, continuous over several tens of meters, may extend into roof or floor of the seam.

Figure 2.13 Description of discontinuity classes in coal seams.

Table 2.5 Types of discontinuities

Feature	Typical length	Comments
Minor joints (cleats)	5 cm to 1 m	Referred to as cleats in coal mining terminology. Minor joints are typically steeply dipping and strike in two nearly orthogonal directions
Joints	1 m to 10 m	Joints in coal seldom extend into the surrounding strata. They may be continuous over several meters and may dip at shallow angles.
Major joints (slips)	10m to > 100m	These are referred to as slips in coal mining terminology. Major joints usually extend into the roof strata resulting in unsafe conditions. They are often drawn onto mine plans and can be seen to extend over several tens of metres

found useful for discussing and comparing coal seams without carrying out formal classifications of the seams.

2.4.2 Frequency based discontinuity mapping system

Since the ultimate objective is to develop a method for estimating the effect of discontinuities on pillar strength, the data collection method was modified to suit that objective. During the initial mapping of discontinuities as much data as possible was collected which would allow the Q-system of Barton and Choubey (1977) to be applied. However, since that rating system does not account for the length of discontinuities and would not discern between the closely spaced, discontinuous cleats and the extensive slips, it was considered to be unsuitable for this application. A mapping system was developed which recognises that the lengths of the discontinuities differ by orders of magnitude and records them on different magnitude scales. The principle of the system is to conduct surveys on three different scales, firstly on a 1m scale in which the minor joints (cleats) are recorded, followed by a survey on a 10m scale in which joints are recorded (which should overlap the initial 1 m survey) and finally a survey on a 100m scale in which the major joints (slips) are recorded. The result is a full description of all the discontinuities in the coal seam. The data thus recorded may then be used in pillar strength estimation.

The following data are collected on the 1m, 10m and 100m scales:

- Frequency : number of discontinuities per metre. In the case of the 100m scale, the major discontinuity (slip) frequency per 100m is recorded.

- Length : The dip length is recorded. The strike length can seldom be assessed since most discontinuities are not visible in the roof or floor of the workings. The dip length is truncated by the height of the mine workings, which is in the order of 2m. The slips are by definition extensive relative to the pillar dimensions.

- Roughness : A simple roughness scale is used as follows:
  1 = smooth, polished
  2 = smooth slickensided
  3 = smooth coal surface
  4 = slightly rough
  5 = rough or striated
  7 = very rough or smooth, stepped
  10 = very rough and stepped

- Waviness : The waviness is taken over 1m as straight and planar, curved or wavy. If a discontinuity is less than 1m long the waviness is observed over its full length.

- Infilling : The strength of the infilling and thickness are recorded. The strength is indicated relative to coal strength as being weaker than coal, equal to coal or stronger than coal. The relative strength is determined by using the sharp end of a geological pick or a pocket knife.

- Wall strength : The discontinuity wall strength is similarly recorded by comparing it to the strength of the coal. It was indicated as being either stronger than coal, equal in strength , weaker than coal or very weak and crumbly.

- Dip : The dip angle of the discontinuity is recorded.

2.5 Results of discontinuity mapping system for coal

Mapping of discontinuities using the method described in section 2.4 was carried out at site 4 and sites 7 to 20, shown in figure 2.1. The individual site numbers and detailed results of mapping at each site are presented in Appendix 1. At each site mapping was carried out at five or six underground locations, the locations being at least one kilometre apart. A total of 88 locations were mapped. The results are summarised and discussed below.

2.5.1 Mean properties of joints at all sites

The mean and standard deviation of the properties of all the observed discontinuities are summarised in table 2.6. It can be seen that there is almost an order of magnitude difference between the frequency of each category of joint. The differences in the mean lengths simply

Table 2.6 Mean discontinuity properties at 16 mine sites

	Frequency (per m)		Dip length (m)		Dip (degrees)		Roughness index		Infill thickness (mm)	
	Mean	Stdev	Mean	Stdev	Mean	Stdev	Mean	Stdev	Mean	Stdev
Cleats	9,2	5,14	0,36	0,21	84	9,1	3,8	1,03	0,85	0,45
Joints	0,83	1,54	1,40	1,30	57	7,5	4,9	1,77	0,87	0,83
Slips	0,079	0,130	3,31	1,88	49,8	9,63	3,7	1,34	1,25	0,82

reflects the different categories of discontinuites. The dip of the structures is interesting in that the mean dip of the cleats is 84 degrees and it decreases to 57 degrees for joints and to about 50 degrees for slips. This implies that the cleats are almost always steeply dipping, and they are a manifestation of the coal structure. The other joint categories were caused by external influences and intersect the coal seam obliquely. The oblique angles of the joints and slips simplifies their identification in underground workings where visibility may be poor. The roughness and infill thickness are both fairly similar for the three discontinuity categories.

2.5.2 Variation of discontinuity properties at individual sites

The variation of jointing at each individual site was evaluated. Since there are many parameters for each category of joint, only the variation in frequency is presented. The frequency of jointing is considered to be the most important in terms of coal pillar strength. Figure 2.14 shows the mean, standard deviation and coefficient of variation of cleats at the different sites. It can be seen that there was a considerable variation in the mean value for each site. At some sites a mean frequency of as little as 2,3 cleats per meter existed and some had more than 16 cleats per meter. The coefficient of variation expresses the standard deviation as a percentage of the mean value. The relatively large values of the coefficient of variation at some of the sites indicates that coal strength can be expected to vary considerably within a single mine property.
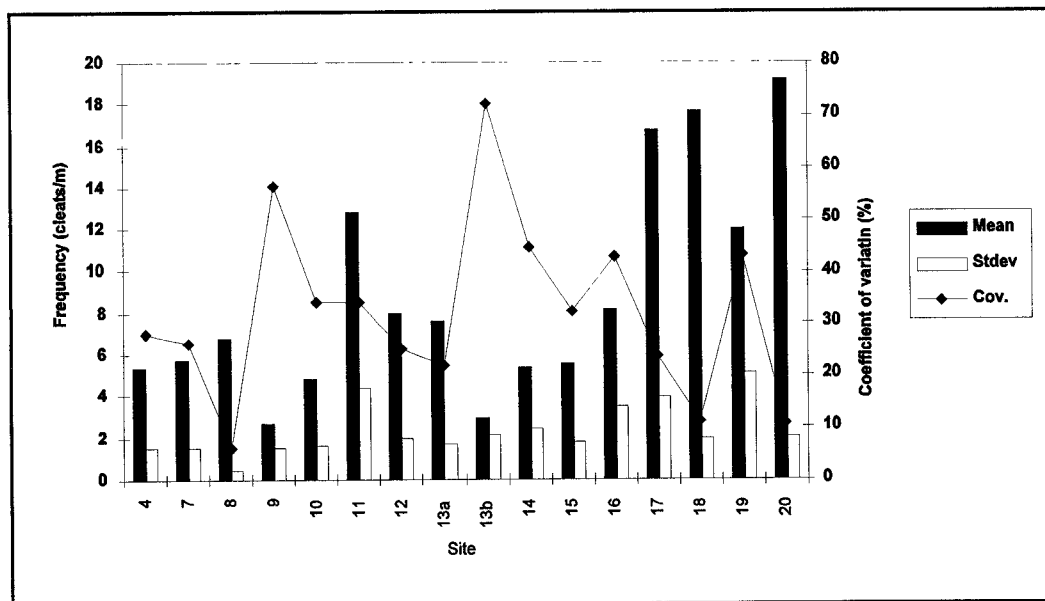
Figure 2.14 Mean, standard deviation and coefficient of variation of cleat frequency at mine sites.

The joint frequency variations at the different sites are shown in figure 2.15. This figure shows that the variation in the joint frequency is much greater than the variation in the frequency of the cleats. At a number of sites, no joints were found.
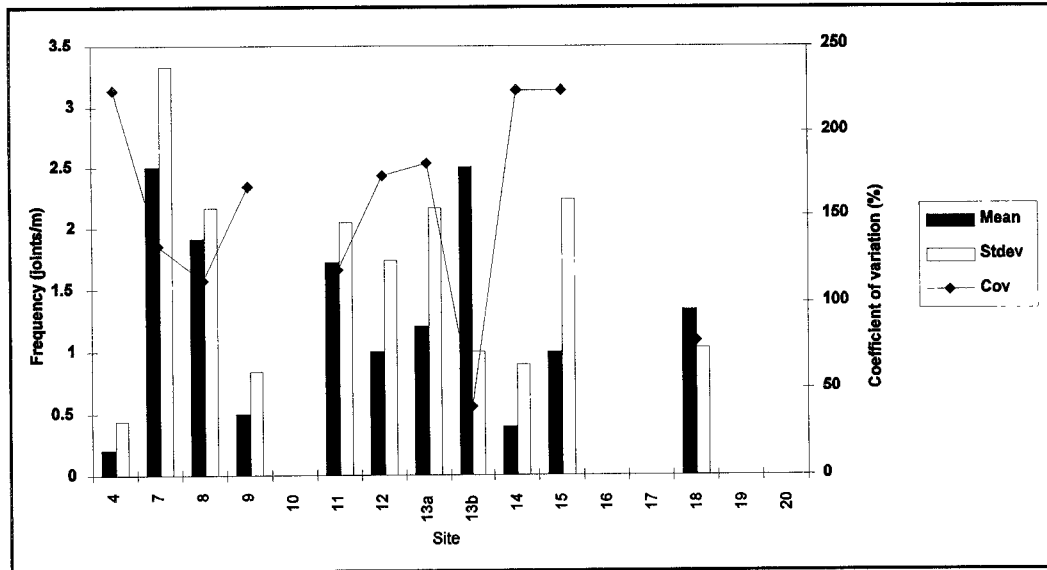
Figure 2.15 Mean, standard deviation and coefficient of variation of joint frequency at mine sites.

At some sites the coefficient of variation is in excess of 100%. The mean joint frequency of all the sites was found to be 0,83 per metre. If one studies the histogram of the joint frequencies, shown in figure 2.16, it can be seen that 59 of 88 locations, that is 67%, had no jointing. Excluding the sites with no jointing, the mean joint frequency is 1,3 joints per meter. It can therefore be said that 67% of the locations were joint free, the remainder of the locations had a mean joint frequency of 1,3 joints per meter. The presence of jointing and the large variation of jointing at the different sites can therefore be expected to result in variations in the coal pillar strength.
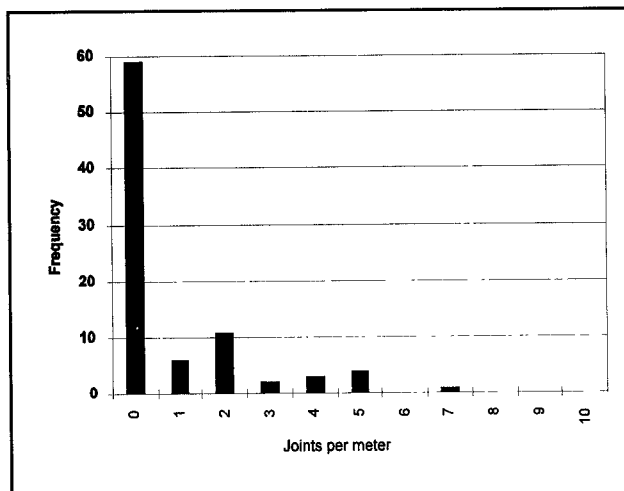
Figure 2.16 Distribution of joints per metre at 86 mapping locations

The frequency of slips per 100 metres is shown in figure 2.17 which shows that slip frequency is not as variable as the joint frequency. Slips were observed at all the sites visited, but not at each location. When compared to typical pillar dimensions, the spacing of slips is often larger than the pillar spacing. In these cases the slips are expected to play a minor role in pillar stability. However at three of the sites the slip frequency exceeded 0,1 indicating spacings of less than 10m. At these sites each pillar would be expected to contain one or more slips.
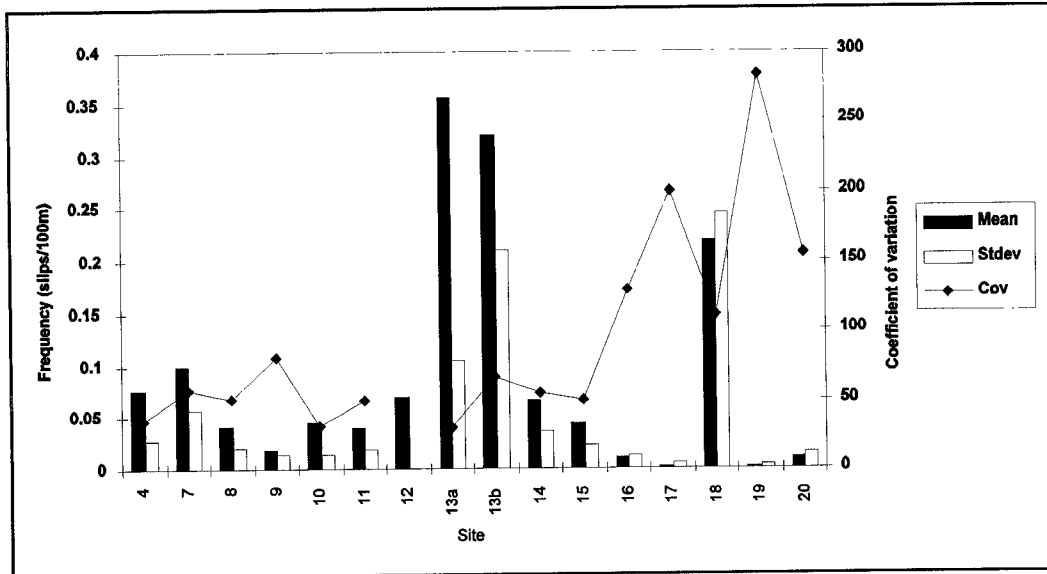
Figure 2.17 Mean, standard deviation and coefficient of variation of slip frequency at mine sites

2.5.3 Correlation between frequencies of different joint categories

The correlation between the different categories of joints was investigated, since it is important to know whether coal containing large numbers of cleats would also contain many joints or slips. The correlation between the different categories are shown in figures
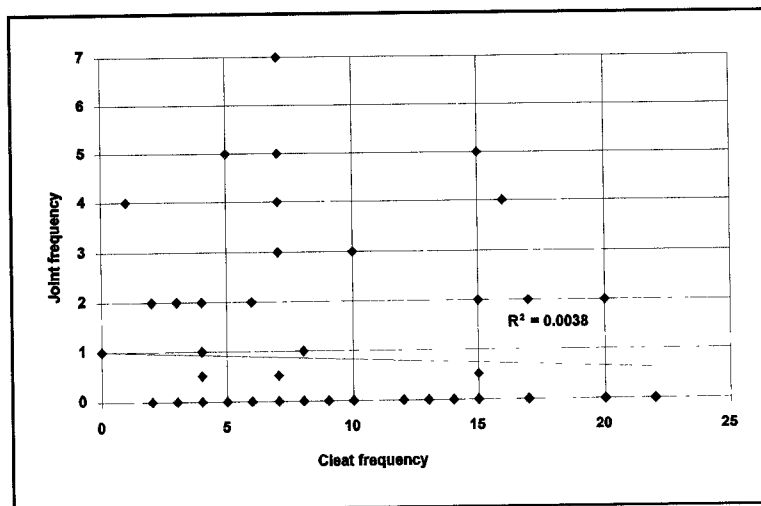
Figure 2.18 Correlation between frequency of cleats and joints.

2.18 to 2.20. The results show that very poor correlation exists between cleats and the other two categories of joints. There is a slight positive correlation between joints and slips, shown in figure 2.20. For the purpose of pillar design, it is concluded that each category of jointing should be considered to be an independent variable.
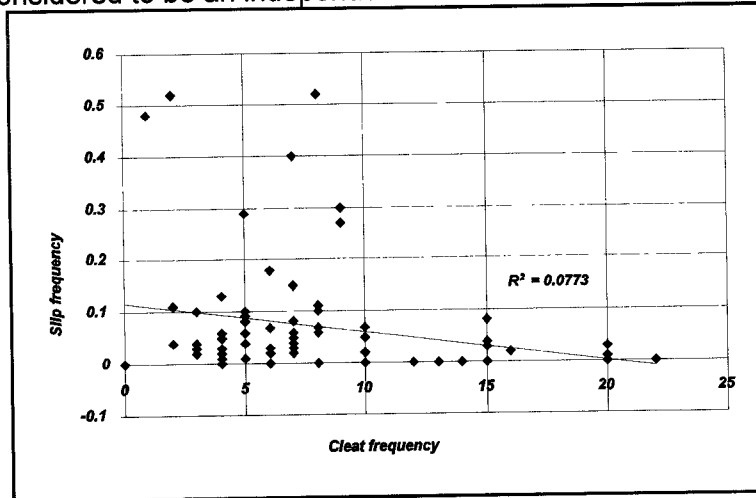
Figure 2.19 Correlation between frequency of slips and cleats.
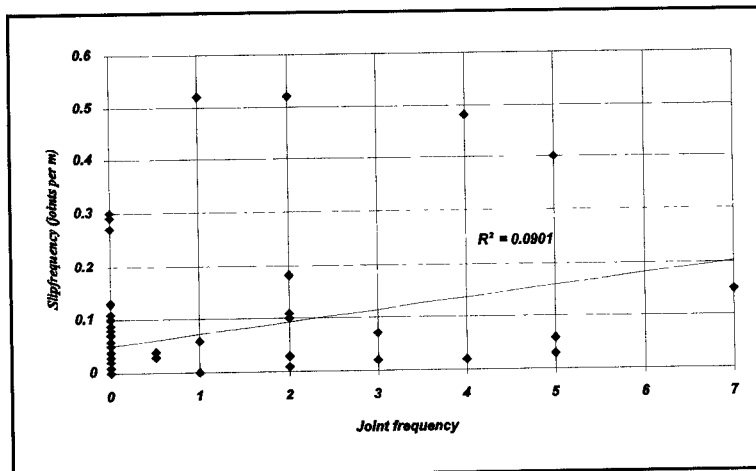
Figure 2.20 Correlation between frequency of joints and slips

2.6 Discussion

South African coal seams were deposited in pre-Karoo valleys and are shallow dipping. Dips in excess of 10 degrees are only found near the edges of the depositional basins. Most coal seams are intersected by dolerite intrusions. Major faulting is rare. Extraction of coal takes place in undisturbed blocks of coal between major structures. Mined areas may be continuous for several kilometres without major faulting. The major structures do not play an important role in the stability of pillars, since the coal in the vicinity is usually left in an unmined state. Pillars are formed in the undisturbed portion of the coal deposits where smaller scale geological discontinuities are present which will not interfere with mining

operations. The discontinuities in coal seams where coal is being extracted have been classified as cleats, joints and slips.

Cleats are defined as minor discontinuities between 5 cm and 1m in length. Cleats exist in coal down to microscopic scale and form part of the coal structure. For the purpose of this report, only those cleat structures longer than 5 cm were considered. Cleats were found to be steeply dipping, are typically 10 cm to 30 cm long and their frequency is typically 9 per metre.

Joints are defined as discontinuities which are more than 1m in length but typically less than 10m. Joints are seldom visible in the surrounding strata, they are almost always confined to the coal seam. It was found that jointing was absent in 67% of the locations visited. Joints are not as steeply dipping a cleats, the average dip of joints was found to be 67 degrees. At locations where joints were observed, the mean frequency was 1,3 per metre.

Slips are defined as discontinuities which are more than 10m long on strike. Slips are often visible in the surrounding strata and may be continuous for more than 100m along strike. The average dip of observed slips was 50 degrees and the average frequency was 0,08 per metre which is an average spacing of 12,5 metres. Slips were absent at 22 of the 88 locations mapped, but were found at all the mine sites visited. Since the spacing of slips is often greater than the pillar spacing, the effect on pillar strength is expected to be minor.

The variability of the different types of discontinuities at the mine sites showed that average values would not be representative for a particular mine site. The cleat frequency has the lowest variability between locations at the mine sites. The joint and slips frequency was highly variable, the coefficient of variation was often more than 100% at individual mine sites.

A study of the correlation between the presence of joints, slips and cleats at the 88 locations showed that these classes of discontinuity are independent of one another. Weak negative correlation was found between cleats and joints and between cleats and slips. There was a weak positive correlation between joints and slips. For the purpose of pillar strength estimation, each of these types of discontinuity should be considered independently.

3 The effect of discontinuities on the strength of coal samples

3.1 Introduction

The results of the study of jointing in coal seams, reported in Section 2, showed that large variations exist in the intensity of discontinuities in South African coal seams. The implication is that the strength of the coal in the seams will vary to a similar extent. A pillar design method which accounts for this variability should result in increased extraction of coal reserves where the coal is relatively unjointed and improved safety where the coal is weak owing to jointing. The contribution of jointing to variability in the strength of small scale and large scale coal samples is evaluated in this chapter. The emphasis is on predicting the strength variations of the coal mass and not of coal pillars. When pillars are considered, the effect of width to height ratio should be included. All discussions of strength in this chapter are based on results of cube or cylinder specimens with width to height ratios of 1,0. Section 4 considers the effect of the width to height ratio of pillars of coal.

3.1.1 Discontinuities and rock mass strength

The effect of discontinuities on the strength of a rock or coal mass will depend on the scale at which it is tested. At the laboratory scale, samples may contain microscopic weakness planes (cleats in coal) but, as the sample size increases, it becomes more representative of the large scale rock mass by including a greater number of weaknesses. With increasing sample size, the heterogeneity of samples decreases, the intensity of discontinuities per sample becomes constant and the scatter of test results decreases. A volume can be reached beyond which the property being tested will become independent of the specimen size. That volume is referred to as the Representative Elementary Volume (REV), (Cunha, 1990). The strengths of most rock materials exhibit scale dependent effects (Cunha, 1990). However, some authors report no influence of specimen size (Hodgson & Cook, 1970) or state that the reduction in strength of coal with sample size cannot be applied universally, (Peng, 1993). The causes of size effects may be related to the testing method, stress gradients, changes in the mode of failure, statistical effects and testing machine effects (Bernaix, 1974).

Hoek and Brown (1980) give the following empirical relationship between the uniaxial compressive strength σ_c of intact rock specimens and the specimen diameter d :

$$\sigma_c = \sigma_{c50} \left(\frac{50}{d} \right)^{0,18} \tag{3.1}$$

where σ_{c50} is the uniaxial compressive strength of a 50 mm diameter specimen. The dimensionless form of the equation eliminates differences due to variations in shape, loading rates, moisture content since these are usually the same for a given set of data. Although the d values range from 10 to 200 mm the above equation has been used successfully to predict the strength of massive quartzites of 2 - 3 m in span, (Wagner, 1987). The equation is only valid for intact rock specimens. When specimens exceed 1m in diameter it becomes difficult to find rock samples which do not contain any through going planes of weakness. The large scale rock mass invariably contains weakness planes which should be included in the estimation of its strength.

3.1.2 Rock mass strength estimation

As the scale increases the practical difficulties of testing large rock samples become excessive. Methods have been developed which allow the large scale strength of a rock mass to be estimated from the discontinuity and intact rock properties, (Hoek & Brown, 1980, Hoek 1996, Palmstrom, 1996 and Ramamurthy & Arora, 1994). Rock classification results are often used

as a basis for providing the input parameters for rock mass strength estimation. The technique has been widely used in rock engineering to estimate rock mass strength around surface excavations and underground excavations. The rock mass strength estimation method of Hoek & Brown (1980) has been used to provide input data to calculate the strength of coal pillars (Barron & Pen, 1992).

In this section, the scale effect of coal strength will be discussed and results of detailed logging of fractures in laboratory scale samples will be presented. The effect of discontinuities on the large scale strength of coal and the potential variation in coal mass strength will be evaluated using rock classification techniques.

3.2   Scale effects of coal strength

With coal, there is overwhelming data to show that the strength this size dependent. Numerous results are available of large scale tests on coal specimens which were compiled by Singh (1980, quoted in Herget 1988) showing clear scale dependence. In South Africa large scale tests were reported by Bieniawski (1968), Bieniawski and van Heerden (1975) and Wagner(1974). These test results indicate strong scale dependence of the strength of coal. Bieniawski reported that when the specimen size exceeded about 1,5m there was no further reduction in the strength of the coal. This may be the REV for coal.

3.2.1 Comparison of scale effects in coal to other rock materials

Data published by Singh (1980, quoted in Herget, 1988) showed that the strength of coal could be approximated as follows:

$$\sigma_c = 303d^{-0,59} \qquad\qquad (3.2)$$

where d is the cube size in mm, (note that Singh's original equation was written for inch - psi units). The equation predicts the strength of a 1 m cube of coal to be 5,16 MPa and a 50 mm cube to be 30,2 MPa. Equation 3.2 for coal may be rewritten in a similar format as equation 3.1:

$$\sigma_c = \sigma_{c50}\left(\frac{50}{d}\right)^{0,59} \qquad\qquad (3.3)$$

The equations 3.1 and 3.3 are plotted in figure 3.1, normalised by σ_{c50}. It can be seen that the strength of coal reduces more rapidly than for other rock types. This phenomenon was discussed by Barron & Yang (1992), who suggested that coal should be tested at cube sample sizes of 13mm to capture the intact strength. However, Trueman & Medhurst (1994) pointed out that minor cleats are concentrated in the brighter coal bands, containing vitrian, and the cleat intensity is expected to vary with coal rank and maceral composition.
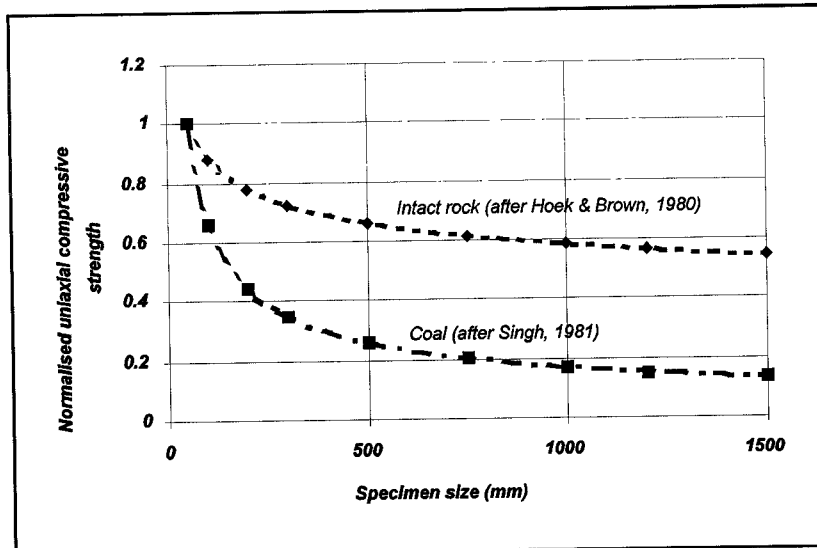
Figure 3.1 Size effect of intact rock and coal

3.2.2 Discussion

The strength equation of Hoek and Brown uses the intact strength of rock samples as a basis for predicting the rock mass strength. Coal cannot be said to be intact, even on the laboratory sample scale. Large samples of coal, contain many imperfections, (cleats) which have an effect on the strength. This explains the rapid decrease in strength of coal with increasing sample size.

3.3 The effect of cleats on laboratory sample strength

Since small laboratory samples may be considered to be models of full scale pillars, the following investigation was carried out to establish the relationship between the intensity of small scale discontinuities and the strength of the samples. It was envisaged that large scale pillars would be affected by discontinuities in a similar manner to the small scale samples.

A programme of laboratory tests on coal samples with different diameters was carried out by Ozbay (1994) on coal samples from the No 2 seam at site 9, shown in Section 2, figure 2.1 The samples were tested using an MTS hydraulic servo controlled stiff testing machine . The tests were displacement controlled and both the load and deformation were recorded during testing. The visible fractures in the samples were mapped by the author and analysed in terms of the strength results.

3.3.1 Method of mapping fractures in laboratory samples and determining fracture length

The laboratory samples were inspected and all visible fractures were traced by placing transparent plastic film over the samples. The result was a fracture map of the top, bottom and sides of each sample. An example of a resulting fracture map is shown in figure 3.2. Once the fracture maps were available, the length of fractures were determined by scanning the fracture maps as black and white computer bitmap images. A computer program was written which counted black pixels and converted these into an equivalent length of line. The program was calibrated by scanning diagrams of known line lengths. Accuracy of better than 90% was obtained.
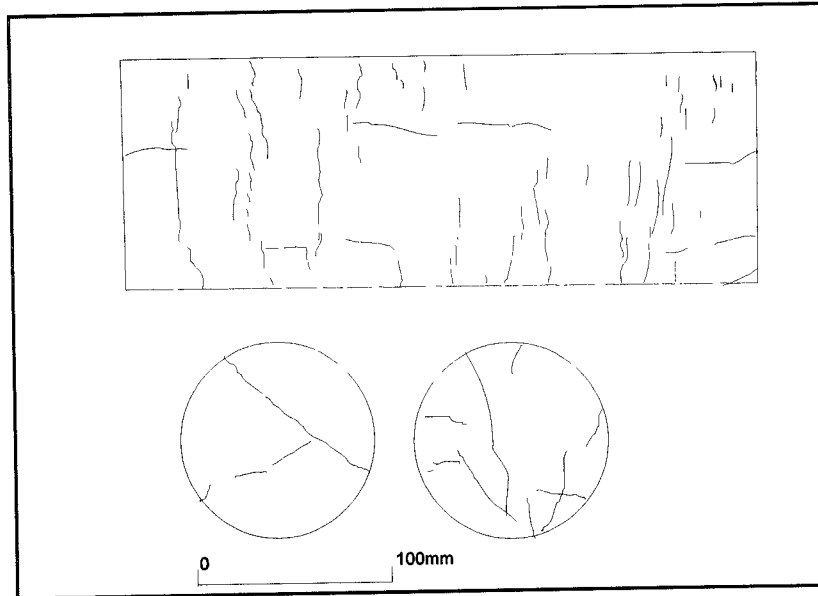
Figure 3.2 Fracture map of a 100mm diameter coal sample with a width to height ratio of 1,0.

3.3.2 Determination of fracture index

The intensity of fracturing in each sample was expressed using a dimensionless index as follows:

$$I = \frac{\Sigma l}{l_e}$$

(3.4)

where Σl is the sum of lengths of all fractures and l_e is the equivalent dimension of the sample. The equivalent dimension was defined as the volume of the sample divided by the area. This corrects for the change in volume to area ratio of larger samples and corrects for changes in the aspect ratio of samples. If the samples all have the same aspect ratio, the equivalent dimension is directly related to the diameter of the sample.

The fracture index provides a dimensionless number which indicates the severity of fracturing in a sample. For example, the sample shown in figure 3.2 had an index of 92,9. Details of all the index calculations are presented in Appendix 2.

Smaller samples tend to be less fractured. If the smaller samples are drawn to a scale such that they appeared to be the same size as the larger samples, they would have the same index if the amount of fracturing appeared to be the same when drawn to the same dimensions. This is illustrated in figure 3.3, where the amount of fracturing and the fracture index for a 25 mm sample and a 100 mm sample are shown, drawn to the same dimensions. The reason for the difference in the fracture index is clearly visible.
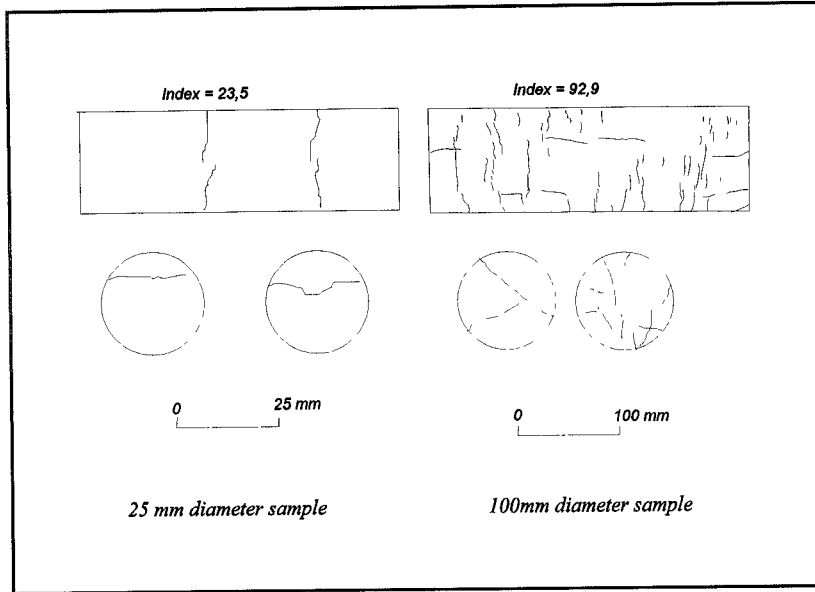
Figure 3.3 Fracture mapping and fracture index for 25 mm and 100 mm samples shown at different scales.

The general trend is for the fracture index to be related to the sample size since larger samples contain more fractures. As the sample size increases, however, the fracture index tends to a constant value, as the samples become more representative of the degree of fracturing. This is shown in figure 3.4, where it can be seen that the fracture index - size relationship may be represented by a logarithmic equation.
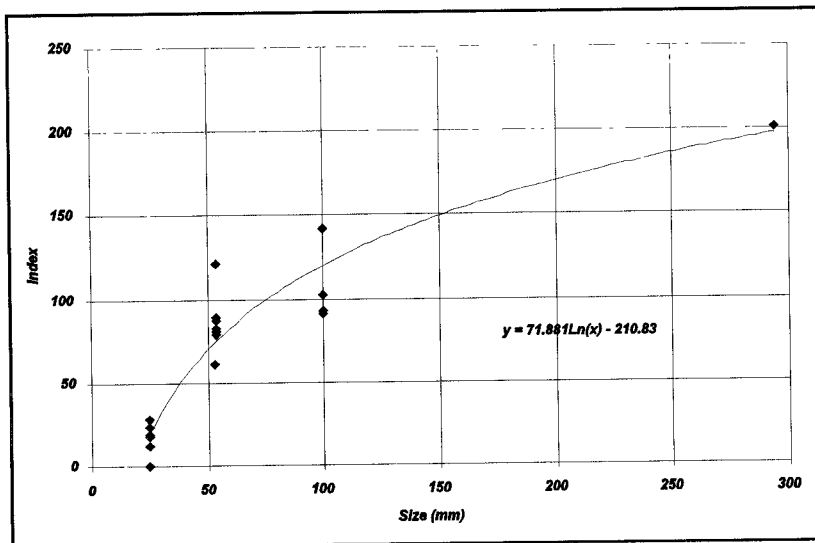
Figure 3.4 Fracture index - sample size relationship
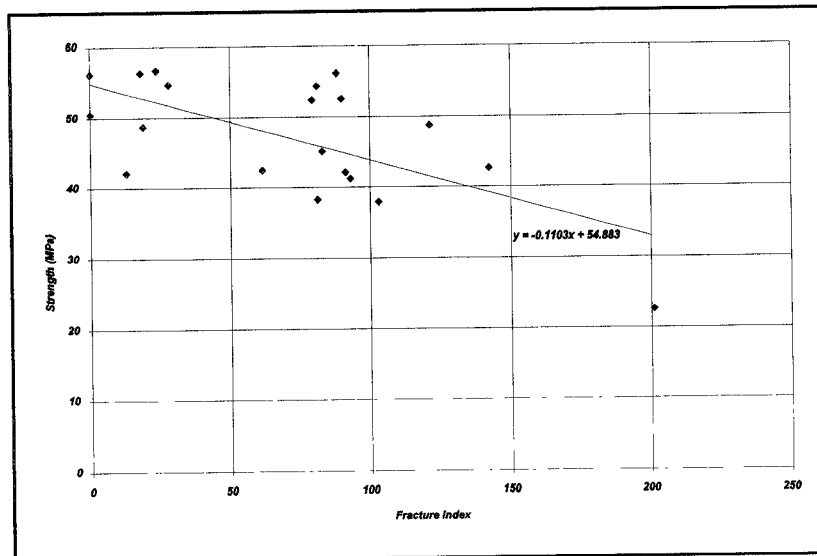
Figure 3.5 Strength - fracture index relationship for samples with a width to height ratio of 1,0

3.3.3 Fracture index and strength results

The results for samples with a width to height ratio of 1,0 were used to determine the relationship between the fracture index and the sample strength. Detailed results are presented in Appendix 2. Figure 3.5 illustrates the relationship between fracture index and sample strength. This figure shows a considerable amount of scatter, but a linear relationship is the best fit to the data. This implies that the strength is directly related to the fracture index, or stated differently, the size effect is a fracture intensity effect. The size effect is compared to the fracture index effect below.

3.3.4 Size effect compared to fracture index

The strength of samples against their size (expressed as the diameter of the sample) is shown in figure 3.6. A negative exponential curve has been fitted through the data. The shape of the curve may not be the best fit for these particular data points, but additional tests, not reported here (Ozbay, 1994), indicated that the strength decreases exponentially with the specimen diameter. By comparing figure 3.6 to figure 3.4, it can be seen that the strength - size relationship is essentially the inverse of the fracture index - size relationship. If the fracture index-size relationship is extrapolated to 1,5 m, using the equation shown in figure 3.4, the predicted fracture index is 315. Using this index in the fracture index- strength relationship, the predicted strength for a 1,5 m sample is 20,13 MPa. If the strength - size relationship is extrapolated to 1,5 m sample size, the predicted strength is 19,6 MPa. The results are summarised in table 3.1.
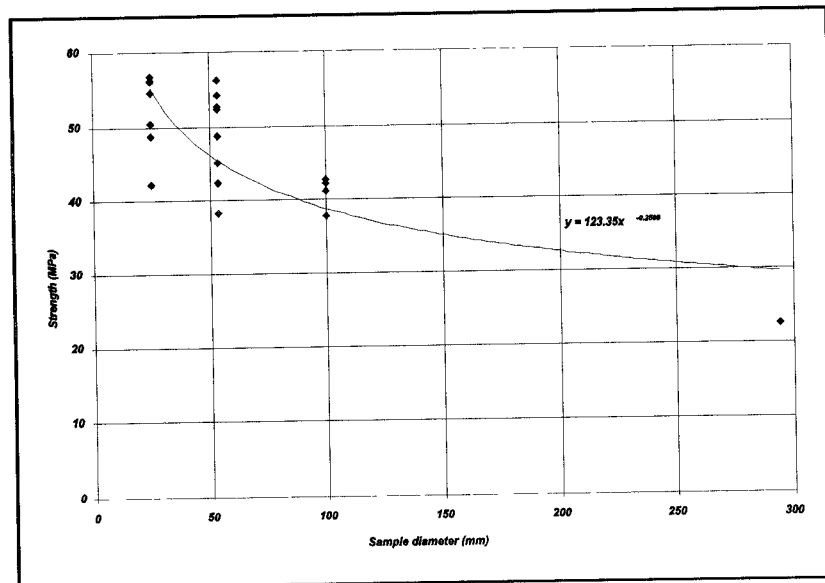
Figure 3.6 Strength - size relationship for samples with a width to height ratio of 1,0.

The results for sample sizes of 25 mm up to 2,0 m, using the size and fracture index approaches are shown in figure 3.7. Here it can be seen that similar results are obtained using the two methods. The difference in strength predicted by the two methods is less than 12% for all sizes considered.

Table 3.1 Results of predicting 1,5 m sample strength using two methods

Method	Equation	Predicted Strength of 1,5m sample
Strength - size(d) relationship	$S = 123.3d^{-0.2509}$	19,69 MPa
Strength - fracture index (i) relationship	$S = -0.1103i + 54.883$	20,13 MPa

The strength of large scale samples predicted above may seem high compared to the results of other workers, but the coal tested in this particular case originated from a mine which is thought to have the strongest coal in South Africa.

3.3.5 Discussion of small scale test results

The above results show that the intensity of fractures appears to be the main cause of the scale effect in sample size strength. If the fracture intensity is expressed in a dimensionless form,

using the fracture index, the larger samples have a higher intensity of fractures and hence a lower strength. The fracture index may be used to predict the strength of coal samples, resulting in similar strength values as obtained by the strength - size relationship. One of the limitations of the above approach is that all samples were prepared by drilling perpendicular to the layering, which resulted that the cleats were aligned parallel to the axial loading. The effect of the cleats on the strength would therefore be minimal since shear stresses were not induced along them. This is however the loading direction in underground workings, and the achieved strength is therefore applicable for designing underground workings.
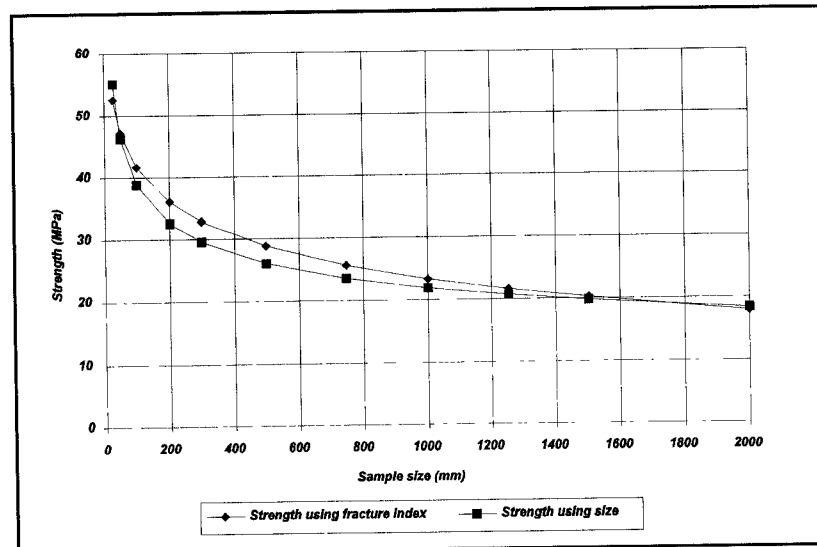
Figure 3.7 Comparison of strength predicted by strength-size relationship and by fracture index - size relationship

Laboratory samples may be considered to be models of full scale pillars. When considering the strength of full scale pillars, large scale discontinuities are likely to have a similar effect on their strength as small scale discontinuities have on laboratory samples.

3.4 Large scale strength of coal using empirical estimation

Empirical methods of estimating the strength of large scale rock masses have been developed from rock classification techniques, (Hoek & Brown, 1980; Hoek et al., 1995; Bieniawski, 1976). In this section one of the classification methods is used together with a failure criterion to establish whether these methods are able to realistically predict the large scale strength of coal.

3.4.1 Application of the Hoek-Brown failure criterion

The Hoek-Brown criterion may be used to estimate the strength of intact rock or rock masses which contain two or more sets of discontinuities (Hoek et al., 1995). In the case of coal the horizontal layering may be considered to be one set of discontinuities and jointing will be additional sets. For the application of the Hoek-Brown criterion, it is necessary to first use the Rock Mass Rating (RMR) classification method of Bieniawski (1976) to obtain the classification of the coal. In the application of the RMR, the cleat structures were not counted as joints, it was assumed that they were part of the "intact" rock . The RMR was therefore based only on the

occurrence of the joints and slips in the coal seams, that is structures which had trace lengths in excess of 1m.

The RMR was determined for all the locations at all the sites visited. The joint spacing was determined by considering both the slip frequency and the joint frequency. The average joint spacing was determined as:

$$S = \frac{1}{F_s + F_j}$$

(3.5)

where F_s and F_j are the frequencies of the slips and joints respectively.

Since the Rock Quality Designation (RQD) was not available for the sites under consideration, the method of Priest and Hudson (1976) was used to estimate the RQD from the joint spacings. This method relates the mean discontinuity spacing to RQD and to the combined rating for RQD and joint spacing in the RMR tables. The relationship is shown in figure 3.8. With regard to the joint condition, all the discontinuities were classed as being slightly rough. The thickness of the fill material in the discontinuities determined whether a rating of 20 was assigned (Slightly rough, separation < 1mm) or a rating of 10 was assigned (Gouge < 5 mm). The discontinuity properties and the assigned ratings are presented as Appendix 3.
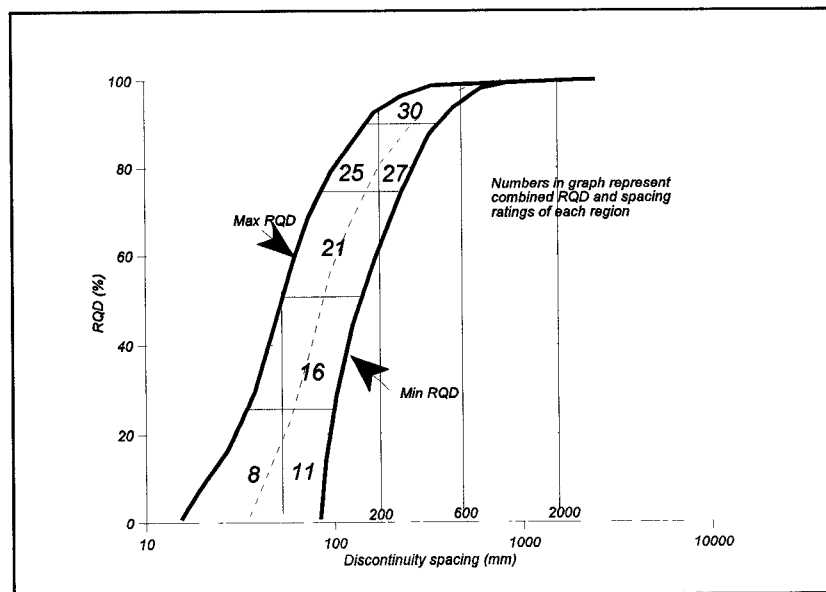
Figure 3.8 Correlation between RQD and discontinuity spacing for the RMR system, after Priest & Hudson, (1976).
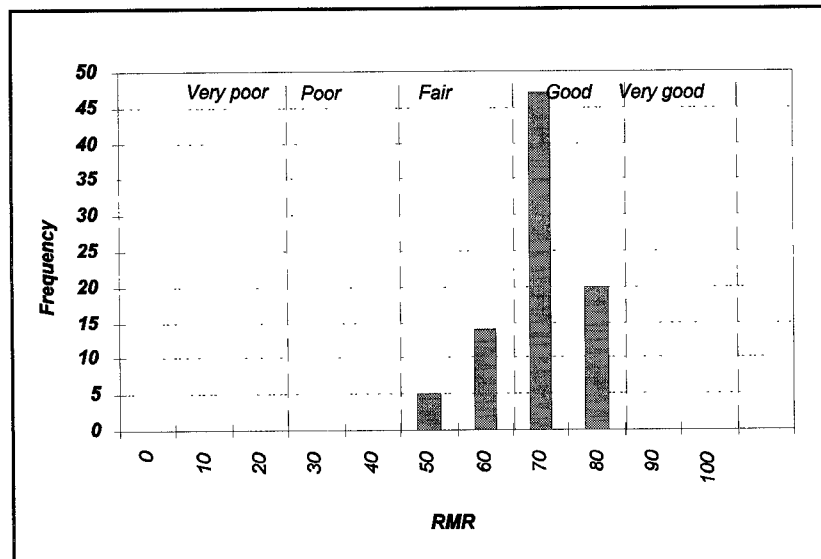
Figure 3.9 Distribution of RMR values in coal seams

In all the cases it was assumed that the workings were dry, and no adjustments were made for the orientation of the excavations, in accordance with the suggestions of Hoek et al (1995).

The resulting distribution of RMR values is shown in figure 3.9. All the values fell within the range of 50 to 79 points on the RMR scale. The mean value was 67,9 with a standard deviation of 8,24. These values were used to calculate the associated rock mass strength of the coal using the point estimate method (Harr, 1985) and the Hoek-Brown criterion (Hoek & Brown, 1988).

The Hoek-Brown criterion in its most general form can be expressed as follows:

$$\sigma_1 = \sigma_3 + \sigma_c \left(m_b \frac{\sigma_3}{\sigma_c} + s \right)^a \qquad (3.6)$$

where:
- m_b is a constant value for the rock mass which may be estimated from rock mass classification and triaxial tests on rock samples;
- s and a are constants which depend on the characteristics of the rock mass, these constants may be estimated using rock classification techniques;
- σ_c is the uniaxial compressive strength of the intact rock pieces determined by standard laboratory tests;
- σ_1 and σ_3 are the axial and confining effective principal stresses.

The criterion has been found to work well for most rock types which consist of tightly interlocking angular pieces of rock. The strength of such rock masses can be defined by setting $a = 0,5$ in equation 3.6. For poor quality rock masses where the interlocking has been destroyed by weathering or shearing (disturbed rock mass), the rock mass has no tensile strength or cohesion and will fall apart in the absence of confinement. In such a case the value of s in equation 3.6 is set to zero.

The values of a, m_b, and s may be estimated using Bieniawski's (1976) Rock Mass Rating (RMR). Hoek et. al (1995) suggest a new parameter, the Geological Strength Index (GSI) be used, which ranges from 100 for intact rock to 10 for extremely poor rock masses. The GSI is determined from the Bieniawski (1976) RMR values and from Barton, Lien and Lunde's Q-system (1974). Note that although the classification method of Bieniawski changed over the years, the 1976 version is used in the determination of the GSI. The GSI was proposed to prevent the stress field, excavation orientation and ground water factors from being accounted for twice in an analysis.

The GSI is determined as follows: Bieniawski's 1976 Rock Mass Rating is determined assuming the rock mass is completely dry, setting the Groundwater rating = 10. No adjustment is made for the joint orientation. The RMR value obtained, called RMR_{76} can be used to estimate the value for GSI as follows:

If $RMR_{76} > 18$: $GSI = RMR_{76}$

If $RMR_{76} < 18$ Barton, Lien and Lunde's Q-system of classification should be used instead. In the case of the coal seams mapped, the value of the RMR_{76} is always above 18 and only the RMR needs to be determined.

Once the GSI value has been estimated, the parameters required for the Hoek-Brown criterion can be calculated as follows:

For GSI > 25 (Undisturbed rock masses)

$$\frac{m_b}{m_i} = \exp\left(\frac{GSI - 100}{28}\right)$$

$$s = \exp\left(\frac{GSI-100}{9}\right) \tag{3.7}$$

$$a = 0{,}5$$

where m_i is the value of the m-parameter for intact rock samples obtained by triaxial laboratory tests. Representative values of m_i have been published by Hoek et al (1995). According to this table a typical value of m_i for coal is 8,0, which was used in the further calculations of the strength of the coal mass.

The resulting parameters for the strength of coal were determined to be as follows, based on the variation of the RMR_{76} values and the assumed m_i value of 8,0:

m = 0,3275 with standard deviation of 0,2371
s = 0,0409 with standard deviation of 0,0296

Using the Hoek-Brown equation, the uniaxial compressive strength (σ_m) of the coal mass is given by:

$$\sigma_m = \sigma_c \sqrt{s} \tag{3.8}$$

The uniaxial compressive strength of intact coal specimens is difficult to obtain since coal usually contains cleats or other discontinuities at the scale required for ucs tests. Test results published by Ozbay (1994) showed average uniaxial compressive strength values of 29,4 MPa and 31,0

MPa for coal from the Delmas and Sigma collieries respectively. Numerous tests have been conducted on cubes of coal or cylindrical samples with width to height ratios of 1,0. Test results reported by Akermann and Canbulat (1994) on samples from nine different coal mines in South Africa showed that the average strength of laboratory samples with a width to height ratio of 1,0 could be expressed as:

$$k = 196,5 \ D^{-0,402} \qquad\qquad (3.9)$$

which results in a average strength of 39,53 MPa for samples with a diameter of 54mm. Since standard ucs tests are carried out on samples with width to height ratios of 0,33 to 0,4 the above average strength should be reduced to account for the change in width to height ratio from 1,0. A 25% reduction was used (Ryder & Ozbay, 1990), reducing the uniaxial compressive strength to a value of 30 MPa.

Testing of small scale samples of coal results in a wide scatter of results. The standard deviation of strength of 54 mm samples tested by Ozbay (1994) was 19,1% of the mean strength. Results published by Bieniawski (1968) of tests carried out at Witbank colliery showed a standard deviation of 22% of the mean value for 50mm samples. For South African coal a standard deviation of 20% of the mean strength was used in the calculation of the coal mass strength. Using the point estimate method and equation 3.8 the average strength of the coal mass becomes:

$$\sigma_m = 30\sqrt{0,0409} = 5,58 \quad (MPa) \qquad\qquad (3.10)$$

and the standard deviation is calculated to be 2,68 MPa (48% coefficient of variation).

Since most pillar strength equations are based on the strength of a coal sample with a width to height ratio of 1,0, the above strength may be increased by 25% to 6,97 MPa to account for the strength increase as the width to height ratio is reduced. Assuming the coefficient of variation remains unchanged at 48%, the standard deviation of the strength would be 3,35 MPa. The resulting strength value of 6,97 MPa lies between the value of 5,5 MPa determined by Madden and 7,17 MPa determined by Salamon & Munro (1967) for the large scale strength of South African coal seams. The technique used above was based on an uniaxial compressive strength of intact coal of 30 MPa. However the intact strength may vary from site to site.

It may be concluded that empirical rock mass strength estimation techniques can be used to estimate the large scale strength of coal measures.

3.5 Pillar condition and discontinuities

The condition of pillars in underground workings may be used as an indicator of their strength. Pillars which are weakened by the presence of discontinuities should show signs of distress sooner than stronger pillars. Observations of the condition of pillars and the intensity of jointing may therefore be used to establish whether joints have a detrimental effect on pillar strength.

A pillar condition rating method was used to assess the condition of pillars in underground workings and was correlated to the intensity of discontinuities in the pillars. The pillar condition rating system is largely based on visual inspection of the perimeter of a pillar. In-situ tests by Wagner (1974) showed that spalling of pillar corners commenced at average stress levels which are well below the peak strength of pillars and that failure of the unconfined sidewall was

independent of the pillar width to height ratio. Therefore the skin of a pillar and particularly the corners are a good indication of the strength to stress ratio of the pillars. This approach has been used by Madden (1995) and Vervoordt & Jack (1992) to estimate the relative strength of coal seams and to deduce the stress distribution in pillars during pillar extraction respectively.

The rating system (Ozan, 1993) used to assess the pillar conditions was developed from the system initially proposed by Madden(1985). The rating system is carried out in two stages. The first stage is a visual rating of condition of a pillar and surrounding strata. The second stage considers the relative importance of each rating parameter. The overall rating of a pillar consists of a rating of the pillar, the roof, support and structural discontinuities. For the purpose of this report only the pillar ratings and the structural discontinuity ratings are considered.

The rating of the performance of coal pillars consists of visual observation of the following:
- fracturing of pillar sidewalls
- scaling of pillar sidewalls
- scaling of pillar corners
- contact of pillar and roof strata
- weaknesses in the pillar.

Perfect conditions in each class are marked with 100 points. The points are reduced as the amount of fracturing and scaling increases. For example, if the scaling of pillar corners exceeds 1,5 m the rating reduces to zero. The total rating is obtained by summing the individual ratings. The maximum total rating is therefore 500 points for a pillar in perfect condition.

The structural discontinuity rating which was part of the pillar rating system simply rated the effects of major structural discontinuities on the condition of the pillar. The rating was 100 for no effect to 0 for serious effects such a pillar corner failure along a discontinuity. Details are listed in Appendix 4. Pillar ratings were carried out at nine of the sites visited. A table listing the sites, their pillar condition ratings, calculated factor of safety, structural discontinuity ratings and discontinuity frequency per meter is presented in Appendix 4. The ratings were first corrected
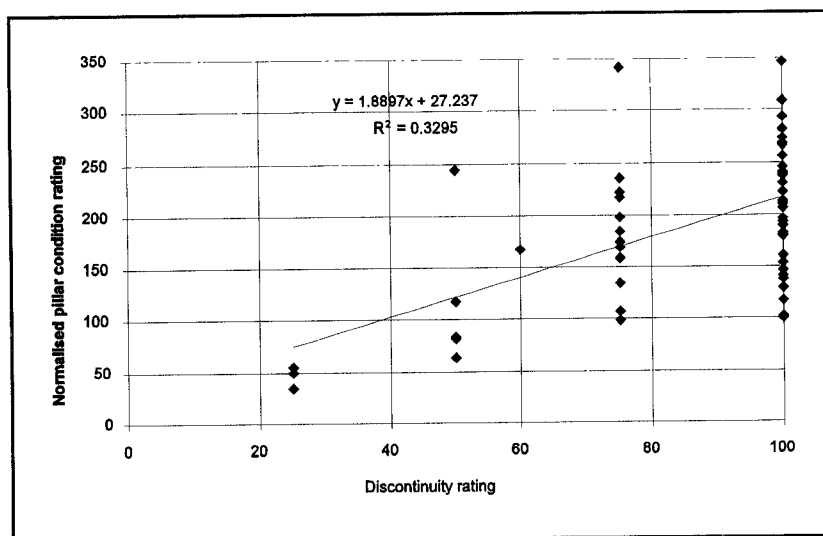
Figure 3.10 Relationship between normalised pillar condition rating and discontinuity rating

for the stress level in the pillar by normalising the rating by the calculated factor of safety, using the Salamon equation. Figure 3.10 shows that as the discontinuity rating increases (improves)

the condition of the pillars also improve. This confirms that discontinuities have an effect on the condition, and hence the strength of pillars in underground workings.

Since the detailed discontinuity mapping data were available for each of the above sites, the discontinuity frequency was plotted against the normalised pillar condition rating shown in figure 3.11. The discontinuity frequency was calculated at each location as the sum of the cleat, joint and slip frequencies. The graph shows that as the frequency of discontinuities increases, the normalised condition decreases. This confirms the trend indicated in figure 3.10 that discontinuities have a detrimental effect on pillar strength in underground workings. The scatter of results shown in figures 3.10 and 3.11 may be attributed to other factors not included in the normalisation process, for example, the intact coal strength, the age of the pillars, mining method and the properties of the contact surfaces with the roof and floor.
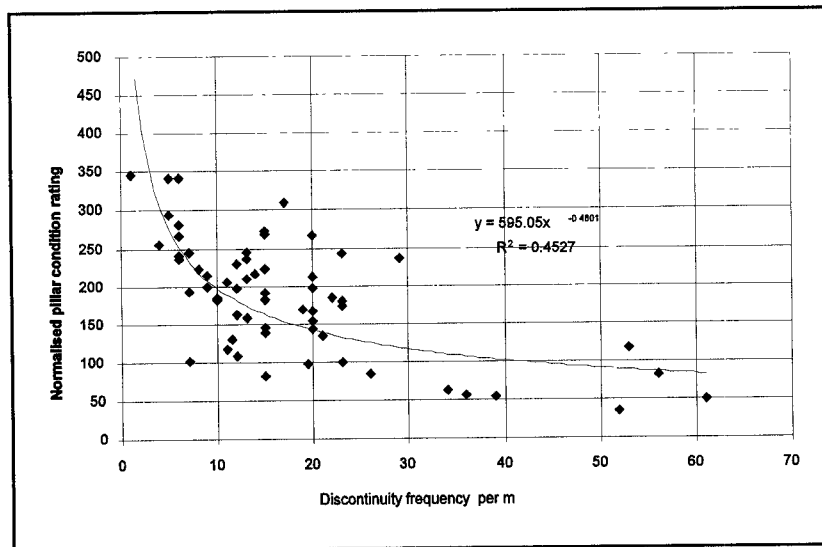
Figure 3.11 Relationship between normalised pillar condition rating and discontinuity frequency

3.6 Discussion

A study of the effect of discontinuities on coal strength has confirmed that discontinuities have a weakening effect on coal. It was first shown that the strength of cleated coal material reduces much more rapidly with size than the strength of other intact rock types. The reason for the rapid decline of coal strength was attributed to the presence of the macroscopic cleats in the coal samples. The cleats in coal were found to be largely responsible for the decrease in coal samples strength up to a size of 300mm tested in the laboratory. By expressing the cleat intensity as a dimensionless number, the strength reduction could be predicted independently of the volume of the sample. Similarly, the strength of a large scale coal pillar is expected to decrease as the intensity of large scale discontinuities in the coal increases.

Empirical rock mass strength prediction methods were used to estimate the effect of large scale discontinuities on the strength of the coal mass. The results showed that the average intact strength of 30 MPa for laboratory sized samples would reduce to approximately 6,9 MPa if the effects of discontinuities are accounted for using Bieniawski's (1976) Rock Mass Rating and the Hoek-Brown (1988) strength criterion. The value of 6,9 MPa is similar to the value of 7,2 MPa obtained by Salamon and Munro (1967) in their back analysis of collapsed and stable pillars.

The condition of pillars in underground workings was observed and the effect of discontinuities on these pillars evaluated. The relationship between pillar condition and discontinuity frequency clearly showed that discontinuities have a detrimental effect on the strength of the pillars.

4 The effect of discontinuities on the strength of pillars

4.1 Introduction

This section of the report first evaluates possible methods of accounting for discontinuities on the strength of coal pillars. It is followed by detailed results of numerical model analyses in which the effect of discontinuities on coal pillar strength were evaluated.

Three approaches exist which allow the engineer to design coal pillars. Each approach is discussed below, and its ability to account for discontinuities is evaluated.

- The empirical approach: The empirical approach makes use of data on stable and failed pillars to derive an equation for pillar strength. The well known pillar strength equation of Salamon & Munro (1976) is an example. Owing to a lack of sufficient failed and unfailed cases, it has not been possible to extend this approach to explicitly account for the effect of discontinuities on pillar strength.
- The analytical approach: Analytical equations are developed which attempt to describe the failure process of a pillar. The sets of equations of Wilson (1983) and Barron and Pen (1992) are good examples of this approach. The analytical equations all make use of the large scale coal strength as an input parameter. It is therefore possible to account for discontinuity effects by reducing the strength of the coal used in the equation. Determining the appropriate strength reduction remains a difficult question. The analytical methods have not found wide acceptance in the mining industry.
- Numerical modelling approach: Recent advances in the capabilities of numerical modelling methods have resulted in a number of researchers attempting to use laboratory testing of coal together with numerical models to design pillars (Duncan Fama, 1995, Sheory et al, 1995, Medhurst, 1996, Madden, 1989). The input parameters for the models may be obtained by back analysis of in situ tests or by laboratory tests on coal samples. The advantage of using numerical models is that, once they are calibrated, they can be used to model new situations for which no previous experience exists. Each of the input parameters may be varied independently to gain insight into their importance in terms of pillar strength. Numerical models allow the effects of discontinuities to be evaluated explicitly.

For the purpose of this research it was decided to make extensive use of numerical models to assess the effects of discontinuities on coal pillar strength. Initially two dimensional models were used. A limited number of three dimensional models were evaluated to confirm the two dimensional results.

4.2 Application of two dimensional numerical models to evaluate the effect of discontinuities on coal pillar strength

Several types of two dimensional numerical models are available to simulate the behaviour of coal pillars. The two dimensional UDEC (Itasca, 1992) program was chosen, since it uses the finite difference approach to solve the equilibrium equations of the model. The finite difference method makes use of a time stepping technique in which the load increase, failure and load shedding is modelled in a controlled manner. Large strains are easily accommodated. The method allows a jointed pillar to be modelled as an assembly of deformable blocks. Each joint surface may be assigned Coulomb shear parameters and the material between the joints can yield according to a strength criterion with strain softening

behaviour. A three dimensional version of the program 3DEC (Itasca, 1994) was used to investigate three dimensional effects of jointing.

4.2.1 Model layout and calibration

A two dimensional UDEC model was set up to simulate a coal pillar with a width to height ratio of 2,0. The objective was to calibrate the model against the full load-deformation curve obtained by Wagner (1974). Although a two dimensional pillar is in effect a rib pillar, it was important to capture the post peak behaviour of the coal correctly. The model layout is shown in figure 4.1. The bottom surface of the model was fixed whilst the sides were free to move in the vertical direction, so that they represent planes of symmetry. The top surface of the model was made to move downwards at a constant velocity of 0,05 m/s, this velocity was selected such that the unbalanced force during yield of the pillar remained below 5% of the initial unbalanced force. The downward moving surface simulated a constant strain compression test on the coal pillar.

The strength of the pillar was obtained by monitoring the value of the vertical stress at a number of points at mid height of the pillar. The average stress was determined at regular intervals as the model was compressed. The peak value of the average vertical stress was taken to be the strength of the pillar. The models were run well into the post peak region, to assess the strain softening behaviour of the pillar.
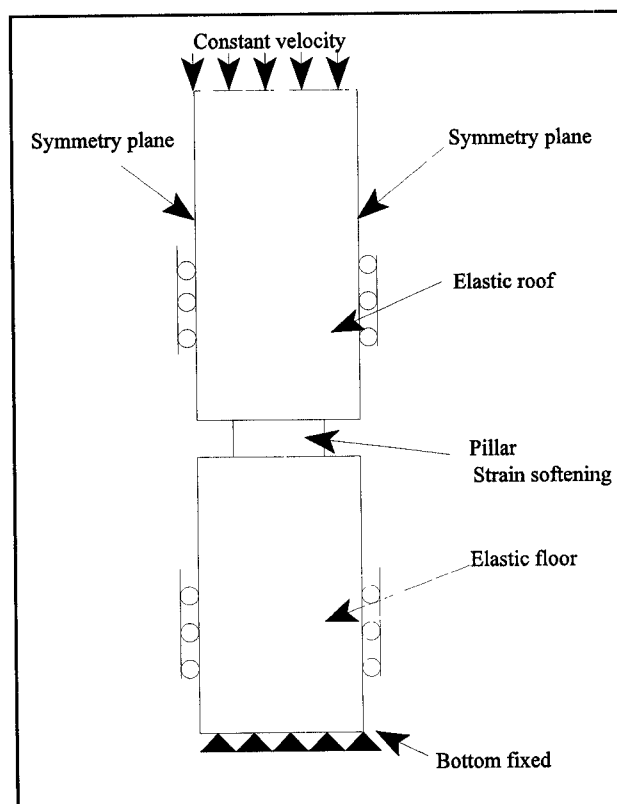
Figure 4.1 Udec model layout and boundary conditions.

The model was divided into two different material types. The pillar was modelled as a strain softening material whilst the roof and floor rock were modelled to be elastic. The elastic

parameters of the rock types are presented in table 4.1. The surrounding rock was therefore approximately three times stiffer than the coal.

The pillar was modelled to be unstressed prior to vertical loading. All stresses generated in the model were the result of the vertical compression of the pillar only. In an underground situation, the pillar will initially be stressed by the virgin stress state, which may provide additional horizontal confinement. The effect of the virgin stress state was not investigated. It was necessary to model the top and bottom contacts of the pillar with the elastic roof and

Table 4.1 Elastic parameters used in numerical models

	Bulk modulus (GPa)	Shear Modulus (GPa)
Pillar	2,67	1,6
Roof & floor	8,0	4,8

floor as joint surfaces. This allowed slip to occur along the joint plane as the failed coal was extruded under compression. Without the joint contacts, the post peak behaviour of the pillar could not be modelled satisfactorily. The contact joints were given zero cohesion and a 20 degrees friction angle.

The coal was modelled as a Coulomb material, with strain softening parameters. The friction angle of the coal was selected to be 20 degrees. This was kept constant in the trial runs of the model. The cohesion of the coal was varied until a peak strength of the pillar of 14,5 MPa was obtained, which was similar to the peak strength obtained by Wagner (1974) from in situ tests. The resultant cohesion used in the models was 2,76 MPa.

Strain softening of the coal was achieved by cohesion softening only. The friction angle was assumed to remain constant, regardless of the strain. The cohesion softening parameters were modified to obtain a similar post peak strength curve as obtained by Wagner. The residual cohesion of the coal was set at 0,1 MPa. It was found that if softening of the coal occurred over a strain of 0,08 the results were very similar to those obtained by Wagner. These values were used in all further analyses of pillars. It was noted that the model behaviour was dependant on the element size selected for the deformable material. As a result, all the models were generated with the same element sizes. The stress-displacement curve obtained for the model pillar with a width to height ratio of 2,0 is shown in figure 4.2 together with an average curve representing the in-situ results obtained by Wagner. It can be seen that the UDEC model behaviour is very similar to that obtained by Wagner. Details of the model input are presented in Appendix 5.

The stress distribution at mid height in the 2:1 pillar at different stages of loading is shown in figure 4.3 The loading sequence of the pillar was divided into nineteen stages from the initial state (S1) where the load has just started to come onto the pillar, to the final stage (S19), where the pillar reaches its peak strength. Here it can be seen that during the initial stages the pillar stress is reasonably uniform across its width. As the average stress increases, peaks start to develop at the outer edges of the pillar, (stage S10). However, the outer parts of the pillar shed stress as the core becomes more highly stressed. At the final stage, when the pillar offers its peak resistance, the core is highly stressed, at 19 MPa, which is almost twice the average stress in the pillar.
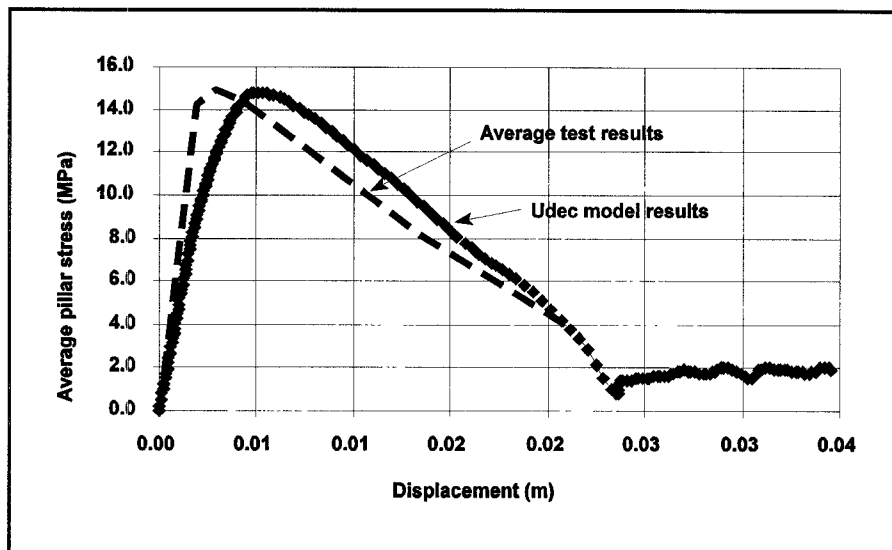
Figure 4.2 Graph showing average pillar stress - displacement curves for pillars with a width to height ratio of 2,0 tested by Wagner (1974) and obtained from Udec model tests.
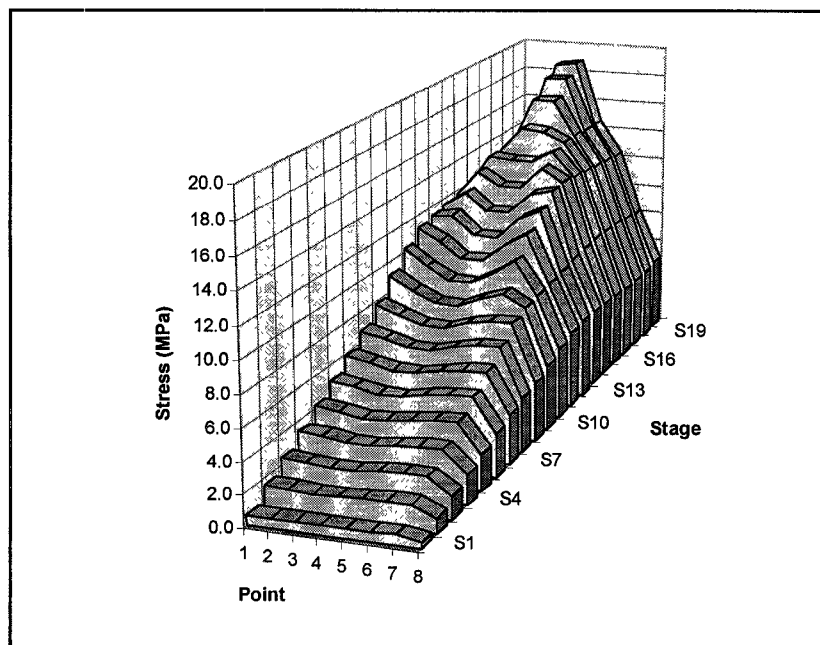
Figure 4.3 UDEC model results of vertical stresses at mid height of a pillar with a width to height ratio of 2,0.

The variation in the horizontal stress at mid height of the pillar for the different loading stages is shown in figure 4.4. The build up of confinement in the pillar is clearly shown up to the final stage when the pillar reaches its peak strength (stage S19). A horizontal stress of 5,5 MPa is indicated in the centre of the pillar. This confinement is generated entirely by the frictional

effects between the pillar and the surrounding rock and the dilation effects of the failed coal. The UDEC model clearly shows the effect of a failed perimeter of coal providing confinement to the central core.

The stages of failure of the UDEC model are shown in figure 4.5. At 50% of the peak strength of the pillar, tensile failure is indicated near the skin of the pillar (indicated by "T" symbols). Yield, according to the Coulomb criterion, is occurring at some of the points (indicated by "+" symbols) and some points have already failed, (indicated by "x" symbols). The core of the pillar is still in an unfailed, elastic state. This stage corresponds to loading stage 10 in figures 4.3 and 4.4.
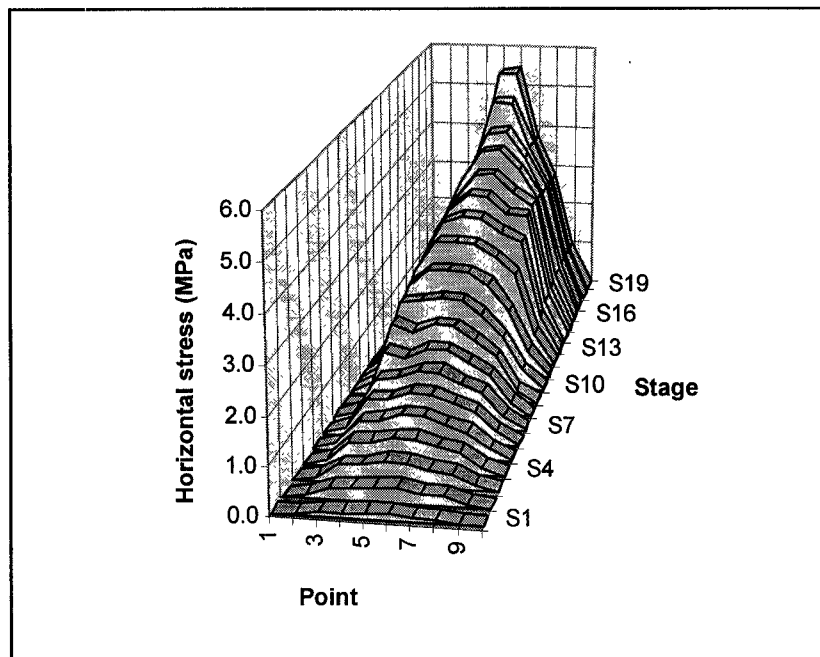
Figure 4.4 UDEC model results of horizontal stress at mid height of a pillar with a width to height ratio of 2,0.

As the load increases to 90% of the ultimate load, the amount of tensile failure increases at the outer parts of the pillar, yield continues almost to the centre of the pillar. This corresponds to loading stage 16 in figure 4.3 and 4.4. The coal at the centre of the pillar is under considerable confinement and does not fail. As the outer parts of the pillar continue to yield, owing to the strain softening behaviour, their ability to sustain high stresses reduces. This can be seen in figure 4.3 and 4.4 where the outer part of the pillar is shown to have shed stresses in the later loading stages.

When the pillar reaches its peak strength, the entire pillar is yielding, as shown in figure 4.5c. The stresses are such that the confinement enables the core to carry high stresses, but any further compression of the pillar causes a reduction in strength of the yielding core, and also a reduction in the load bearing capacity of the pillar.

The stages of failure of the UDEC model are very similar to the stages of failure observed by Wagner (1974). The role of the outer skin of failed material in generating confinement to the pillar core is clearly illustrated. It is concluded that the UDEC model is a good representation of the actual stages of failure of a coal pillar.

The role of the top and bottom contacts of the pillar in providing shear resistance to the extrusion of the pillar was studied by plotting the shear stresses at these contacts at different stages of loading the UDEC model pillar. The results are summarised in figure 4.6 where the shear stresses are plotted for the three loading stages shown in figure 4.5. At the initial stage, where the average pillar stress is 50% of the ultimate stress, the maximum shear stress at the contacts is 1,8 MPa. As the stress in the pillar increases to 90% of its ultimate load, the maximum shear stresses also increase to 3,25 MPa. The peak values of shear stress are not at the edges of the pillar, probably because the normal stress has reduced at the edges owing to failure of the coal. When the pillar is at its peak strength, the maximum shear stress at the contacts increases to 3,7 MPa. At the centre of the pillar the shear stresses are zero owing to symmetry.

In order to compare the model results with the empirically derived Salamon equation and the squat pillar equation (Wagner & Madden, 1984), the peak strength of the coal in the Udec model was reduced so that the model results agreed with the empirical pillar strength at a width to height ratio of 1,0. To achieve the required strength, it was necessary to reduce the cohesion of the coal to 2,61 MPa. All the other strength and strain softening parameters were left unchanged. The cohesion value of 2,61 MPa and the friction angle of 20 degrees results in a uniaxial compressive strength of the coal of 7,17 MPa, which is almost identical to the value obtained by Salamon & Munro (1967) in their study of pillar strength. The results of the empirical equations and the models at different width to height ratios are shown in figure 4.7. All the results of the UDEC models are higher than those predicted by the empirical equations, except for the 1:1 pillar, which was the calibration point. The trend in the curves is similar however, both indicate a more rapid increase in strength once the width to height ratio exceeds 4,0. The UDEC model is expected to result in a more rapid increase in strength than predicted by the empirical equations since the modelled pillars are rib pillars while the empirical equations were derived for square pillars.

It is concluded that the UDEC model is a good representation of the strength of coal pillars. The more rapid increase in strength in the UDEC model compared to empirical equations can be explained since it models a rib pillar. The further evaluation of the effects of discontinuities on pillar strength was carried out using the UDEC model.

4.2.2 Effect of variations in coal mass strength on UDEC model pillar strength

An evaluation of the effect of variations in the coal mass strength on the strength of modelled coal pillars was carried out. The variation in coal mass strength was evaluated by allowing the cohesion of the model material to vary. Variations of 30% above and below the mean cohesion of 2,51 MPa were modelled, assuming that the cohesion varied according to a normal distribution. The point estimate method, explained in Section 3, was used to determine the 95% lower limit of the strength, and the required factor of safety to ensure that the probability of failure of a pillar would be 5% or less. This required that two models be evaluated for each width to height ratio. The resulting pillar strength, 95% upper and lower confidence limits and required factor of safety are shown in figure 4.8. It is clear from this graph that as the width to height ratio increases, the sensitivity of a pillar to the strength of the coal mass decreases. The required factor of safety to ensure that 95% of the pillars will be stable decreases as the width to height ratio increases.

UDEC 1.82

Cycle   1610
block plot
no. zones : total   332
            elastic (.)   274
  at yield surface (+)   18
  yielded in past (x)   14
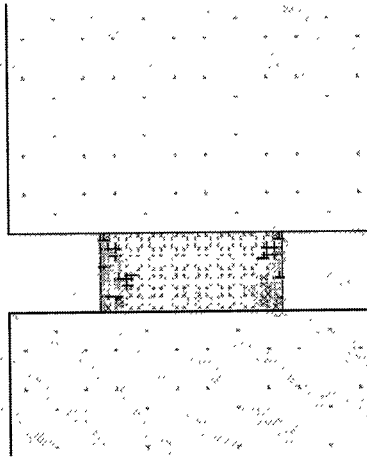
a) Pillar loaded to 50% of its ultimate strength

UDEC 1.82

Cycle   3210
block plot
no. zones : total   332
            elastic (.)   128
  at yield surface (+)   168
  yielded in past (x)   6
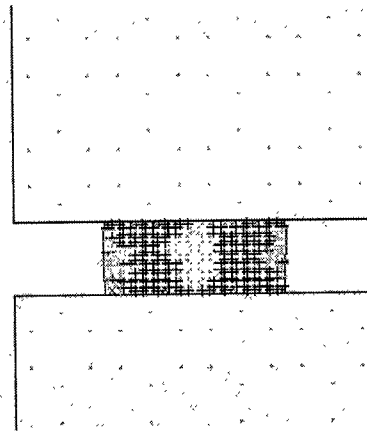
b) Pillar loaded to 90% of its ultimate strength

UDEC 1.82

Cycle   3810
block plot
no. zones : total   332
            elastic (.)   77
  at yield surface (+)   222
  yielded in past (x)   2
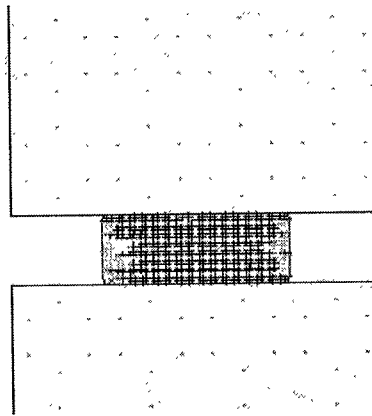
c) Pillar loaded to its peak strength

Figure 4.5 Progression of failure in a UDEC model of a 2:1 pillar at different loading stages
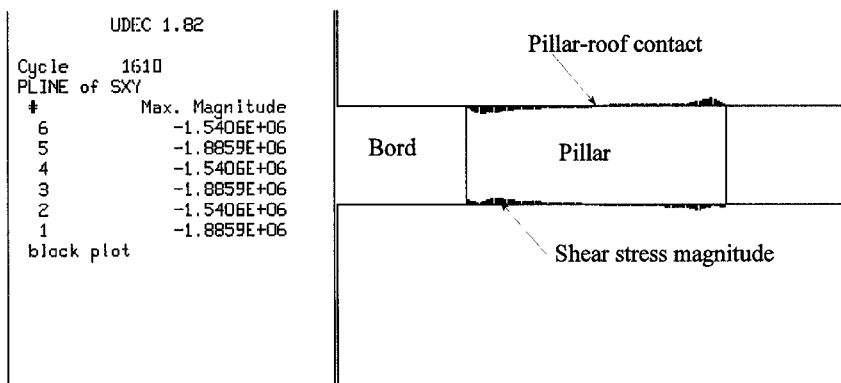
UDEC 1.82

Cycle   1610
PLINE of SXY
  #   Max. Magnitude
  6   -1.5406E+06
  5   -1.8859E+06
  4   -1.5406E+06
  3   -1.8859E+06
  2   -1.5406E+06
  1   -1.8859E+06
block plot

Pillar-roof contact

Bord   Pillar

Shear stress magnitude

a) Pillar loaded to 50% of its ultimate strength

UDEC 1.82

Cycle   3210
PLINE of SXY
  #   Max. Magnitude
  2   3.2529E+06
  1   3.0012E+06
block plot

Bord   Pillar

b) Pillar loaded to 90% of its ultimate strength

UDEC 1.82

Cycle   3810
PLINE of SXY
  #   Max. Magnitude
  2   -3.7056E+06
  1   3.4333E+06
block plot

Bord   Pillar
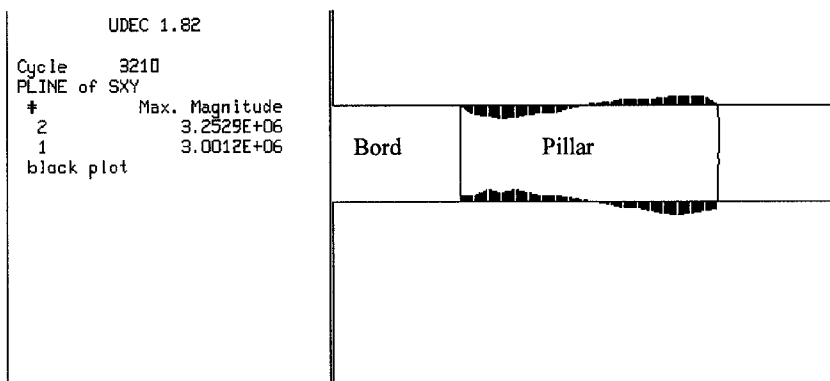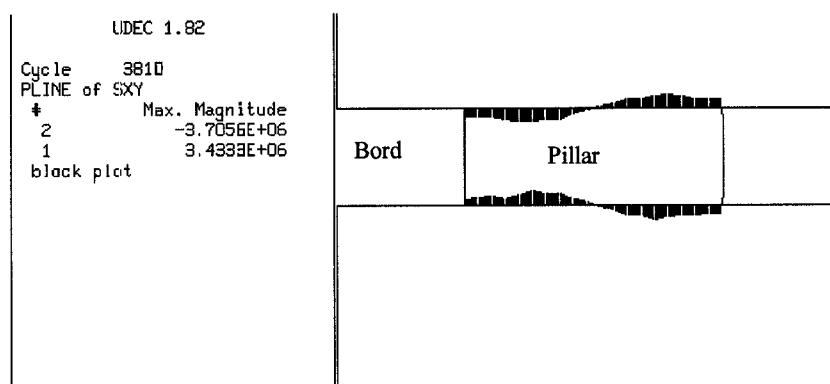
c) Pillar loaded to its ultimate strength

Figure 4.6 UDEC model results showing the development of shear stresses at the top and bottom contacts of a 2:1 pillar at different stages of loading
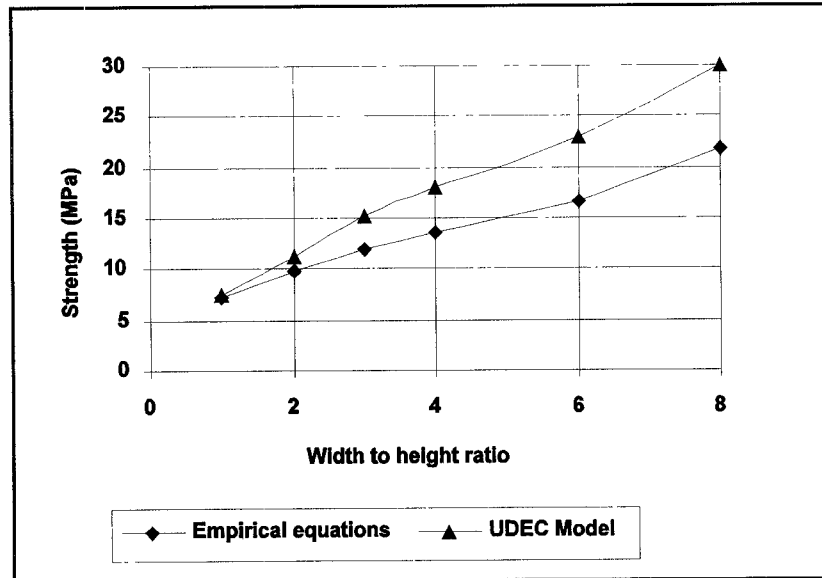
Figure 4.7 Comparison of pillar strength predicted by empirical equations and determined by UDEC models

Table 4.2 UDEC model results showing the effect of the variation in coal strength on pillar strength

Width to height ratio	1	2	3	6	8
Calculated mean strength (MPa)	6,48	10,95	14,9	22,45	29,7
Standard deviation (MPa)	1,73	3,05	3,5	2,45	2,7
Coefficient of variation %	26,64	27,85	23,49	10,91	9,09
95% upper limit (MPa)	9,31	15,97	20,66	26,48	34,14
95% lower limit (MPa)	3,64	5,93	9,14	18,42	25,26
Required factor of safety	1,78	1,85	1,63	1,22	1,18

An interesting result is obtained if the percent reduction in pillar strength caused by a 30% reduction in the coal mass strength is plotted against the width to height ratio of the pillars. This is shown in figure 4.9 with a fitted trend line. It can be seen that the strength of pillars with width to height ratios of 1,0 reduces by about 30% if the coal strength reduces by 30%, but a pillar with a width to height ratio of 8,0 will only suffer a loss in strength of 10%. The results are summarised in table 4.2.

The behaviour of the UDEC model pillars clearly shows that the increasing confinement provided by the greater width of squat pillars reduces the sensitivity of the pillars to variations in strength.

4.2.3 Effect of a single discontinuity on the strength of UDEC model pillars

Since the UDEC numerical model appears to model pillar behaviour satisfactorily, the next stage was to investigate the effect of a single discontinuity on the strength of pillars at different width to height ratios. A single discontinuity dipping at 45 degrees was modelled in the centre of each pillar. The discontinuity had a friction angle of 20 degrees, similar to the roof and floor contacts of the pillar. All the other parameters in the models were left unchanged. The models were run until the peak strength of the jointed pillar was achieved.
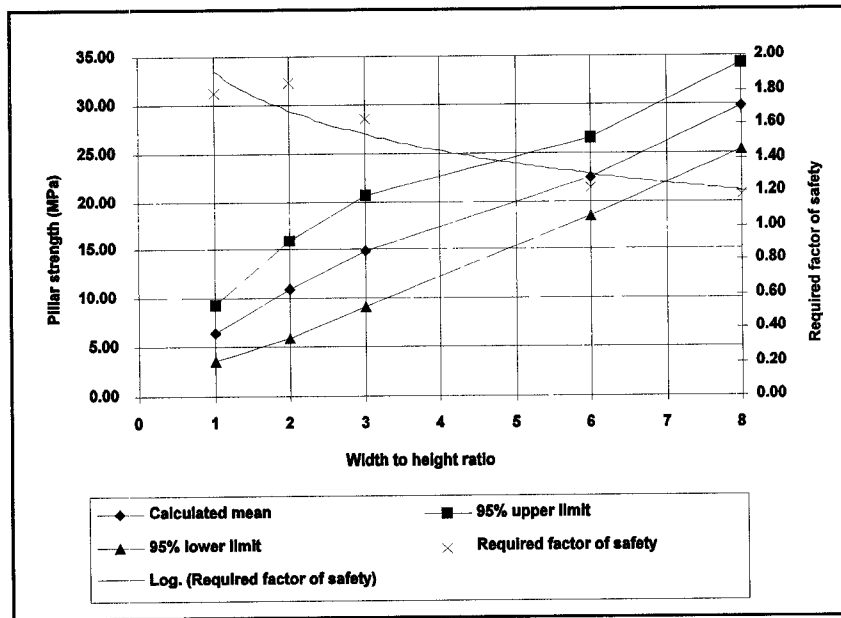
Figure 4.8 Calculated mean and 95% confidence limits of pillar strength based on UDEC models of pillars
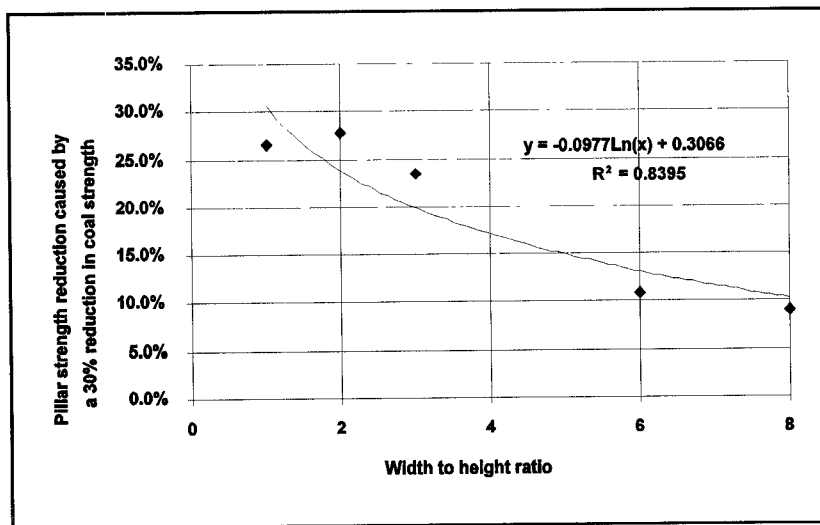
Figure 4.9 Effect of a 30% reduction in coal mass strength on the strength of coal pillars based on UDEC model results

The overall results are shown graphically in figure 4.10. The effect of a single joint on a pillar with a width to height ratio of 1,0 is shown to be drastic, it suffers a loss in strength of 90%. As the width to height ratio increases, the effect of the joint becomes less important. At a width to height ratio in excess of 6,0 the joint reduces the strength by less than 10%.
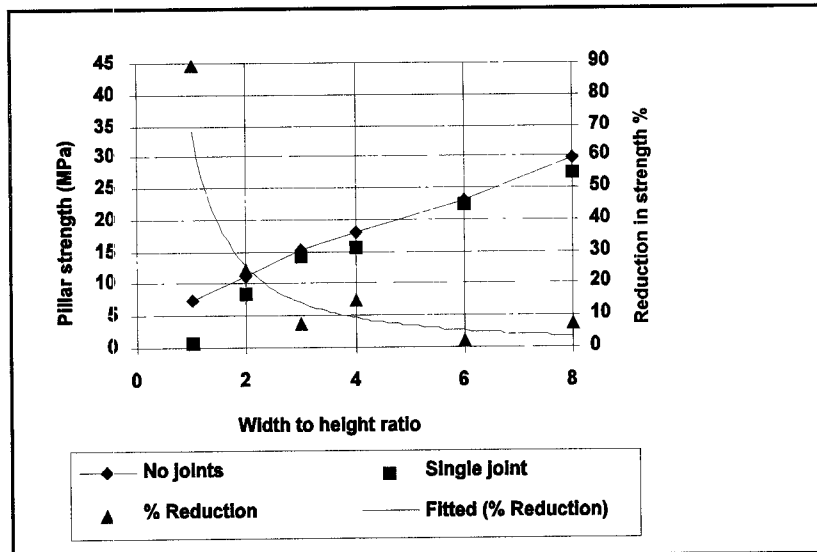
Figure 4.10 UDEC model results showing the effect of a single discontinuity on the strength of pillars with different width to height ratios

4.2.4 Effect of the position of multiple joints on the strength of UDEC model pillars

The effect of a series of joints intersecting a pillar was evaluated by setting up UDEC models of pillars with different width to height ratios. Initial analyses were carried out by generating joints which were continuous over the height of the pillar, spaced 0,75 m apart and dipping at various dip angles. The friction angle of the joints was 20 degrees and the cohesion set to zero.

During the initial analyses it was found that the strength of pillars with smaller width to height ratios was sensitive to the location of the joints within the pillar. To test the sensitivity, a number of runs were carried out in which the horizontal position of the joints were varied in increments of 0,15m between the different analyses. The joint spacing and dip was constant at 0,75m and 75 degrees respectively in all the runs. It was found that the narrow pillars are more sensitive to the effect of the position of the joints in the pillars. The strength of the 1:1 pillar may reduce from 7,2 MPa if there are no joints to as little as 1,5 MPa. One of the runs of the 1:1 pillar resulted in a slight increase in strength, but this was followed by a sudden drop in strength in the post peak region, which would probably manifest itself as a catastrophic failure of the pillar.

The 2:1 and 3:1 pillars showed a reduced amount of scatter in their strength compared to the 1:1 pillar. In the case of the 3:1 pillar, the post peak curves of some of the pillars dropped very rapidly. Inspection of the models at different stages of loading revealed that this was the result of individual joint defined blocks in the pillars suddenly starting to slide outwards. In practice, this behaviour could result in unstable failure. The 6:1 pillar was essentially unaffected by the location of the joints in the pillar.

An important observation is that in the pre-peak curves, the pillars all follow essentially the same load curve. In a practical mine situation, provided no pillars are over loaded, there would be no obvious difference in the behaviour of the pillars. It is only when they approach say 90% of their ultimate load, that there is a difference in their behaviour.

A table was prepared indicating the mean and standard deviation of the peak strengths of the different analyses for each width to height ratio evaluated, presented as table 4.3. The variation in peak strength was used to calculate the 95% upper and lower confidence limits of the strength, also shown in the table. Using the 95% lower limit of the strength, the factor of safety required to ensure that 95% of the pillars will be stable, was calculated. It can be seen from the results that the 1:1 pillars would require a factor of safety of 5,86 whilst the 6:1 pillars would only require a factor of safety of 1,37. This result further confirms the observation that at increasing width to height ratios the pillars become less sensitive to jointing effects. It appears from the results that there are two types of behaviour, the narrow pillars, with width to height ratio of less than 4, are severely affected and required factors of safety of approximately 1,6. The squat pillars, with width to height ratios in excess of 4, are essentially unaffected by the position of the joints and would therefore require lower factors

Table 4.3 Statistics of the effect of the horizontal joint position on the strength of pillars for joints dipping at 75 degrees, 0,75m apart

	Width to height ratio			
	1	2	3	6
Mean strength (MPa)	4,39	8,86	11,81	16,67
Standard deviation (MPa)	1,94	1,18	1,45	0,62
Coeff, of variation %	44,24	13,29	12,24	3,69
95% upper limit	7,58	10,79	14,19	17,68
95% lower limit	1,19	6,92	9,44	15,66
Required F,O,S,	5,86	1,66	1,61	1,37

of safety. The reduced scatter of results with increasing width to height ratio is shown graphically in figure 4.11.
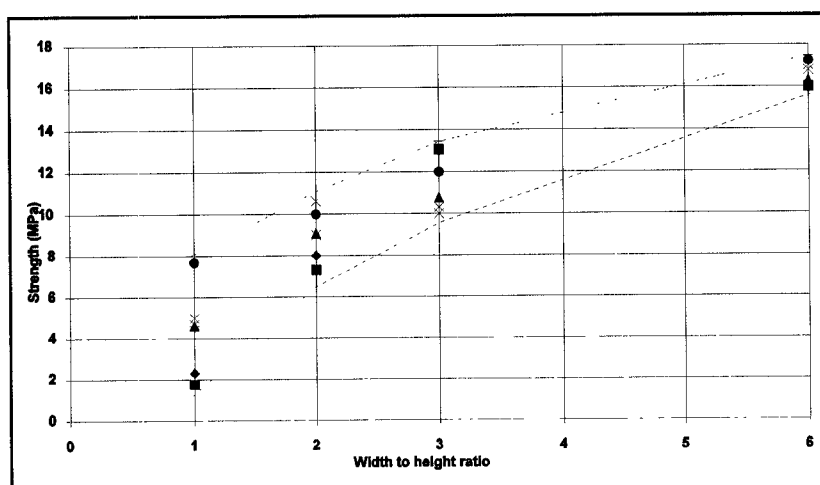
Figure 4.11 Graph showing scatter of peak strength of pillars owing to varying the position of joints in the pillars. Joints dip at 75 degrees and are spaced 0,75m apart.

4.2.5 Effect of the dip of multiple joints on the strength of UDEC model pillars

The dip of joints relative to the maximum load direction is important in terms of the rock mass strength. The effect of the joint orientation on pillars with different width to height ratios was studied by modelling joints spaced 0,5 m apart in pillars which were 1 m high. The dip of the joints was varied from 15 degrees to 90 degrees in 15 degree intervals. Owing to the sensitivity of the strength of a pillar to the exact location of the joints in the pillar, five analyses were carried out for each dip of the joints, in which the relative position of the joints was shifted by 0,1m horizontally. The resulting peak strength of each pillar was determined by running the UDEC model well into the post peak region. As a result, five peak strength values were obtained for each dip value of the joints. The results are summarised in table 4.4, which presents the peak pillar strengths obtained from the different UDEC analyses. The results include the mean, standard deviation and coefficient of variation for the different model geometries. The results for the pillars with width to height ratios of 2, 4 and 6 are shown in figure 4.12.
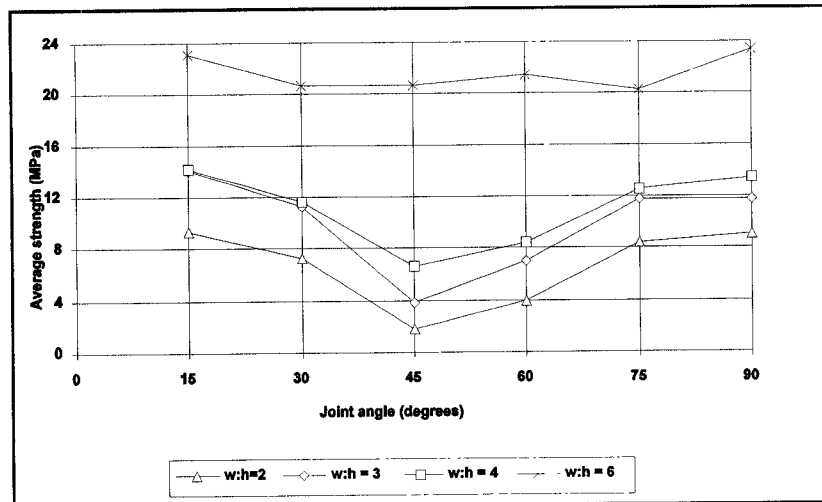
Figure 4.12 Average results of UDEC models showing the effect of joint orientation on pillar strength

The results show that:

- Joints dipping at 45 degrees have the most detrimental effect on the strength of a pillar.
- The effect of the joints on the strength decreases as the dip angle changes from 45 degrees. The effect is not symmetrical about 45 degrees.
- As the width to height ratio increases, the percentage drop in strength owing to joints becomes less pronounced. At a width to height ratio of 6,0 the effect of the joint dip is essentially obscured.
- The greatest degree of scatter, indicated by high values of the coefficient of variation, is found when the dip of the joints is 45 degrees.
- As the width to height ratio increases, the degree of scatter of peak strengths decreases, indicated, for example, by the reduction in the coefficient of variation for joints dipping at 45 degrees.

The results show the importance of the joint dip on pillar strength and confirms the trend observed earlier that as the width to height ratio increases, a pillar becomes less sensitive to the effect of joints. A number of analyses were carried out for pillars with a width to height

ratio of 8,0 in which the effect of jointing on the strength was insignificant. However, these pillars showed typical strain hardening behaviour, and a peak strength value could not be identified.

4.2.6 Effect of the frictional properties of multiple joints on the strength of UDEC model pillars

All the UDEC models discussed above were analysed with joints having a friction angle of 20 degrees. The effect of changing the friction angle from 20 degrees down to 15 degrees, which is a 26 percent reduction in coefficient of friction, was studied. The friction angle of the contact planes between the pillar and the surrounding rock was maintained at 20 degrees. Only one set of analyses were carried out for a fixed position of the joints within the pillar. As a result, the peak strength values obtained are more erratic than those obtained by running five different joint positions for each dip value. The results are summarised in figure 4.13 for pillars with width to height ratios of 2, 4 and 6. The results show that:

• A reduction in the joint strength has the most pronounced effect on the strength of pillars when the dip is 45 degrees.
• The effect of a weaker joint becomes less pronounced as the width to height ratio of the pillars increases. According to the models, the strength of a pillar with a width to height ratio of 6,0 is essentially unaffected by the joint strength.
• At steep dips and shallow dips, the effect of the joint strength becomes less pronounced. In some of the analyses the pillar strength with weak joints was greater than stronger joints. The reason is probably owing to the path dependence of non-linear models and an element of randomness in the post peak behaviour of the models.
• A 26 percent reduction of the friction angle of the joints results in a 71, 42 and 3 percent reduction in the peak strength of pillars with width to height ratios of 2, 4 and 6 respectively.

These results show that the strength of joints can have a pronounced effect on the strength of a pillar. However, as the width to height ratio of the pillar increases, the effect becomes less important. An important reservation is that the strength of the contact planes between the pillar and the surrounding rock remains unchanged. The effect of the strength of the contact planes is evaluated below.

4.2.7 The effect of the frictional properties of the contact surfaces between the pillar and the surrounding rock on the strength of UDEC model pillars

The contact surfaces were all modelled with a friction angle of 20 degrees. Since the friction between the pillar and the surrounding rock is one of the ways in which confinement is generated in a pillar, the frictional properties are expected to have a significant impact on the strength of a pillar. UDEC models were set up in which the friction angle of the contact surfaces was reduced to 15 degrees. The pillars were modelled with joints spaced 0,5m apart at various dip angles. The results are summarised in figure 4.14. From the results the following observations were made:

• A reduction in the strength of the contact surface can have an overriding effect on the strength of a jointed pillar since it affects the build up of confinement in the pillar, which is the source of its strength.
• Weak contact planes have a most detrimental effect on pillars with joints dipping at about 45 degrees.

- The effect of weak contacts reduces as the width to height ratio increases, but the effect remains significant even at width to height ratios of 6,0. The model with a width to height ratio of 6,0 suffered a reduction in strength of approximately 20 percent for a 26 percent reduction in the contact frictional resistance.

The results show the importance of the frictional properties of the contact surfaces between a pillar and the surrounding rock. It is significant that pillars with large width to height ratios may be affected quite severely, which is contrary to the effect of the internal joints in a pillar.

4.3 Three dimensional model tests to verify two dimensional model results

Since two dimensional models are only able to simulate rib pillars, it was necessary to carry out a number of test runs in which fully three dimensional pillars were modelled. The two dimensional models are limited in their capability of modelling joint and pillar configurations. The two dimensional models can only model situations where the joints are parallel to the pillar edges. In addition, the two dimensional models do not take into account the effect of all four free faces of a pillar. Three dimensional models are capable of studying all these effects and were used to verify the two dimensional model results. The three dimensional models were evaluated using the 3DEC version 1.5 finite difference stress analysis program (Itsaca, 1994). The 3DEC program is similar to UDEC in its mathematical basis, except that it allows fully three dimensional models to be evaluated. One important difference between the two programs was that the 3DEC program could not model strain softening behaviour. The post peak weakening of the failed coal around the perimeter of a pillar could not, therefore, be modelled correctly. The result was that the peak strengths of the three dimensional model pillars was higher than obtained in the two dimensional models. However, the intention was to evaluate the effect of joints, which was achieved by relative comparison of the results.

Three dimensional models were set up to simulate pillars with width to height ratios of 2:1, 3:1 and 6:1. The pillars were modelled as square pillars, with contact planes separating them from the surrounding rock. Constant velocity boundary conditions were applied to the top surface of the model, which was placed 12m above the top of the pillar. The rock mass was confined in the horizontal direction, representing vertical planes of symmetry. The rock mass was modelled as an elastic material, whilst the pillar was modelled as a Coulomb material. An example of one of the models is shown in figure 4.15. The models were analysed with the coal strength as follows: cohesion of 2,51 MPa and friction angle of 20 degrees. Details of other input data are presented in Appendix 5. These input data resulted in a strength of 14,5 MPa for an unjointed pillar with a width to height ratio of 2,0. Owing to the inability to model strain softening, these models did not shed their strength after reaching a peak value, but remained at approximately constant strength. The pillars with a width to height ratio of 6,0 did not reach a strength plateau, but simply continued to increase until the model became numerically unstable. Their results were not used in the further analysis.

Table 4.4 Results of UDEC analyses showing effect of joint inclination on peak strength of pillars, joints were spaced 0,5m apart and were shifted by 0,1m horizontally between the different runs

W:H ratio	Run no.	Joint dip (degrees)					
		90	75	60	45	30	15
w:h = 2	1	8,99	8,77	4,87	2,51	6,46	10,3
	2	10,79	8,78	5,3	3,08	6,42	9,7
	3	9,17	9,6	5,47	5,32	6,72	10,86
	4	9,8	8,3	6,79	3,61	6,3	8,5
	5	9,5	8,03	4,35	1,08	7,96	7,79
Mean		9,65	8,696	5,356	3,12	6,772	9,43
St Dev		0,708978	0,597938	0,911142	1,550435	0,681557	1,267793
Coef var %		7,346924	6,876013	17,01162	49,69344	10,06434	13,44426
w:h = 3	1	13,5	13,3	6,03	4,16	8,68	13,6
	2	13,61		6,08	3,91	9,59	12,53
	3	12,81	11,76	6,37	4,13	13,62	12,42
	4	13,81	11,31	7,39	4,25	8,03	13,59
	5	11,51	12,11	7,09	9,72	12,21	14,09
Mean		13,048	12,12	6,592	5,234	10,426	13,246
St Dev		0,938467	0,852095	0,614833	2,510862	2,391261	0,733301
Coef var %		7,192419	7,030491	9,326962	47,97215	22,93556	5,536017
w:h = 4	1	14,1	12,4	8,35	7,22	9,13	14,2
	2	13,72	12,11	8,36	5,84	9,3	14,09
	3	15,68	11,42	10,18	8,39	8,45	12,25
	4	15,3	14,2	7,53	8,74	11,66	13,16
	5	13,83	12,04	9,88	4,88	10,44	13,02
Mean		14,526	12,434	8,86	7,014	9,796	13,344
St Dev		0,900877	1,0498	1,124922	1,646748	1,263974	0,81008
Coef var %		6,201827	8,442979	12,69664	23,47802	12,90296	6,070745
w:h = 6	1	23,3	21,1	21	19,2	20,1	20,6
	2	22,02	20,64	20,66	19,14	21,64	22,3
	3	22,12	22,07	19,64	20,59	21,23	21,72
	4	24,75	19,83	19,31	23,65	24,63	23,36
	5	24,14	21,48	19,15	22,77	20,98	22,46
Mean		23,266	21,024	19,952	21,07	21,716	22,088
St Dev		1,207593	0,848664	0,8295	2,061468	1,723842	1,018685
Coef var %		5,190375	4,036642	4,157477	9,783901	7,938118	4,611941

W:H = 2

Peak strength (MPa)

12
10
8
6
4
2
0

0   15   30   45   60   75   90

Dip angle (degrees)

—■— Joint friction 15 degrees   —♦— Series1

W:H = 4

Peak strength (MPa)

16
14
12
10
8
6
4
2
0

0   15   30   45   60   75   90

Dip angle (degrees)

—♦— Joint friction 20 degrees   —■— Joint friction 15 degrees

W:H = 6

Peak strength (MPa)

25
20
15
10
5
0

0   10   20   30   40   50   60   70   80   90

Dip angle (degrees)

—♦— Joint friction 20 degrees   —■— Joint friction 15 degrees
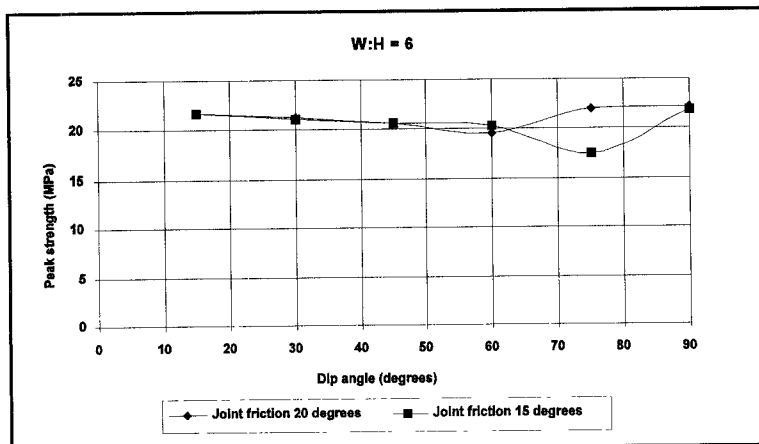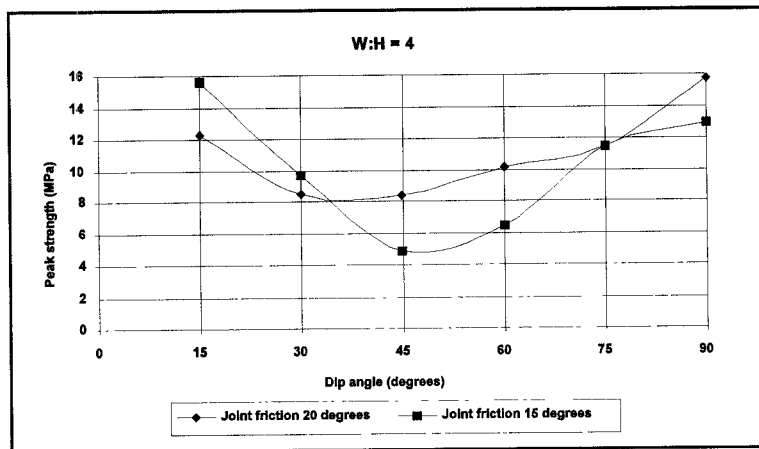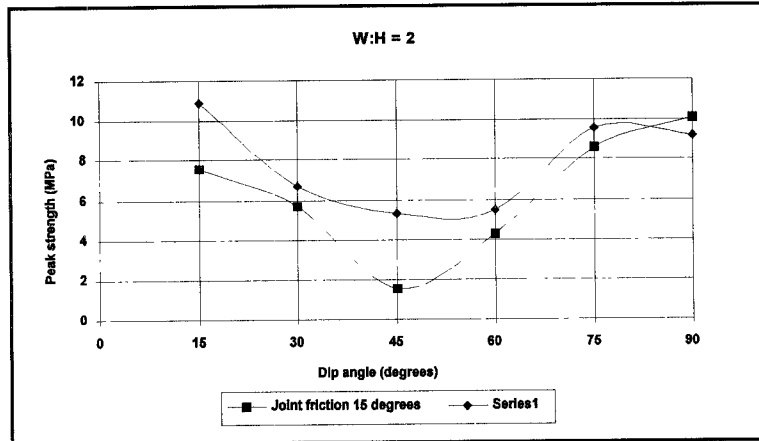
Figure 4.13 Graphs showing the effect of a reduction in the joint strength from 20 degrees to 15 degrees on the peak pillar strength. The friction angle of the contact planes between the pillar and the surrounding rock was maintained at 20 degrees
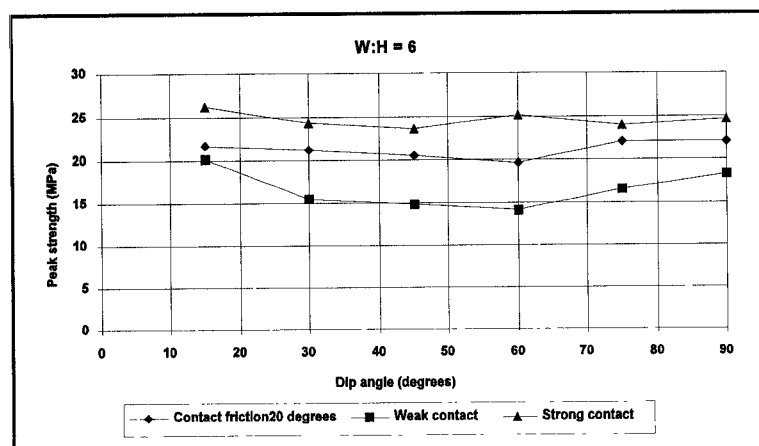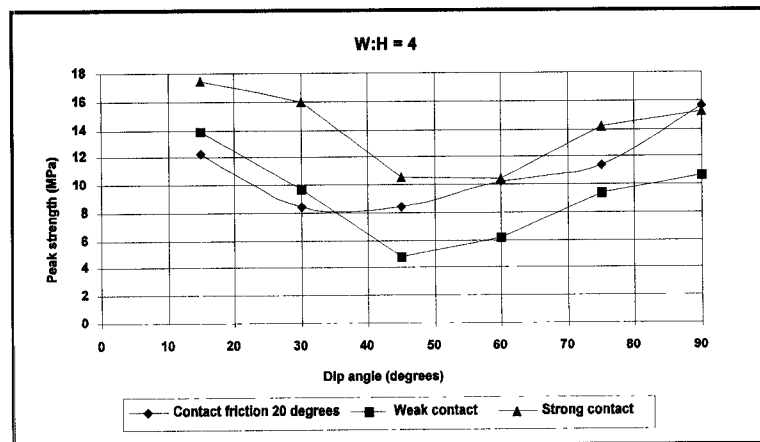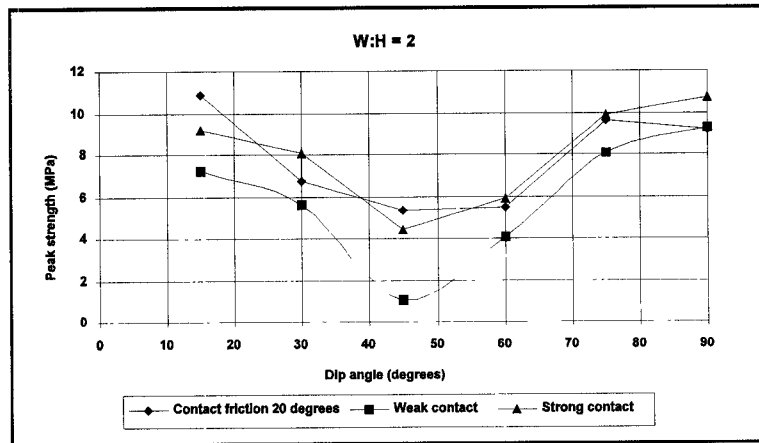
Figure 4.14 UDEC model results showing the effect of the frictional properties of the contacts between a jointed pillar and the surrounding rock for different width to height ratios and different joint dip angles
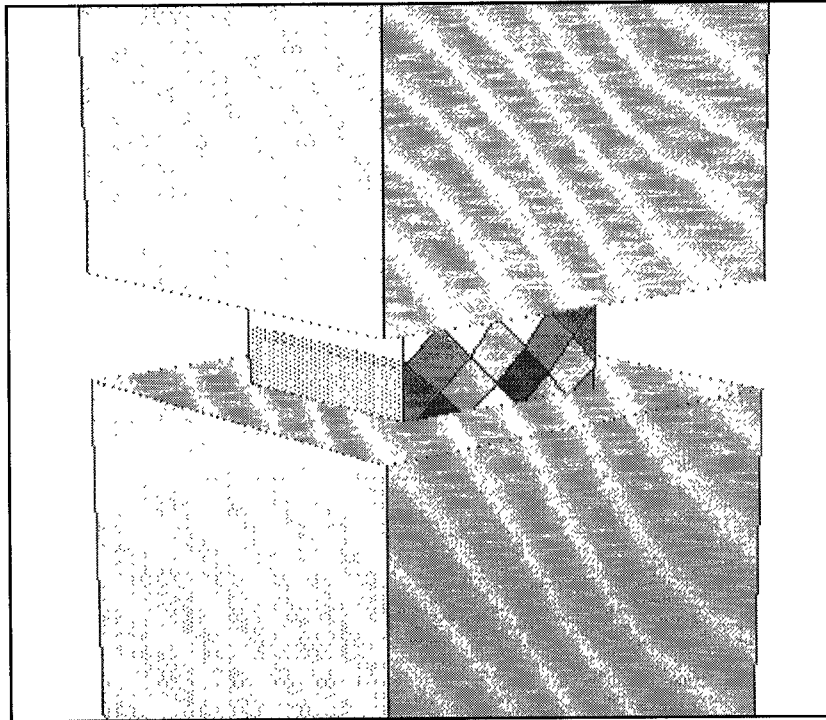
Figure 4.15 Three dimensional model of a pillar with two joint sets dipping at 45 degrees, the joints are parallel to the pillar edges

4.3.1 The effect of a single set of joints on the strength of a three dimensional pillar

The initial three dimensional analyses were carried out for a pillar with a width to height ratio
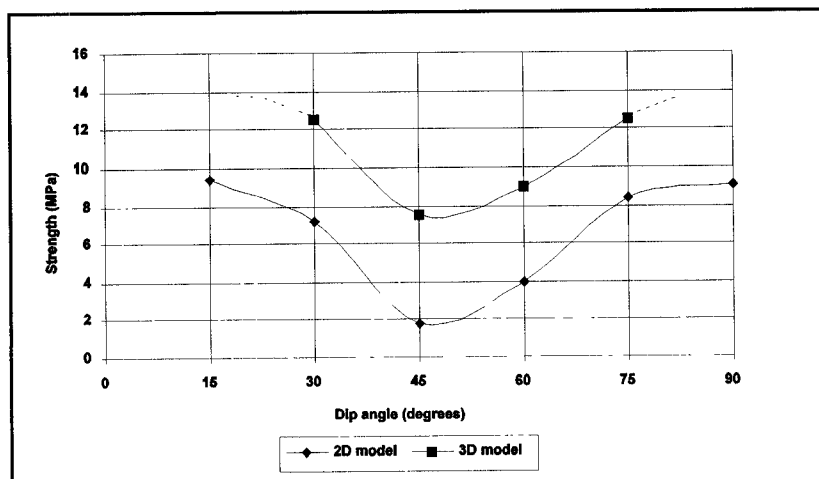
Figure 4.16 The effect of joint dip angle on the strength of two dimensional and three dimensional numerical model pillars

of 2,0. The pillar was modelled with one set of joints spaced 0,5 m apart, dipping at 30, 45 , 60 and 75 degrees. The peak strength of the pillar was obtained by monitoring the vertical stress at mid height of the pillar along a line through the centre of the pillar and diagonally across the pillar. The average vertical stress was determined and used as an indicator of the mobilised pillar strength as the pillar was compressed. The resulting peak strength values are summarised in figure 4.16, which also shows the strength obtained for two dimensional model analysis. It can be seen that the shape of the curve is similar for the two model types. The strength drop is a maximum when the joints dip at 45 degrees for both model types. The absence of strain softening of the coal material resulted in higher strengths being achieved in the three dimensional models.

4.3.2 The effect of joints which are not parallel to the pillar edges

In the UDEC models all the joints are modelled as if they are parallel to the pillar edges. The 3DEC model allows joints to be modelled at any orientation in the pillar. Models were set up to investigate the effect of joints dipping at 45 degrees and striking diagonally through a pillar with a width to height ratio of 2,0. The results showed that if the joints are not parallel to the pillar edges, as shown in figure 4.17, the pillar is 9,6% weaker than the case where the joints are parallel to the edges. This difference is not significant and the two dimensional models may be considered to be representative of cases where the joints are not parallel to the pillar edges. Details of the input data are presented in the appendices.
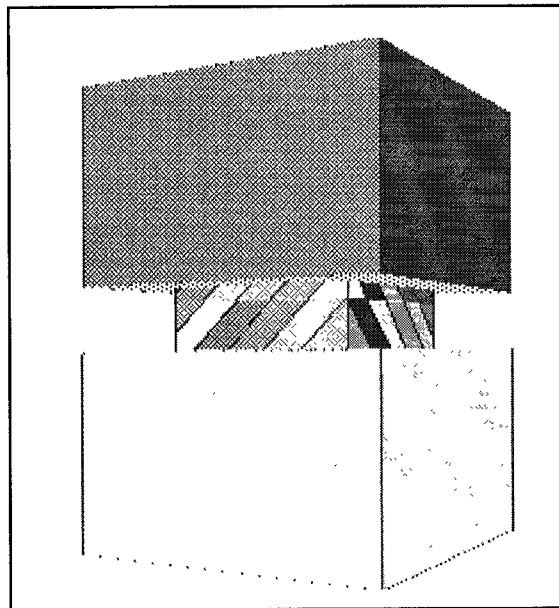
Figure 4.17 Three dimensional model with 45 degree joints which strike diagonally to the pillar edges

4.3.3 Discussion of three dimensional model results

The three dimensional model analyses showed that the difference between the behaviour of the two dimensional model and the three dimensional model analyses was not significant. The effect of the joint dip on pillar strength was similar in both cases. The similarity was

probably a result of the fact that the two dimensional model parameters were initially calibrated to the strength of fully three dimensional pillars modelled by empirical equations.

The results also showed that pillar strength is not significantly different if the joints do not strike parallel to the pillar edges, as in the two dimensional models. It was concluded that the two dimensional model results could be used to indicate trends in the effect of jointing on three dimensional pillars.

4.4 Discussion

A numerical modelling technique was used which allows discontinuities to be modelled explicitly and is able to model the failure of the coal material in a realistic manner. Two-dimensional numerical models were calibrated against empirical pillar strength equations for pillars without major joints. It was possible to study the effect of through going discontinuities on the strength of pillars with different width to height ratios. The results showed that as the width to height ratio increases the effect of joints on the strength of a pillar diminishes. Further studies showed the importance of the joint orientation, the joint frictional properties and the position of joints within a pillar. The model studies showed a reducing sensitivity to variations in joint properties as the width to height ratio of a pillar increases.

Limited three dimensional model analyses confirmed the results of the two dimensional analyses. The three dimensional geometrical effects, for example joints which are not parallel to the pillar edges, were shown to be minor in terms of overall pillar strength.

It is recognised that the numerical model results are not directly applicable to the behaviour of actual coal pillars in underground workings. The general trends observed and relative importance of the different jointing characteristics are, however, important for the development of an improved method of pillar design.

5 Conclusions

5.1 Conclusions regarding discontinuities

The conclusions of the research are presented below in italics, followed by explanatory text, explaining the reasons for the conclusions:

Discontinuities in coal seams may be divided into three categories: cleat, joints and slips.

Coal seams are divided into major mining blocks by faults and dolerite intrusions. Within the blocks the coal seams are relatively undisturbed. Within the relatively undisturbed blocks of coal, discontinuities exist which affect the strength of the coal pillars. The discontinuities exist from the microscopic scale to several tens of metres. For the purposes of this research, cleats were described as those discontinuities which are 5 cm to 1m in length and form part of the coal structure. The frequency of cleats may be as high as 100 per metre in disturbed coal or may be absent in some coal seams. Cleats are usually orthogonal to the bedding of the coal.
Joints were described as discontinuities which are more than 1m in length, and are typically spaced 1m apart. Joints are not as pervasive as cleats; joints were present in only 33% of the sites mapped. The average dip of joints was found to be 67 degrees.
Slips are major joints which may be continuous over several hundred meters and may displace the coal by a few centimetres. Slips are typically spaced several metres to several tens of metres apart and have an average dip of 50 degrees. Slips were observed in 75% of the locations mapped.

The intensity of discontinuities is highly variable between the different seams and within individual mine sites.

It was observed that the frequency of joints and slips was highly variable at individual mine sites, the standard deviation of the frequency often exceeding the mean value. The reason is that coal seams with a low intensity of jointing may be highly jointed in isolated locations such as the vicinity of dykes or faults. It is therefore not advisable to categorise the different seams on the basis of the amount of jointing. Some of the seams were consistently highly jointed, for example the sites in the Zululand coal field and the Klipriver coal field.

5.2 Conclusions regarding the determination of discontinuity properties

Field estimation techniques are adequate to determine the strength of discontinuities for pillar design purposes.

Laboratory shear tests and field estimation methods provided similar results for the strength of discontinuities in coal. The field estimation technique makes use of the base friction angle of the coal, the roughness of the discontinuities and the infill strength properties to estimate the friction angle and cohesion.

Empirical methods of estimating rock mass strength provide acceptable estimates of the coal mass strength.

The discontinuity mapping data and published coal strength data were used to calculate the coal mass strength using the criterion of Hoek and Brown (1988). It was found that the average strength of a cube of the coal mass was 6,97 MPa which is similar to the strength of 7,2 MPa obtained by Salamon & Munro (1967). It must be borne in mind that the standard deviation in the strength was found to be 3,35 MPa which would require factors of safety of 2,7 to ensure that 95% of the pillars are stable. In addition, empirical methods assume that the coal mass is uniformly jointed in all directions which may result in an underestimation of the coal pillar strength when joints are favourably oriented for stability.

5.3 Conclusions regarding the effect of discontinuities on the strength of coal

The reduction in the strength of coal samples with increasing volume can partially be explained by the increasing number of cleats in the samples.

Detailed mapping of cleats on the surface of coal samples indicated that there was a linear relationship between the cleat intensity, normalised to the sample diameter, and the strength of the sample. As the sample size increases, the normalised cleat intensity also increases, and hence the strength is reduced. A similar trend may therefore be expected in coal pillars.

5.4 Conclusions regarding the effect of discontinuities on the strength of pillars

Discontinuities have a weakening effect on coal pillars in underground workings.

The results of a study of the discontinuity frequency and the condition of coal pillars in underground workings indicated that an increased intensity of discontinuities resulted in poorer pillar conditions. This confirms that discontinuities reduce the strength of coal pillars. Numerical model studies confirmed that through-going discontinuities may result in significant reductions in the strength of pillars.

Pillar strength is likely to vary within individual seams and between seams, owing to the variability of the discontinuities.

The observations of the properties of discontinuities in the different coal seams indicated that the frequency and strength properties of discontinuities are highly variable. This variability will therefore result in variable pillar strength.

The effect of discontinuities on coal pillar strength is not constant, but decreases with increasing width to height ratio of a pillar

Numerical model results indicated that pillars with large width to height ratios (6,0 and above) are less sensitive to the weakening effects of discontinuities. The strength of narrower pillars is significantly reduced by the presence of discontinuities.

The existence of a confined core in a pillar may explain the above mentioned weakening effect of discontinuities.

The existence of a confined core in a pillar increases the resistance to shear failure along discontinuities. A wide pillar with a large confined core will therefore be less sensitive to the presence of discontinuities than a narrow pillar. Numerical models, which are able to simulate the presence of discontinuities in pillars, confirmed the above conclusion.

Discontinuities inclined at 45⁰ have the most severe effect on the strength of pillars.

Unlike rock samples, where discontinuities dipping at about $60°$ to $75°$ have the most severe effect on their strength, coal pillars are most severely affected when the discontinuities dip at $45°$. The reason is that the width to height ratio of pillars in coal mines is almost always greater than 2,0 and steeply dipping discontinuities cannot daylight on two opposing sides of a pillar at once. When testing rock samples, which are about twice as high as their diameter, steeply dipping discontinuities may daylight on opposing sides of the samples.

An improved method of designing coal pillars should take into account the presence of discontinuities as a parameter which is dependent on the width to height ratio of the pillars.

The results of this study show that discontinuities play an important part in the strength of coal pillars. Any improved method of coal pillar design should consider discontinuities as an contributing factor. Since the weakening effect of discontinuities depends on the width to height ratio, an improved method should account for discontinuities accordingly.

6 REFERENCES

Akermann, K.A. & Canbulat, I. 1994. A reassessment of coal pillar design in South African collieries. *Safety in Mines Research Advisory Committee*. Report: Project COL021A, Johannesburg.

Bandis, S.C. 1990. Scale effects in the strength and deformability of rocks and rock joints. *Proc. Scale effects in rock masses*. ed. Pinto Cunha. Balkema, Rotterdam. pp. 59-75.

Barron, K. & Pen, Y. 1992. A revised model for coal pillars. *Proc. Workshop on coal pillar mechanics and design*. US Bureau of Mines, IC9315. pp.144 - 157.

Barron, K. & Yang, T. 1992. Influence of specimen size and shape on the strength of coal. *Proc. Workshop on coal pillar mechanics and design*. US Bureau of Mines, IC9315. pp.5 - 25.

Barton, N. & Choubey, V. 1977. The shear strength of rock joints in theory and practice. *Rock Mechanics* No. 10.

Barton, N. & Bandis, S. 1982. Effects of block size on the shear behaviour of jointed rock. *23 rd U.S. Symp. Rock. Mech.*, Berkeley.

Bieniawski Z.T. 1968. The effect of specimen size on compressive strength of coal. *Int. J. Rock Mech. Min. Sci.* Vol 5. pp.325 - 335.

Bieniawski, Z.T. 1976. Rock mass classification in rock engineering. *Exploration for rock engineering*, ed. Z.T. Bieniawski. AA Balkema, Rotterdam. pp.97-106.

Bieniawski, Z.T. & van Heerden, W.L. 1975.The significance of in situ tests on large rock specimens. *Int. J. Rock Mech. Min. Sci. & Geom. Abstr.*, Vol. 2: pp.101 - 113.

Cunha, A.P. 1990. Scale effects in rock mechanics. *Scale effects in rock masses*, ed. Pinto da Cunha, Balkema, Rotterdam, pp.3 - 27.

De Jager, F.S.J. 1976. *Mineral Resources of the Republic of South Africa*, 5th ed., Handbook 7, ed. C.B. Coetzee, Geological Survey of South Africa.

Duncan Fama, M.E., Trueman, R. & Craig, M.S. 1995.Two- and three-dimensional elasto-plastic analysis for coal pillar design and its application to highwall mining. *Int. J. Rock Mech. Min. Sci. & Geom. Abstr.*, Vol. 32: pp.215 - 225.

Falcon, R. & Ham,A.J. 1988. The characteristics of Southern African coals. *J.S. Afr. Inst. Min. Metall.* Vol. 88 pp. 145-161.

Fauconnier, C.J. & Kersten, R.W.O. 1982. Increased underground extraction of coal. *S. Afr. Inst. Min. Metall.* Monograph series No. 4, Johannesburg.

Gaigher, J.L. 1980. The mineral matter in some South African coals. *MSc thesis, University of Pretoria*, Pretoria.

Green. 1982. The macromolecular structure of coal, *Coal structure,* ed. Meyers R.A., Academic Press, pp.199 - 282.

Hoek, E. & Brown, E.T. 1988. The Hoek and Brown failure criterion - a 1988 update. *Proc.15th Canadian Rock Mech. Symposium,* Toronto, pp.31 - 38.

Hoek, E., Kaiser P.K. & Bawden W.F. 1995. Support of underground excavations in hard rock. A.A. Balkema, Rotterdam.

Harr, M.E. 1985. *Reliability based design in civil engineering,* Mc Graw Hill.

Herget, G. 1988. *Stresses in rock.* AA Balkema, Rotterdam.

Hoek, E. & Brown, E.T. 1980. *Underground excavations in rock.* Inst. Mining & Metall., London.

Itasca Consulting Group. 1992. *User's manual UDEC,* V1.8. Minnesota.

Itasca Consulting Group. 1994. *User's manual 3DEC,* V1.5. Minnesota.

Madden, B.J. 1989. Re-assessment of coal pillar design, *School : The total utilisation of coal resources.* S. Afr. Inst. Min. & Metall., Witbank.

Madden, B.J. 1985. A study of the in-situ strength properties of coal seams in South African collieries, *Symp. Rock mass characterisation,* S. Afr. National Group on Rock Mechanics, Randburg, pp.21-27.

Madden, B.J. 1995. Coal pillar design procedures. *Safey in Mines Research Advisory Committee,* Report: Project COL337, Johannesburg.

Medhurst, T.P. 1997. Estimation of the in situ strength and deformability of coal for engineering design. *Thesis (Ph.D.)* University of Queensland, 1997.

Ozan, T.T. 1993. Reassessment of coal pillar design procedures, *Safey in Mines Research Advisory Committee,* Report: Project COL021A, Johannesburg.

Ozbay, M.U. 1994. Strength of laboratory-sized coal samples from Delmas and Sigma collieries. *Safey in Mines Research Advisory Committee,* Report: Project COL021A, Johannesburg.

Palmstrom, A. 1996. Characterizing rock masses by the RMi for use in practical rock engineering. Part 1: The development of the rock mass index (RMi). *Tunnelling and underground space technology* Vol. 11.

Peng, S.S. 1993. Strength of laboratory-sized specimens vs. underground coal pillars. *Mining Engineering,* Feb. 1993. pp.157-158.

Priest, S.D. & Hudson, J.A. 1976. Discontinuity spacings in rock. *Int. J. Rock Mech. & Min. Sci.* Vol. 13. pp. 135-148.

Ramamurthy, T. & Arora, V.K. 1994. Strength predictions for jointed rocks in confined and unconfined states. *Int. J. Rock Mech. Min. Sci. & Geomech. Abstr.* Vol 31 No 1 pp.9-22.

Robertson, A. Mc G. 1970. The interpretation of geological factors for use in slope theory. *Proc. Symp. The theoretical background to the planning of open pit mines with special reference to slope stability,* S. Afr. Inst. Min. Metall., Johannesburg. pp.55-71.

Salamon, M.D.G. & Munro, A.H. 1967. A study of the strength of coal pillars. *J.S. Afr. Inst Min. Metall.* Vol. 67. pp. 56-67.

Salamon, M.D.G. 1967. A method of designing bord and pillar workings. *J.S. Afr. Inst Min. Metall.* Vol. 68. pp. 68-78.

Serafim, J.L. & Perreira, J.P. 1983. Consideration of the geomechanics classification of Bieniawski. *Proc.Int Symp. Engng. Geol. and Underground Construction,* Lisbon, Portugal, pp. 1133-1144.

Sheory, P.R., Barat, D., Mukherjee, K.P., Prasad, R.K., Das, M.N., Banerjee, G. & Das K.K. 1995. Application of successful depillaring under stiff strata. *Int. J. Rock Mech. Min. Sci. & Geomech. Abstr.* Vol. 2 No. 7 pp. 699 - 708.

Trueman, R. & Medhurst, T.P. 1994. The influence of scale effects on the strength and deformability of coal. *Proc.IV CSMR/ Integral approach to applied rock mechanics,* Santiago Chile.

Van der Merwe, J.N. 1993. Revised strength factor for coal in the Vaal basin, *J. S. Afr. Inst. Min. Metall.* Vol. 93. pp. 71-77

Vervoordt, A. & Jack, B. 1992. Analysis of sidewall fracturing and spalling during coal-pillar extraction. *J.S. Afr. Inst. Min. Metall.* Vol. 92, pp.3-11.

Wagner, H. 1974. Determination of the complete load deformation characteristics of coal pillars. *Proc.3rd Congr. Int. Soc. Rock Mech.* Denver, Colorado.

Wagner, H. & Madden, B.J. 1984. Fifteen years of experience with the design of coal pillars in shallow South African collieries: An evaluation of the performance of the design procedures and recent improvements. *Design and performance of underground excavations.* ISRM/BGS, Cambridge. pp.391-399.

Wilson, A.H. 1983. The stability of underground workings in the soft rocks of the coal measures. *Int. J. Min. Eng.* Vol. 1. pp. 91-187.

Appendix 1

Discontinuity mapping data

The results of field mapping of discontinuities are given in this Appendix. The discontinuities were mapped at site 4 and sites 7 to 20. The locations of the sites are shown in the main body of the report, in figure 2.1. The data collected at sites 1, 2, 3, 5 and 6 are not presented here since they were collected using a different technique.

Discontinuities were mapped using the following method:

- Frequency : number of discontinuities per metre. In the case of the 100m scale, the major discontinuity (slip) frequency per 100m is recorded.

- Length : The dip length is recorded. The strike length can seldom be assessed since most discontinuities are not visible in the roof or floor of the workings. The dip length is truncated by the height of the mine workings, which is in the order of 2m. The slips are by definition extensive relative to the pillar dimensions.

- Roughness : A simple roughness scale is used as follows:
  1 = smooth, polished
  2 = smooth slickensided
  3 = smooth coal surface
  4 = slightly rough
  5 = rough or striated
  7 = very rough or smooth, stepped
  10 = very rough and stepped

- Waviness : The waviness is taken over 1m as s=straight and planar,c= curved or w=wavy. If a discontinuity is less than 1m long the waviness is observed over its full length.

- Infilling : The strength of the infilling and thickness are recorded. The strength is indicated relative to coal strength as being w=weaker than coal, u= unaltered, equal to coal or s=stronger than coal. The relative strength is determined by using the sharp end of a geological pick or a pocket knife.

- Wall strength : The discontinuity wall strength is similarly recorded by comparing it to the strength of the coal. It was indicated as being either s=stronger than coal,u=unaltered, equal in strength , w=weaker than coal or wc=very weak and crumbly.

- Dip : The dip angle of the discontinuity is recorded.

- Ground water : Groundwater conditions are noted, d=dry, w=wet/damp.
The following tables list the mapping data for the cleats, joints and slips seperately.

CLEATS

Site	Location	Frequency	Length	Roughness	Waviness	Fill-strength	Fill Thickness	Wall strength	Ave dip	Ground water
7	1	7	25	4	s	w		1 w		80 d
	2	5	50	5	s	w		1 w		90 d
	3	7	75	4	w	w		2 w		90 d
	4	4	74	4	s	w		1 w		90 d
8	1	7	35	3	s	w		1 w		85 d
	2	7	35	2.5	s	w		1 w		85 d
	3	7	40	2.5	s	w		1.5 c		85 d
	4	7	40	2.5	s	w		1.5 c		85 d
	5	6	45	3.5	s	w		1 w		87 d
	6	7	35	3.5	s	w		1 w		87 d
11	1	15	50	3	s	w		1 w		85 d
	2	16	30	3.5	s	w		1 w		85 d
	3	15	30	4	s			0 u		70 d
	4	10	50	4	s	w		1 u		85 d
	5	15	40	3	s			0 u		70 d
	6	15	30	4	s	w		1 u		80 d
*Near dyke	7	4	80	4	c	w		1 u		70 d
16	1	10	30	4	s	w		1 w		90 d
	2	4	10	4	s	w		1 w		90 d
	3	4	40	4	s	w		2 w		90 d
	4	6	25	4	s	w		1 w		90 d
	5	10	60	4	s	w		1.5 w		90 d
	6	10		4	s	w		1 w		70 d

Site	Location	Frequency	Length	Roughness	Waviness	Fill-strength	Fill Thickness	Wall strength	Ave dip	Ground water
	7	13	35	3	w		0	w	90	d
14	1	8	40	5	s	w	1	w	60	d
	2	7	25	4	s	w	1	w	80	d
	3	6	30	5	w	w	1	w	90	d
	4	4	25	7	c	w	1	w	90	d
	5	2	45	7	w		0	u	45	d
15	1	4	30	5	s	w	0	u	60	d
	2	7	90	5	w	w	2	w	80	d
	3	4	70	5	w	w	1	w	90	d
	4	5	75	5	s	w	0	u	90	d
	5	8	105	5	s	w	2	c	90	d
4	1	4	20	4	w	w	1	w	90	d
	2	5	30	5	s		0	w	90	d
	3	5	25	4	s	w	1	w	90	d
	4	8	30	5	w	w	1	w	60	d
	5	5	20	5	w	w	1	w	80	d
9	1	0								
	2	4	30	5	s		0	w	85	d
	3	4	30	5	s		1	w	90	d
	4	2	20	5	c	w	1	w	80	d
	5	3	30	4	c	w	1	w	90	d
	6	3	30	4	w	w	1	w	90	d
10	1	7	50	5	c	w	1	w	90	d
	2	6	20	4	c	w	0.5	w	90	d

Site	Location	Frequency	Length	Roughness	Waviness	Fill-strength	Fill Thickness	Wall strength	Ave dip	Ground water
	3	4	20	5	c	w	0.5	w	90	d
	4	3	10	5	w	w	0.5	w	90	d
	5	4	20	5	w	w	0.5	w	90	d
12	1	8	10	4	c	w	0.5	w	90	d
	2	10	12	4	w	w	0.5	w	90	d
	3	6	15	4	w	w	1	w	90	d
13A	1	9	30	2	w	w	1.5	c	85	d
	2	9	30	4	w	w	1	w	90	d
	3	8	45	4	w	w	1	w	90	d
	4	7	30	4	w	w	1	c	85	d
	5	5	30	4	s	w	1	w	80	d
13B	1	2	30	4	s	w	1	c	90	d
	2	1	25	4	s	w	1	c	90	d
	3	6	25	4	c	c	1	c	90	d
	4	3	30	4	s	w	1	c	90	d
20	1	20	90	2.5	s	w	1	c	80	d
	2	20	30	2	s	w	1	w	70	d
	3	20	40	3	s	w	0.5	c	80	d
	4	15	30	3	s	w	0.5	w	60	d
	5	20	30	3	s	w	0.5	w	70	d
	6	20	30	3	s	w	0.5	w	70	d
19	1	12	15	2	s		0.5	u	90	d
	2	10	25	3	s		0.5	u	90	d
	3	14	15	3	s	w	0.5	u	80	d

71

Site	Location	Frequency	Length	Roughness	Waviness	Fill-strength	Fill Thickness	Wall strength	Ave dip	Ground water
	4	5	10	3	s	c	0.5	c	80	d
	5	8	10	3	s	w	0.5	u	90	d
	6	22	15	3	s	w	0.5	u	90	d
	7	15	20	3	s	w	0.5	u	90	d
	8	10	20	3	s	w	0.5	u	90	d
17	1	20	30	1	s	w	1	u	90	d
	2	15	90	3	c		0.5	u	85	d
	3	12	80	3	s		0.5	u	85	d
	4	20	10	3	s		0	u	85	d
18	1	15	80	3	s	w	1	u	80	d
	2	20	80	3	s	w	1	u	85	d
	3	20	30	3	s	w	1.5	u	90	d
	4	17	30	2	s	w	1	u	90	d
	5	17	30	3	s	w	1	u	90	d
	6	17	30	3	s	w	1	u	90	d

JOINTS

Site	Location	Frequency	Length	Roughness	Waviness	Fill-strength	Thickness	Wall strength	Ave dip	Ground Water
7	1	3	40	7	c	s	1	u	55	d
	2	0								
	3	7	75	4	w	w	1	c	45	w
	4	0								
8	1	0								
	2	0								
	3	0								
	4	0								
	5	0								
	6	0								
11	1	0								
	2	4	500	4	w	w	0.5	u	40	d
	3	5	400	3	w		0	u	50	d
	4	0								
	5	2	200	5	s		0	u	70	d
	6	0.5	300	5	w	w	1	u	45	d
*N e a r dyke	7	0.5	200	4	w		0	u	45	d
16	1	0								
	2	0								
	3	0								
	4	0								
	5	0								
	6	0								

Site	Location	Frequency	Length	Roughness	Waviness	Fill-strength	Thickness	Wall strength	Ave dip	Ground Water
14	7	0								
	1	0								
	2	0								
	3	0								
	4	0								
	5	2	45	7	w	s	0	u	45	d
15	1	0								
	2	0								
	3	0								
	4	5	75	5	s	w	0	u	90	d
	5	0								
4	1	1	60	7	c	s	0	u	45	d
	2	0								
	3	0								
	4	0								
	5	0								
9	1	1	100	4	s	s	1.5	c	82	d
	2	2	100	10	c	w	2	w	85	d
	3	0								
	4	0								
	5	0								
	6	0								
10	1	0								
	2	0								
	3	0								
	4	0								

74

Site	Location	Frequency	Length	Roughness	Waviness	Fill-strength	Thickness	Wall strength	Ave dip	Ground Water
	5	0								
12	1	0								
	2	3	100	5	w	w	1	w	45	d
	3	0								
13A	1	0								
	2	0								
	3	1	20	4	w	w	1	c	85	d
	4	5	15	5	c	w	0	u	60	d
	5	0								
13B	1	2	45	4	d	s	1	c	50	d
	2	4	69	7	w	w	1.5	u	60	d
	3	2	60	7	s	w	2	w	60	d
	4	2	50	7	s	s	0	s	50	d
20	1	0								
	2	0								
	3	0								
	4	0								
	5	0								
	6	0								
19	1	0								
	2	0								
	3	0								
	4	0								
	5	0								
	6	0								
	7	0								

Site	Location	Frequency	Length	Roughness	Waviness	Fill-strength	Thickness	Wall strength	Ave dip	Ground Water
	8	0								
17	1	0								
	2	0								
	3	0								
	4	0								
18	1	2	140	3	s	w	1	u	45	d
	2	2	140	3	s	w	2	u	45	d
	3	2	160	3	c	w	3	w	45	d
	4	0								
	5	0								
	6	2	130	3	s	w	2	u	90	d

SLIPS

Site	Location	Frequency	Length	Roughness	Waviness	Fill - strength	Thickness	Wall strength	Average dip	Ground Water
7	1	2	3.5	4	s	w	3	u	40	d
	2	10	2.5	4	s	w	2	c	55	d
	3	15	2	7	w	w	2	u	55	d
	4	13	2.5	4	c	w	1	c	45	d
8	1	0								
	2	0								
	3	6	3	4	w	w	1	w	75	d
	4	3	3	2	w	w	1	w	35	d
	5	0								
	6	0								
11	1	8	4	2	w	w	0.5	u	50	d
	2	2	4	2	w	w	0.5	w	50	d
	3	3	4	2	w	w	0.5	w	50	d
	4	5	4	3	w	w	1	w	45	d
	5	3	3	4	w	w	1	w	60	d
	6	4	4	4	w	w	1	w	50	d
* N e a r dyke	7	3	4	3	w	w	1	w	50	d
16	1	0								
	2	3	4.5	4	w	w	2	w	50	d
	3	2	4.5	5	w		0	w	60	d
	4	0								
	5	2	4.5	5	w	w	0	w	60	d

Site	Location	Frequency	Length	Roughness	Waviness	Fill - strength	Thickness	Wall strength	Average dip	Ground Water
	6	0								
	7	0								
14	1	10	3	7	s	w	2	w	45	d
	2	4	4	5	c	w	1	c	45	d
	3	3	3	3	s	w	0	s	45	d
	4	5	1.5	5	c	w	1	w	45	d
	5	11	1	5	w	w	1	c	45	d
15	1	2	0.6	2	c	w	1	s	60	d
	2	6	2.5	4	w	w	2	c	60	d
	3	2	0.4	5	c	w	1	u	90	d
	4	6	2	4	c	w	2	c	45	d
	5	6	1	4	w	w	2	c	45	d
4	1	6	1.5	5	s	s	0	u	45	d
	2	9	1	4	c	s	0	w	45	d
	3	8	1.2	4	s	s	0	w	45	d
	4	11	1.1	4	c	w	2	c	45	d
	5	4	2.5	4	c	w	1	c	45	d
9	1	0								
	2	1	3.5	5	c	w	1.5	w	45	d
	3	1	3.5	4	c	w	1	w	45	d
	4	4	3	3	s	w	2	u	45	d
	5	3	3.5	2	w	w	1	c	45	d
	6	2	3	2	w	s	1	w	45	d
10	1	2	7	4	s	w	1	w	50	
	2	2	7	5	s	w	1	w	60	
	3	2	7	5	s	w	1	w	45	

78

Site	Location	Frequency	Length	Roughness	Waviness	Fill - strength	Thickness	Wall - strength	Average dip	Ground Water
	4	4	5	4	s	w	1	w	50	
	5	0								
12	1	7	5	5	w	w	1	w	50	d
	2	7	5	4	w	w	1	w	50	d
	3	7	5	4	w	w	1	w	90	d
13A	1	30	2.5	7	c	w	1.5	c	45	d
	2	27	2	5	w	w	2	c	45	d
	3	52	2.5	2	w	w	1.5	c	45	d
	4	40	2.5	2	w	w	1	s	45	d
	5	29	2	2	s	w	1	u	45	d
13B	1	52	3	2	c	w	1.5	s	45	d
	2	48	3	2	s	w	1	u	30	d
	3	18	3.5	2	s	w	1.5	s	45	d
	4	10	2.5	2	s	w	1	s	40	d
20	1	0								
	2	3	3	6	w	s	0.5	c	45	d
	3	0								
	4	0								
	5	3	3	3	w	w	0.5	c	50	d
	6	0								
19	1	0								
	2	0								
	3	0								
	4	1	3	3	w	s	1	c	70	d
	5	0								
	6	0								

79

Site	Location	Frequency	Length	Roughness	Waviness	Fill - strength	Thickness	Wall strength	Average dip	Ground Water
	7	0								
	8	0								
17	1	1	2	4	w	w	1	w	45	d
	2	0								
	3	0								
	4	0								
18	1	50	0.5	3	c	w	4	w	50	d
	2	0								
	3	2	1.6	3	c	w	3	w	45	d
	4	50	3	2	c	w	2	c	60	d
	5	30	3	4	w	w	4	c	45	d
	6	0								

Appendix 2

Fracture index calculations

The laboratory samples were inspected and all visible fractures were traced by placing transparent plastic film over the samples. The result was a fracture map of the top, bottom and sides of each sample. Once the fracture maps were available, the length of fractures were determined by scanning the fracture maps as black and white computer bitmap images. A computer program was written which counted black pixels and converted these into an equivalent length of line. The program was calibrated by scanning diagrams of known line lengths. Accuracy of better than 90% was obtained.

The intensity of fracturing in each sample was expressed using a dimensionless index as follows:

$$I = \frac{\Sigma l}{l_e}$$

where Σl is the sum of lengths of all fractures and l_e is the equivalent dimension of the sample. The equivalent dimension was defined as the volume of the sample divided by the area.

The following table summarises the fracture length, sample dimensions and index values for samples with a width to height ratio of approximately 1,0.

Table A2.1 Data and calculation of fracture index for samples with width to height ratio of 1,0.

Fracture length Top (mm)	Fracture length Bottom (mm)	Fracture length Sides (mm)	Diameter (mm)	Height (mm)	Volume (cubic mm)	Fractures total (mm)	Surface Area (mm²)	Fractures/surface (mm/mm²*)	Strength MPa	W/H	Index
717.7	308.4	1348.3	100	100.5	789325.1542	2374.4	47280.969	0.0502189	42.7	1.00	142.2277413
291.1	0	1419.1	100	99.5	781471.1726	1710.2	46966.81	0.0364129	37.9	1.01	102.7838794
182.2	188.4	162.3	53.2	50.6	112476.9841	532.9	12902.647	0.0413016	42.5	1.05	61.13091028
116.4	273.8	390.9	53.4	50.2	112428.4213	781.1	12900.825	0.0605465	52.6	1.06	89.62888521
138.5	136.1	423.3	53.3	49	109330.2596	697.9	12667.357	0.0550944	38.3	1.09	80.86094881
253.4	174.2	278.2	53.4	50.2	112428.4213	705.8	12900.825	0.0547097	54.2	0.00	80.98843577
260.9	147.8	351.7	53.4	49.2	110188.8114	760.4	12733.064	0.0597185	56.2	1.09	87.8693706
118.4	320.7	300.2	53.6	53.8	121395.2619	739.3	13572.183	0.0544717	45.1	1.00	82.65491317
113.3	203.1	366.7	53.3	48.9	109107.1367	683.1	12650.612	0.0539974	52.4	1.09	79.20319064
316.1	247.5	492.1	53.4	50	111980.4993	1055.7	12867.272	0.0820454	48.7	1.07	121.3066517
25.8	21.3	30.9	24.6	25.4	12072.40544	78	2913.5759	0.0267712	48.8	0.97	18.82465911
0	0	0	24.6	24	11406.99726	0	2805.3794	0	56.1	1.03	0
13.6	24.9	78.2	24.6	25.8	12262.52206	116.7	2944.4891	0.0396334	54.6	0.95	28.02212138
0	0	52.4	24.6	25.5	12119.93459	52.4	2921.3042	0.0179372	42.2	0.96	12.63012912
26.8	19.7	52.9	24.6	26.9	12785.34276	99.4	3029.5006	0.0328107	56.7	0.91	23.5529362
0	0	74.7	24.6	25	11882.28881	74.7	2882.6626	0.0259135	56.3	0.98	18.12234146
0	0	0	24.6	24.9	11834.75966	0	2874.9343	0	50.4	0.99	0
2084.3	2348.2	7505.4	294	294	19958682.64	9853.6	407320.05	0.0241913	22.5	1.00	201.0938776
1222.8	320.7	0	100	99	777544.1818	1543.5	46809.731	0.0329739	41.2	1.01	92.92181818
972.3	147.9	394.3	100	100	785398.1634	1514.5	47123.89	0.0321387	42.2	1.00	90.87

82

Appendix 3

Rock mass rating data

The joint data presented in Appendix 1 was used to rate the coal mass at the different sites. The rating was based on the Rock Mass Rating system of Bieniawski (1976).

Table A3.1 Rock mass rating data

Site No	Intact rock Rating	RQD & Joint spacing Rating	Roughness Rating	Ground water Rating	Total Rating
7	4	35	10	10	59
	4	50	10	10	74
	4	26.25	10	10	50.25
	4	50	10	10	74
8	4	50	10	10	74
	4	35	10	10	59
	4	26.25	10	10	50.25
	4	50	10	10	74
	4	35	10	10	59
	4	43.75	10	10	67.75
11	4	50	10	10	74
	4	35	10	10	59
	4	26.25	10	10	50.25
	4	50	10	10	74
	4	35	10	10	59
	4	43.75	10	10	67.75
*Near dyke	4	43.75	10	10	67.75
16	4	50	20	10	84
	4	50	10	10	74
	4	50	10	10	74
	4	50	20	10	84

84

Site No	Intact rock Rating	RQD & Joint spacing Rating	Roughness Rating	Ground water Rating	Total Rating
	4	50	10	10	74
	4	50	20	10	84
	4	50	20	10	84
14	4	50	10	10	74
	4	50	10	10	74
	4	50	10	10	74
	4	50	10	10	74
	4	35	10	10	59
15	4	50	10	10	74
	4	50	10	10	74
	4	50	10	10	74
	4	26.25	10	10	50.25
	4	50	10	10	74
4	4	43.75	10	10	67.75
	4	50	10	10	74
	4	50	10	10	74
	4	50	10	10	74
	4	50	10	10	74
9	4	43.75	20	10	77.75
	4	35	10	10	59
	4	50	10	10	74
	4	50	10	10	74
	4	50	10	10	74
	4	50	10	10	74
10	4	50	10	10	74
	4	50	10	10	74
	4	50	10	10	74
	4	50	10	10	74
	4	50	20	10	84
12	4	50	10	10	74
	4	35	10	10	59
	4	50	10	10	74
13a	4	50	10	10	74
	4	50	10	10	74
	4	43.75	10	10	67.75
	4	26.25	10	10	50.25
	4	50	10	10	74
13b	4	35	10	10	59
	4	35	10	10	59
	4	35	10	10	59

Site No	Intact rock Rating	RQD & Joint spacing Rating	Roughness Rating	Ground water Rating	Total Rating
	4	35	10	10	59
20	4	50	20	10	84
	4	50	10	10	74
	4	50	20	10	84
	4	50	20	10	84
	4	50	10	10	74
	4	50	20	10	84
19	4	50	20	10	84
	4	50	20	10	84
	4	50	20	10	84
	4	50	10	10	74
	4	50	20	10	84
	4	50	20	10	84
	4	50	20	10	84
	4	50	20	10	84
17	4	50	10	10	74
	4	50	20	10	84
	4	50	20	10	84
	4	50	20	10	84
18	4	35	10	10	59
	4	35	20	10	69
	4	35	10	10	59
	4	50	10	10	74
	4	50	10	10	74
	4	35	20	10	69

Appendix 4

Effect of discontinuities on pillar conditions

The pillar classification metod of Ozan (1993) was used to rate the pillars at a number of the mine sites. The rating system is carried out in two stages. The first stage is a visual rating of condition of a pillar and surrounding strata. The second stage considers the relative importance of each rating parameter. The overall rating of a pillar consists of a rating of the pillars, the roof, support and structural discontinuities. In the following table, only the pillar ratings and the structural discontinuity ratings are considered. Ratings were carried out at eleven of the coal mine sites. The site numbers indicated in the table below refer to the sites shown in figure 2.1 of the main body of this report.

The rating of the performance of coal pillars consists of visual observation of the following:

- fracturing of pillar sidewalls
- scaling of pillar sidewalls
- scaling of pillar corners
- contact of pillar and roof strata
- weaknesses in the pillar.

Perfect conditions in each class are marked with 100 points. The points are reduced as the amount of fracturing and scaling increases. For example, if the scaling of pillar corners exceeds 1,5 m the rating reduces to zero. The total rating is obtained by summing the individual ratings. The maximum total rating is therefore 500 points for a pillar in perfect condition.

The structural discontinuity rating which was part of the pillar rating system simply rated the effects of major structural discontinuities on the condition of the pillar. The rating was 100 for no effect to 0 for serious effects such a pillar corner failure along a discontinuity.

The frequency of discontinuities was taken from the discontinuity mapping data presented in appendix 1.

Table A4.1 Pillar condition rating and discontinuity rating

Site	Location	Pillar condition rating	Discon- tinuity rating	Factor of safety	Frequency of discon- tinuities
7	1	450	100	2.79	12
	2	400	100	2.74	15
	3	425	75	1.8	29
	4	500	100	1.62	17
8	1	400	100	2.2	15
	2	475	100	2.26	13
	3	450	100	3.24	15
	4	425	75	3.94	12
	5	425	100	3.62	11
	6	450	100	3.46	11.5
11	1	475	100	4.74	23
	2	475	75	2.58	22
	3	475	75	2.73	23
	4	425	100	1.56	15
	5	400	100	2.6	20
	6	475	75	4.83	19.5
*Near dyke	7				7.5
16	1	400	100	2.18	10
	2	425	100	2.2	7
	3	400	100	1.69	6
	4	500	100	2.09	6
	5	325	100	1.65	12
	6	325	100	1.78	10
	7	400	100	1.69	13
4	1	250	100	1.21	11
	2	275	75	1.27	14
	3	325	75	2.05	13
	4	350	75	2.08	19
	5	450	100	2.11	9
9	1	450	100	1.3	1
	2	375	100	3.65	7
	3	400	75	1.17	5
	4	400	75	1.17	6
	5	375	100	1.33	6

Site	Location	Pillar condition rating	Discon-tinuity rating	Factor of safety	Frequency of discon-tinuities
	6	450	100	1.53	5
10	1	450	75	2.27	9
	2	475	100	2.14	8
	3	500	100	1.88	6
	4	500	100	2.04	7
	5	500	100	1.95	4
12	1	500	100	1.87	15
	2	475	100	2.41	20
	3	450	50	1.84	13
13A	1	325	25	6	39
	2	300	25	5.43	36
	3	300	25	5.97	61
	4	225	25	6.55	52
	5	350	50	5.59	34
13B	1	250	50	3.05	56
	2	375	50	3.2	53
	3	250	50	2.97	26
	4	250	50	3.05	15
20	1	425	100	2	20
	2	500	100	2.78	23
	3	500	100	1.88	20
	4	400	100	2.11	15
	5	425	100	1.76	23
	6	250	100	1.76	20
17	1	430	75	3.2	21
	2	400	75	1.8	15
	3	460	100	2	12
	4	400	60	2.4	20

Appendix 5

Numerical modeling parameters

The following pages present input data and results of selected numerical models used in the analyses presented in Section 4 of this report.

Udec data file to simulate a 2:1 pillar

```
* no joints 2:1
new
tit
Pillar with - w:h=2
set vga
block 0 0 0 13 4 13 4 0
round=0.02
crack 0 6 4 6
crack 0 7 4 7
crack 1 6 1 7
crack 3 6 3 7
jregion 1,6 1,7 3,7 3,6
jdel
gen 0,4 0,6 edge 1
gen 0,4 6,7 edge 0.2
gen 0,4 7,13 edge 1
del area=0.02
*boundaries
bo -1 5 12 14 yvel -0.5e-1
bo -1 1 -1 14 xvel=0
bo 3.5,4.5 -1,14 xvel=0
bo -1,5 -1,1 yvel=0
* properties
* rock
prop mat=1 bulk=8e9 sh=4.8e9
dens=2500
* coal
prop mat=2 bulk=2.67e9 sh=1.6e9
den=1500
*joints
prop jmat=1 jcoh=0 jks=10e9 jkn=20e9
jfric=20 jdil=5 jten=0
* assign props
* rock is elastic

change -1 5 -1 14 cons=1 mat=1 jmat=1
jcons=2
* coal is Coulomb
change -1 5 6 7 cons=3 mat=2
* define SS zone
zone -1 5 6,7 mo=ss ftable=1 ctable=2
bulk=2.67e9 sh=1.6e9 dil=10
zone -1 5 6,7 coh=2.51e6 fric=20
tens=0.01e6
table 1 0,20
table 2 0,2.51e6 0.08,0.1e6
* histories
his ncyc=200
his unbal
his damp
his yd 2.1,7
his yd 2.1,6
his syy 1.1,6.5
his syy 1.3,6.5
his syy 1.5,6.5
his syy 1.7,6.5
his syy 1.9,6.5
his syy 2.1,6.5
his syy 2.3,6.5
his syy 2.5,6.5
his syy 2.7,6.5
his syy 2.9,6.5
damp auto
delete 0,1 6,7
delete 3,4 6,7
cy 10000
sav s2nil.sav
```

Udec data file to simulate a pillar with a width to height ratio of 3 containing joints spaced at 0,5m apart dipping at 75 degrees

new

set vga

tit

W:H = 3 - Joints at 75 deg - coh=0

spacing 0.5

block 0 0 0 19 5 19 5 0

round=0.02

crack 0 9 5 9

crack 0 10 5 10

crack 1 9 1 10

crack 4 9 4 10

jregion 1,9 1,10 4,10 4,9

jset 75 0 10 0 0 0 0 0.5 0.0 0.2

*jset 135 0 10 0 0 0 0 0.5 0.0 0.2

jdel

gen 0,5 0,9 edge 1

gen 0,5 9,10 edge 0.2

gen 0,5 10,19 edge 1

del area=0.02

*boundaries

bo -1 6 18,20 yvel -0.5e-1

bo -1 1 -1 20 xvel=0

bo 4.5,5.5 -1,20 xvel=0

bo -1,6 -1,1 yvel=0

* properties

* rock

prop mat=1 bulk=8e9 sh=4.8e9

dens=2500

* coal

prop mat=2 bulk=2.67e9 sh=1.6e9

den=1500

*joints

prop jmat=1 jcoh=0.0e6 jks=10e9

jkn=20e9 jfric=20 jdil=5 jten=0

* assign props

* rock is elastic

change -1 6 -1 20 cons=1 mat=1 jmat=1

jcons=2

* coal is Coulomb

change -1 6 9 10 cons=3 mat=2

* define SS zone

zone -1 6 9,10 mo=ss ftable=1 ctable=2

bulk=2.67e9 sh=1.6e9 dil=10

zone -1 6 9,10 coh=2.51e6 fric=20

tens=0.01e6

table 1 0,20

table 2 0,2.51e6 0.08,0.1e6

* histories

his ncyc=50

his unbal

his damp

his yd 2.5,10

his yd 2.5,9

his syy 1.1,9.5

his syy 1.3,9.5

his syy 1.5,9.5

his syy 1.7,9.5

his syy 1.9,9.5

his syy 2.1,9.5

his syy 2.3,9.5

his syy 2.5,9.5

```
his syy 2.7,9.5
his syy 2.9,9.5
his syy 3.1,9.5
his syy 3.3,9.5
his syy 3.5,9.5
his syy 3.7,9.5
his syy 3.9,9.5
damp auto
delete 0,1 9,10
delete 4,5 9,10
cy 11000
save s3175.sav
```

Input data file for 3DEC model of pillar with a width to heightratio of 3:1

```
*************************
* 3 to 1 coal pillar   *
* for SIMRAC COL 005   *
* PREPARED BY          *
* P. G. CARVILL        *
* ISCOR MINING DIVISION *
************************
* GEOMETRY SET UP


POLY BRICK 0 15 0 21  0  15



JSET DIP 0 DD 180 ORG 0 9 0
MARK DIP 0 DD 180 ORG 0 9 0 BELOW
REG 2 * BASE BLOCK
HIDE REG 2


JSET  DIP 0 DD 180 ORG 0 12 0
MARK  DIP 0 DD 180 ORG 0 12 0
BELOW REG 3 * COAL SEAM
MARK DIP 0 DD 180 ORG 0 12 0 ABOVE
REG 5 * TOP BLOCK
HIDE REG 5


* SET UP PILLAR AND BORD


JSET DIP 90 DD 90 ORG 3 9 0
MARK DIP 90 DD 90 ORG 3 9 0 BELOW
REG 4
HIDE REG 4


JSET DIP 90 DD 90 ORG 12 9 0
MARK DIP 90 DD 90 ORG 12 9 0 ABOVE
REG 4
```

```
HIDE REG 4


JSET DIP 90 DD 180 ORG 0 9 3
MARK DIP 90 DD 180 ORG 0 9 3 ABOVE
REG 4
HIDE REG 4


JSET DIP 90 DD 180 ORG 0 9 12
MARK DIP 90 DD 180 ORG 0 9 12
BELOW REG 4
HIDE REG 4


* REGION 3 IS COAL PILLAR
* REGION 4 IS BORD
* joints to change to off parallel change dd
to 45 /135
*jset dip 45 dd 90 org 7.5 10.5 7.5 num 6
spac 1.32
*jset dip 45 dd 180 org 7.5 10.5 7.5 num 6
spac 1.32


FIND
* SET UP ZONES


GEN REG 3 EDGE 0.5
GEN REG 4 EDGE 1.5
GEN REG 2 5 EDGE 4.5
*SAVE 3TO1GEN.SAV


*es 4to1gen.sav
* boundaries


bou -0.25 0.25 0 21 0 15 xvel=0
bou 14.75 15.25 0 21 0 15 xvel=0
```

bou 0 15 0 21 -0.25 0.25 zvel=0

bou 0 15 0 21 14.75 15.25 zvel=0

bou 0 15 -0.25 0.25 0 15 yvel=0

bou 0 15 20.75 21.25 0 15 yvel=-0.15

* cons models

change reg 3 4 cons 2 mat 2 jcons 2 jmat
2

change reg 2 5 cons 2 mat 3 jcons 2 jmat
3

change mint 2 3 jcons 2 jmat 4

change mint 3 5 jcons 2 jmat 4

change mint 2 4 jcons 2 jmat 4

change mint 4 5 jcons 2 jmat 4

* properties

*initial elastic

* rock

prop mat 3 bu=8e9 g=4.8e9 dens=2500
bcoh=100e6 phi=45 bten=100e6

prop jmat 3 ks=2e10 kn=1e10 coh=100e6
ten=100e6 fric=1 dil=0.245

*coal

prop mat 2 bu=2.67e9 g=1.6e9 den=1500
bcoh=100e6 phi=45 bten=100e6

prop jmat 2 ks=2e10 kn=1e10 coh=100e6
ten=100e6 fric=1 dil= 0.245

* interface properties

prop jmat 4 ks=2e10 kn=1e10 coh=100e6
ten=100e6 fric=1 dil=0.245

*histories

his unbal

his damp

*pillar middle

*edge

his sxx 3.1 10.5 7.5

his syy 3.1 10.5 7.5

his xdis 3.1 10.5 7.5

his ydis 3.1 10.5 7.5

*0.5 m

his sxx 3.5 10.5 7.5

his syy 3.5 10.5 7.5

his xdis 3.5 10.5 7.5

his ydis 3.5 10.5 7.5

* 1m in

his sxx 4.0 10.5 7.5

his syy 4.0 10.5 7.5

his xdis 4.0 10.5 7.5

his ydis 4.0 10.5 7.5

* 1.5 m in

his sxx 4.5 10.5 7.5

his syy 4.5 10.5 7.5

his xdis 4.5 10.5 7.5

his ydis 4.5 10.5 7.5

* 2 m in

his sxx 5.0 10.5 7.5

his syy 5.0 10.5 7.5

his xdis 5.0 10.5 7.5

his ydis 5.0 10.5 7.5

*2.5 m in

his sxx 5.5 10.5 7.5

his syy 5.5 10.5 7.5

his xdis 5.5 10.5 7.5

his ydis 5.5 10.5 7.5

```
* 3.0 m in                          his xdis 5.5 9.0 5.5
his sxx 6.0 10.5 7.5                his ydis 5.5 9.0 5.5
his syy 6.0 10.5 7.5
his xdis 6.0 10.5 7.5               his sxx 6.5 9.0 6.5
his ydis 6.0 10.5 7.5               his syy 6.5 9.0 6.5
                                    his xdis 6.5 9.0 6.5
* 4.5 m in                          his ydis 6.5 9.0 6.5
his sxx 7.5 10.5 7.5
his syy 7.5 10.5 7.5                his sxx 7.5 9.0 7.5
his xdis 7.5 10.5 7.5               his syy 7.5 9.0 7.5
his ydis 7.5 10.5 7.5               his xdis 7.5 9.0 7.5
                                    his ydis 7.5 9.0 7.5


* histories corner                  * close joints and setup
his sxx 3.1 9.0 3.1                 * change to realistic properties
his syy 3.1 9.0 3.1
his xdis 3.1 9.0 3.1                * properties
his ydis 3.1 9.0 3.1                * correct
                                    * rock
his sxx 3.5 9.0 3.5                 prop mat 3 bu=8e9 g=4.8e9 dens=2500
his syy 3.5 9.0 3.5                 bcoh=10e6 phi=44 bten=4e6
his xdis 3.5 9.0 3.5                prop jmat 3 ks=2e10 kn=1e10 coh=10e6
his ydis 3.5 9.0 3.5                ten=1e6 fric=1  dil=0.245
                                    *coal
his sxx 4.0 9.0 4.0                 prop mat 2 bu=2.67e9 g=1.6e9 den=1500
his syy 4.0 9.0 4.0                 bcoh=1.25e6 phi=21 bten=1e5
his xdis 4.0 9.0 4.0                prop jmat 2 ks=2e10 kn=1e10 coh=1e5
his ydis 4.0 9.0 4.0                ten=1e4 fric=0.38 dil= 0.09
                                    * interface properties
his sxx 4.5 9.0 4.5                 prop jmat 4 ks=2e9 kn=1e9 coh=1e5
his syy 4.5 9.0 4.5                 ten=1e4 fric=0.38 dil=0.09
his xdis 4.5 9.0 4.5
his ydis 4.5 9.0 4.5                * isolate pillar
                                    del reg 4
his sxx 5.5 9.0 5.5                 set tens off
his syy 5.5 9.0 5.5                 cyc 200
```

```
pr line 3 10.5  9 9 10.5 9 13 zone stress
pr line 3 10.5 3 9 10.5 9 13 zone stress

set tens on
cyc 5000
save 31test.sav

ret

cyc 2000
pr line 3 10.5  7.5 7.5 10.5 7.5 10 zone
stress
pr line 3 10.5 3 7.5 10.5 7.5 10 zone stress

save 31test.sav
cyc 2000
pr line 3 10.5  7.5 7.5 10.5 7.5 10 zone
stress
pr line 3 10.5 3 7.5 10.5 7.5 10 zone stress
save 3_1c57e2.2so
cyc 2000
pr line 3 10.5  7.5 7.5 10.5 7.5 10 zone
stress
pr line 3 10.5 3 7.5 10.5 7.5 10 zone stress
save 3_1c77e2.2so
cyc 2000
pr line 3 10.5  7.5 7.5 10.5 7.5 10 zone
stress
pr line 3 10.5 3 7.5 10.5 7.5 10 zone stress
save 3_1c97e2.2so
cyc 2000
pr line 3 10.5  7.5 7.5 10.5 7.5 10 zone
stress
pr line 3 10.5 3 7.5 10.5 7.5 10 zone stress
save 3_1117e2.2so
cyc 2000
```

```
pr line 3 10.5  7.5 7.5 10.5 7.5 10 zone
stress
pr line 3 10.5 3 7.5 10.5 7.5 10 zone stress
save 3_1137e2.2so
cyc 2000
pr line 3 10.5  7.5 7.5 10.5 7.5 10 zone
stress
pr line 3 10.5 3 7.5 10.5 7.5 10 zone stress
save 3_1157e2.2so
cyc 2000
pr line 3 10.5  7.5 7.5 10.5 7.5 10 zone
stress
pr line 3 10.5 3 7.5 10.5 7.5 10 zone stress
save 3_1177e2.2so
cyc 2000
pr line 3 10.5  7.5 7.5 10.5 7.5 10 zone
stress
pr line 3 10.5 3 7.5 10.5 7.5 10 zone stress
save 3_1197e3.2so
```